THESIS FOR THE DEGREE OF DOCTOR OF PHILOSOPHY

Thermodynamic constraints on noise

LUDOVICO TESSER

Department of Microtechnology and Nanoscience (MC2)
Applied Quantum Physics Laboratory
CHALMERS UNIVERSITY OF TECHNOLOGY

Göteborg, Sweden 2025

Thermodynamic constraints on noise
LUDOVICO TESSER
Göteborg, Sweden 2025
ISBN 978-91-8103-141-6

Doktorsavhandlingar vid Chalmers tekniska högskola
Ny serie Nr 5599
ISSN 0346-718X

Applied Quantum Physics Laboratory
Department of Microtechnology and Nanoscience (MC2)
Chalmers University of Technology
SE-412 96 Göteborg, Sweden
Telephone: +46 (0)31-772 1000

Cover
Artistic depiction of nanoscale heat engine connecting hot and cold sides.
Image by Carina Schultz

Printed by Chalmers Digitaltryck
Göteborg, Sweden 2025

Thermodynamic constraints on noise
LUDOVICO TESSER
Applied Quantum Physics Laboratory
Department of Microtechnology and Nanoscience (MC2)
Chalmers University of Technology

Abstract

The recent progress in nanotechnology has allowed the fabrication of smaller and smaller devices. On the one hand, this development allows to fit more of such devices on a chip, improving its performance. On the other hand, as the size of the device decreases, new phenomena emerge, such as quantum effects and sizable fluctuations. Indeed, when the size of the device is comparable with the coherence length, the quantum nature of particles cannot be neglected. Furthermore, the smaller a device is, the more it is affected by random changes in one of its few components, leading to fluctuations and noise that are comparable with the average quantities. While these phenomena pose new challenges, they also offer new opportunities both in terms of understanding the underlying physical system, and of realizing new devices that exploit such phenomena.

This thesis studies, from a theoretical perspective, the noise in such nanodevices where both quantum effects and fluctuations play an important role. While noise has already been investigated for systems at thermodynamic equilibrium, most devices need to operate out of equilibrium in order to be useful. Here we show that such out-of-equilibrium conditions set constraints on how large or how small the noise can be, and how these constraints affect the precision of the device.

The appended papers discuss these constraints starting from a quantum transport perspective, and study the impact they have on the performance of thermal machines. In this thesis we do not follow the same route. Instead, we first introduce out-of-equilibrium fluctuations in the context of quantum stochastic thermodynamics, and then use this framework to describe transport. This different approach aims at providing a broader perspective on the constraints on noise found in the appended papers, putting them into context with previously known results such as the fluctuation-dissipation theorem, and both thermodynamic and kinetic uncertainty relations.

Keywords: quantum transport, quantum thermodynamics, out-of-equilibrium noise, limits on precision

Acknowledgements

First, I want to thank my supervisor Janine Splettstößer for all the guidance (and also the coffee) she gave me in these years. I hope the risk you took in choosing me as a student paid off, even if just a small fraction of the one I took in choosing you as supervisor.

I also want expres my gratitude to all the members of the research group I have been part of for creating such a welcoming and open environment. Special thanks go to Matteo Acciai, who endured my ramblings on physics throughout our collaborations, to Juliette Monsel, who taught me a lot, even though we didn't work together as much, and to Didrik Palmqvist, who I may have infected with the inequality "disease".

Furthermore, I acknowledge all the collaborators who took the time to discuss with me and made the projects possible.

Finally, I appreciate the patience of all those who bore discussing physics and answering my (sometimes annoying) questions.

Squished by the soles of giants.

List of publications

This thesis presents an introduction, summary and extension to the following appended papers:

[I] J. Eriksson, M. Acciai, L. Tesser, and J. Splettstoesser, "General Bounds on Electronic Shot Noise in the Absence of Currents", Phys. Rev. Lett. **127**, 136801 (2021).

[II] L. Tesser, M. Acciai, C. Spånslätt, J. Monsel, and J. Splettstoesser, "Charge, spin, and heat shot noises in the absence of average currents: Conditions on bounds at zero and finite frequencies", Phys. Rev. B **107**, 075409 (2023).

[III] L. Tesser and J. Splettstoesser, "Out-of-Equilibrium Fluctuation-Dissipation Bounds", Phys. Rev. Lett. **132**, 186304 (2024).

[IV] L. Tesser, M. Acciai, C. Spånslätt, I. Safi, and J. Splettstoesser, "Thermodynamic and energetic constraints on out-of-equilibrium tunneling rates", arXiv (2024) 10.48550/arXiv.2409.00981, eprint: 2409.00981.

[V] M. Acciai, L. Tesser, J. Eriksson, R. Sánchez, R. S. Whitney, and J. Splettstoesser, "Constraints between entropy production and its fluctuations in nonthermal engines", Phys. Rev. B **109**, 075405 (2024).

[VI] D. Palmqvist, L. Tesser, and J. Splettstoesser, "Kinetic uncertainty relations for quantum transport", arXiv (2024) 10.48550/arXiv.2410.10793, eprint: 2410.10793.

We always refer to these publications as paper I, II, ..., according to the labeling in the list above.
The following papers were published during my PhD studies, but are outside the scope of this thesis.

[A] L. Tesser, B. Bhandari, P. A. Erdman, E. Paladino, R. Fazio, F. Taddei: "Heat rectification through single and coupled quantum dots", New J. Phys. **24**, 035001 (2022).

[B] L. Tesser, R. S. Whitney, J. Splettstoesser: "Thermodynamic Performance of Hot-Carrier Solar Cells: A Quantum Transport Model", Phys. Rev. Appl. **19**, 044038 (2023).

List of figures

Contents

1 Introduction

Thermodynamics was developed to quantify and optimize the performance of engines. From its early stages, it was clear that a macroscopic engine in contact with a *single* thermal reservoir could not perform any useful task, such as producing work. For the engine to function, it must interact with (at least) two thermal reservoirs at *different temperatures* [1]. This *out-of-equilibrium* condition, created by the temperature difference, is what allows the engine to operate. In such setups, the laws of thermodynamics describe energy transformations, e.g. heat conversion into work by a heat engine, and establish fundamental limits on the efficiency of these processes. These laws were originally formulated by observing macroscopic systems, i.e. systems made of a huge number of inaccessible degrees of freedom, such as the position and momentum of all particles in a mole.

Today, the developments in nanotechnology allow to realize and observe small-scale systems, which are instead made of few degrees of freedom, as, for example, the single electron transistor [2], in which the addition or removal of a single electron determines the operation of the device. One could then use thermodynamics to understand the limitations of such small-scale devices. However, the original laws of thermodynamics do not capture completely the behavior of small-scale systems because in such systems fluctuations (or noise), i.e. deviations from the average behavior, cannot be neglected. Furthermore, quantum effects, such as interference, tunneling and entanglement, affect the system's behavior when the system's size is smaller than its coherence length, which is typically achieved by cooling down the system to temperatures ranging from 100 K to sub-Kelvin [3]. To tackle these new challenges and understand what new opportunities they may offer, thermodynamics has evolved to account for the effects of fluctuations and quantum effects. This evolution came in the form of stochastic [4, 5] and quantum thermodynamics [6], which provide tools for understanding out-of-equilibrium processes.

In the appended papers we study the noise in such small-scale devices operating out-of-equilibrium in the context of quantum transport [7, 8]. This framework focuses on studing the current flows in devices described by quantum mechanics. Concretely, quantum transport studies the properties of the current operators, such as its average and its noise. Typically, a lot of focus is put on charge and energy currents because these are crucial when it comes to power production. However, depending on the context, different currents, for instance spin currents, may be considered. In the appended papers, we derive constraints on the current

noise that depend on the out-of-equilibrium conditions that the system is subject to. This is particularly interesting when the transport systems considered are viewed as an instance of a thermodynamic engine [9, 10]. Indeed, using quantum transport, one can study the heat flowing into reservoirs that are connected by a central system, which may act as an engine. Then, the thermodynamic constraints on the noise derived in the appended papers allow for a better understanding of the performance in such out-of-equilibrium, quantum systems.

This thesis aims at connecting the quantum stochastic thermodynamics framework with the quantum transport one. Indeed, the tools and techniques developed in quantum stochastic thermodynamics can provide additional insights into the fluctuations in the currents studied in quantum transport. To this end, we first describe fluctuations from a point of view based on quantum stochastic thermodynamics, and then use this framework to derive the same statistics obtained with transport techniques. This allows us to put the results of the appended paper into context with previously obtained results in the field of quantum stochastic thermodynamics, and to understand in what ways they are similar, and where they differ.

1.1 Fluctuations in small-scale systems

In classical thermodynamics fluctuations are often neglected because their relative strength decreases with the number of elements N in the system. This can be understood by considering a "macroscopic" observable $Q = \sum_{i=1}^{N} q_i$ given by the sum of "microscopic", independent and identically distributed observables $\{q_i\}_{i=1}^{N}$. Its first two moments are

$$\langle Q \rangle = N\langle q \rangle, \qquad \langle Q^2 \rangle = \sum_{ij} \langle q_i q_j \rangle = N\langle q^2 \rangle + N(N-1)\langle q \rangle^2, \tag{1.1}$$

where $\langle q^k \rangle = \langle q_i^k \rangle$ for all $i \in \{1, \cdots, N\}$ are the moments of the microscopic variables. Comparing the variance $\mathrm{Var}[Q] \equiv \langle Q^2 \rangle - \langle Q \rangle^2$ with the squared average $\langle Q \rangle^2$, the precision of Q is

$$\frac{\langle Q \rangle^2}{\mathrm{Var}[Q]} = \frac{N^2 \langle q \rangle^2}{N \mathrm{Var}[q]} \sim N. \tag{1.2}$$

So, in the thermodynamic limit, i.e. when N is large, the average behavior dominates over the fluctuations around such average. However, when the system considered has a small number of elements, i.e. $N \sim 1$, this is no longer true. We refer to such systems as *small-scale systems*. Indeed, in small-scale systems the fluctuations of variables around their average are comparable with the average itself.

On the one hand, the sizable fluctuations mean that small-scale systems are noisy. In particular, one may wonder *how precise* these small-scale systems can

be. This question is answered by *trade-off* relations, which often take the form of inequalities limiting from above the precision on the right-hand side of Eq. (1.2). Examples of such trade-off relations are the thermodynamic uncertainty relation (TUR) [11–19] and the kinetic uncertainty relation (KUR) [20–27], which were initially derived for classical Markovian systems, and are now being investigated in quantum systems as well.

While noise is a hindrance to precision, it can, on the other hand, provide additional insight into the system. Indeed, the presence of sizable noise allows to access more information about, for instance, the underlying probability distribution governing the behavior of our system. Thanks to this additional information, noise measurements are a valuable tool in sensing, and see use in, for instance, the detection of (fractional) charges [28–31], thermometry [32–36], tomography [37–39]. These applications of noise measurements are possible because the noise is connected to other physical quantities. For example, in the case of thermometry, the so-called Johnson-Nyquist noise [40, 41] of a charge current is proportional to the temperature of the sample. The Johnson-Nyquist noise is an early instance of the fluctuation-dissipation theorem (FDT), which was further generalized into the Green-Kubo relations [42–44]. This pivotal result in the study of fluctuations establishes a relation between the *correlations* (which quantify the fluctuations, e.g. $\mathrm{Var}[Q]$) and the *response* of the system to external perturbations (which is then related to the dissipation).

However, the FDT holds for systems close to equilibrium. Importantly, many devices, engines in particular, operate out of equilibrium, e.g. under a voltage or a temperature bias, where fluctuations have more intricate features. To understand such features, fluctuation theorems (FTs) have been developed [45–57]. These results allow, for example, to develop an extension of the FDT to the presence of a voltage bias, albeit in the weakly coupled, equal temperature regime [58, 59], and also to prove that the FDT relation between correlation and response holds in nonequilibrium setups where the average current vanishes [60, 61]. In this thesis we investigate how the presence of both a temperature bias and possibly finite average currents affect the relation between the current correlations and its average value. Indeed, both ingredients are crucial for a whole class of devices, namely thermal machines.

In particular, Papers I-IV are dedicated to the study of out-of-equilibrium noise in the presence of a temperature bias. There, we show that, even in regimes where the FDT does not hold, there are constraints on this out-of-equilibrium noise. Instead, Papers V,VI study the noise in out-of-equilibrium setups that go beyond the presence of a temperature bias. Indeed, we consider *nonthermal* reservoir, which cannot be described by unique intensive properties, such as a temperature, but instead are described by an arbitrary, energy-dependent average occupation number. Even in those more general out-of-equilibrium conditions we provide constraints on the current noise.

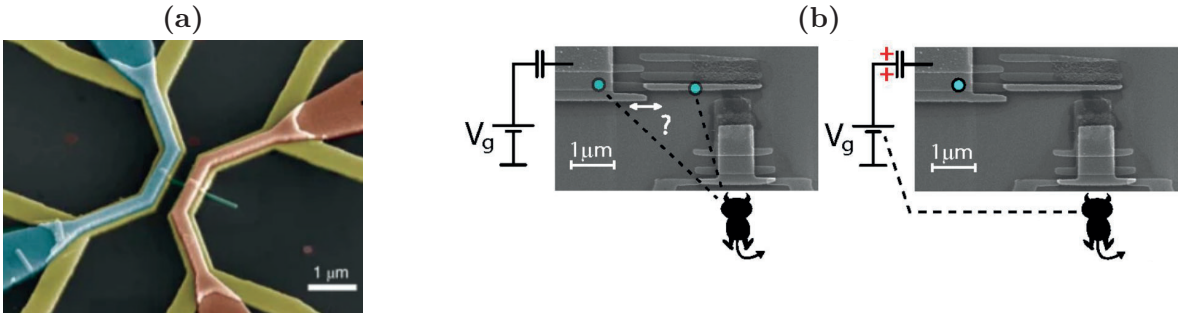

Figure 1.1: (a)*: False-coloured scanning electron microscope picture of a thermoelectric heat engine. A temperature bias is established between the metallic leads (yellow) using the heaters (blue and red), and induces a current through a nanowire (green).* **Source:** [62]. **(b)***: Experimental realization of a Szilard engine using a single-electron box. A single (excess) electron is on one of two metallic islands. Measuring the position of the electron allows to extract work in a feedback operation.* **Source:** [63].

1.2 Engines at the nanoscale

The developments in nanofabrication techniques have made it possible to realize engines using small-scale systems. As discussed previously, these devices are typically noisier than their macroscopic counterparts due to the significant role of fluctuations. However, reducing the size of the system not only presents challenges, but also offers opportunities to improve the efficiency of engines. This is the case, for instance, in thermoelectric heat engines, where heat is converted into electrical power [62, 64–66]. In such devices, nanostructured materials can be engineered to improve the efficiency of power production [67–69], as happens for example in the device shown in Fig. 1.1(a).

Furthermore, the presence of sizable fluctuations also allows for the development of new kinds of devices. A foundational example is the Szilard engine [70], where the information gained by measuring fluctuations allows to extract work from a single thermal reservoir. While this seemingly violates the second law of thermodynamics, it actually highlights the role of information and its connections to thermodynamics [71]. These small-scale systems are not just a theoretical construction, but are also being realized [63, 72, 73], as is the case in the device shown in Fig. 1.1(b).

In addition to fluctuations, quantum effects also appear in small-scale systems where the decoherence time is larger than the typical time-scale of the system's dynamics. These phenomena, which include interference and entanglement, also affect the behavior of small-scale systems, and can be exploited to devise thermal machines with different goals, such as work extraction or refriferation [74–84], or even generation of entangled states [85–87]. However, the delicate nature of quantum states raises concerns about whether it is actually worthwhile to rely on such states in thermal machines.

Indeed, since realizing small-scale devices requires a considerable amount of effort, it is critical to understand and quantify their performance accounting not only for average work or heat, but also for their fluctuations. To this end, trade-off relations have attracted increasing interest as a way to formulate constraints on the performance of large classes of devices. The constraints on the out-of-equilibrium noise derived in the appended papers can be understood as instances of such trade-off relations. For example, in Paper III we study systems where coherent transport makes the thermodynamic uncertainty relation fail [88–96], and we develop a trade-off relation between the charge current and its noise. This result allows us to limit the precision of electrical power production in the presence of coherent transport in terms of the heat dissipated in the cold reservoir, as later discussed in Sec. 4.1. While in Paper III the trade-off relation between current and noise holds for the particle current, the constraint developed in Paper VI applied to arbitrary currents, and highlights the difference in the achievable precision between fermionic and bosonic transport.

1.3 Organization of this thesis

Having introduced the general context behind the appended papers, as well as the goal of this thesis, we now move on to a more detailed discussion of the theoretical background and the main results of the appended papers. Specifically, Chapter 2 gives an overview of a common framework in the field of quantum stochastic thermodynamics, namely the two-point measurement scheme. Within this framework, we discuss the results on out-of-equilibrium fluctuations introduced in Sec. 1.1: the fluctuation theorems, the fluctuation-dissipation theorem, and both the thermodynamic and the kinetic uncertainty relation. These results serve both as a starting point and as means of comparison for the constraints on out-of-equilibrium noise derived in the appended papers.

Then, in Chapter 3 we discuss the transport statistics using the two-point measurement scheme. While this is not how it is presented in the appended papers, the derivations in Chapter 3 show how the two-point measurement and the quantum transport approach lead to the same statistics, and therefore helps in giving a broader perspective on the study of out-of-equilibrium noise.

The discussion of the main results of the appended papers is then provided in Chapter 4. Finally, the conclusions are drawn in Chapter 5.

2 Fluctuations out of equilibrium

In this chapter we discuss a general framework to describe out-of-equilibrium fluctuations in quantum systems: The two-point measurement scheme. Using this framework we show some general properties of the out-of-equilibrium fluctuations, and use them to derive the fluctuation-dissipation theorem and trade-off relations on the precision of observables.

2.1 Two-point measurement scheme

An isolated quantum system described by the density matrix $\rho(t)$ evolves according to the von Neumann equation [97]

$$\partial_t \rho(t) = -\frac{i}{\hbar}[\hat{H}(t), \rho(t)], \tag{2.1}$$

where $\hat{H}(t)$ is the generally time-dependent Hamiltonian of the system. The formal solution is given in terms of the unitary transformation of the state,

$$\rho(t) = \hat{\mathcal{U}}(t,0)\rho(0)\hat{\mathcal{U}}^\dagger(t,0) \tag{2.2}$$

with the unitary operator $\hat{\mathcal{U}}(t,0)$. This is obtained from the system's Hamiltonian through the so-called time-ordered exponential

$$\hat{\mathcal{U}}(t,0) = \mathcal{T}\left\{\exp\left[-\frac{i}{\hbar}\int_0^t \hat{H}(s)ds\right]\right\}. \tag{2.3}$$

Here, $\mathcal{T}\{\bullet\}$ denotes the time-ordering operation. However, the unitary transformation of Eq. (2.2) does not describe the effect that *measurements* have on the system. Consider for instance the measurement of the observable $\hat{A} = \hat{A}^\dagger$ on the state $\rho(0)$. The hermiticity of the observable guarantees that it can always be decomposed as $\hat{A} = \sum_a a\hat{\Pi}_a$, where $\hat{\Pi}_a = \hat{\Pi}_a^2$ are the projectors on the observable's eigenspaces. Then, an ideal measurement of $\hat{A}$ distinguishes perfectly these eigenspaces. The probability of observing the outcome a when measuring the state $\rho(0)$ is given by the Born rule

$$p(a,0) = \mathrm{Tr}\left\{\hat{\Pi}_a\rho(0)\right\}, \tag{2.4}$$

and the state after the measurement collapses to the state

$$\rho(0|a,0) = \frac{\hat{\Pi}_a \rho(0) \hat{\Pi}_a}{p(a,0)}, \tag{2.5}$$

which is conditioned on the outcome a of the measurement.

We now combine the unitary transformation of Eq. (2.2) with the transformation induced by the measurements of Eq. (2.5) to access the statistics before and after the unitary transformation. This is particularly interesting when the (stochastic) change in an observable, e.g. the energy of the system, is considered. The protocol that we consider here is the two-point measurement scheme, sketched in Fig. 2.1(a), which is characterized by the following steps:

0. At the beginning of the protocol the system is in the state $\rho(0)$.

1. An ideal measurement of the observable $\hat{A} = \sum_a a\hat{\Pi}_a$ is performed at $t = 0$. Calling a the outcome of the measurement, the probability $p(a,0)$ of obtaining such an outcome is given by Eq. (2.4) and the post-measurement state $\rho(0|a,0)$ is given by Eq. (2.5).

2. The system undergoes a unitary transformation until time t. In contrast with Eq. (2.2), here the initial state is the post-measurement state $\rho(0|a,0)$, and the final state of the transformation is

$$\rho(t|a,0) = \hat{\mathcal{U}}(t,0)\rho(0|a,0)\hat{\mathcal{U}}^\dagger(t,0). \tag{2.6}$$

3. An ideal measurement of the observable $\hat{B} = \sum_b b\hat{\tilde{\Pi}}_b$ is performed at time t. The observable $\hat{B}$ is also decomposed in terms of projectors $\hat{\tilde{\Pi}}_b = \hat{\tilde{\Pi}}_b^2$. However, these projectors are in general different from the projectors of the observable $\hat{A}$, meaning that the two observable may not have the same eigenspaces and therefore may not commute. Calling b the outcome of this second measurement, the probability of obtaining such an outcome *given that* the outcome of the first measurement was a follows by the Born rule Eq. (2.4) applied to the state $\rho(t|a,0)$. The probability thus reads

$$\begin{aligned} p(b,t|a,0) &= \mathrm{Tr}\left\{\hat{\tilde{\Pi}}_b \rho(t|a,0) \hat{\tilde{\Pi}}_b\right\} \\ &= \mathrm{Tr}\left\{\hat{\tilde{\Pi}}_b \hat{\mathcal{U}}(t,0) \left(\frac{\hat{\Pi}_a \rho(0) \hat{\Pi}_a}{p(a,0)}\right) \hat{\mathcal{U}}^\dagger(t,0) \hat{\tilde{\Pi}}_b\right\}. \end{aligned} \tag{2.7}$$

Therefore, the *joint* probability distribution of observing the outcome a at time 0 and the outcome b at time t is given by

$$p(b,t;a,0) = \mathrm{Tr}\left\{\hat{\tilde{\Pi}}_b \hat{\mathcal{U}}(t,0) \hat{\Pi}_a \rho(0) \hat{\Pi}_a \hat{\mathcal{U}}^\dagger(t,0) \hat{\tilde{\Pi}}_b\right\}. \tag{2.8}$$

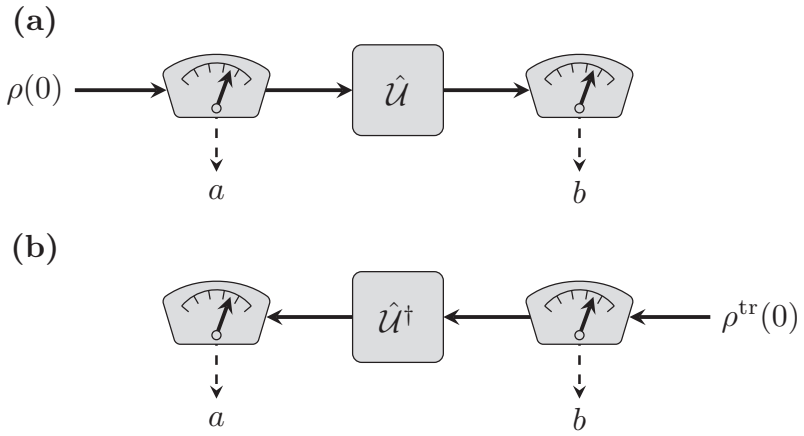

Figure 2.1: *Forward* **(a)** *and time-reversed* **(b)** *two-point measurement schemes. In the forward (time-reversed) protocol the observable $\hat{A}$ ($\hat{B}$) is measured on the initial state $\rho(0)$ ($\rho^{tr}(0)$), and the measurement has outcome a (b). Then, the system evolves according to the unitary $\hat{\mathcal{U}}$ ($\hat{\mathcal{U}}^\dagger$). Finally, the observable $\hat{B}$ ($\hat{A}$) is measured on the system, and the measurement has outcome b (a).*

Note that the presence of the first measurement affects the statistics of the second outcome because the measurement back action destroys the coherences between the different eigenspaces of $\hat{A}$. Concretely, this means that the marginal probability for the second outcome $p(b,t)$ does not coincide with the probability $\tilde{p}(b,t)$ of a protocol in which the first measurement did not happen

$$\begin{aligned} p(b,t) = \sum_a p(b,t;a,0) &= \mathrm{Tr}\left\{\hat{\tilde{\Pi}}_b \hat{\mathcal{U}}(t,0)\left(\sum_a \hat{\Pi}_a \rho(0)\hat{\Pi}_a\right)\hat{\mathcal{U}}^\dagger(t,0)\hat{\tilde{\Pi}}_b\right\} \\ &\neq \mathrm{Tr}\left\{\hat{\tilde{\Pi}}_b \hat{\mathcal{U}}(t,0)\rho(0)\hat{\mathcal{U}}^\dagger(t,0)\hat{\tilde{\Pi}}_b\right\} = \tilde{p}(b,t). \end{aligned} \tag{2.9}$$

2.2 Fluctuation theorems

The two-point measurement scheme offers a simple framework where one can study the thermodynamics of the process, and in particular, its irreversibility. However, the two-point probability distribution of Eq. (2.8) on its own is not sufficient to quantify the irreversibility of a (stochastic) process. Indeed, one typically compares the probability of a process with the probability of its "opposite" process. For example, drawing from a classical thermodynamics intuition, we want to compare the probability of heat flowing from a hot bath to a cold bath to the probability of heat flowing from the cold bath to the hot bath. Following this idea, we consider the *time-reversed process*, in which the order of the measurement and the unitary transformation of the system are inverted [6, 51, 98]. This process is sketched in Fig. 2.1(b), and is described by the following steps:

0. At the beginning of the time-reversed protocol the system is in the state $\rho^{\mathrm{tr}}(0)$.

1. An ideal measurement of the observable $\hat{B} = \sum_b b\hat{\tilde{\Pi}}_b$ is performed at $t = 0$, and has outcome b.

2. The system undergoes a unitary transformation until time t. In contrast with Eq. (2.2), here the initial state is the post-measurement state $\rho^{\mathrm{tr}}(0|b,0)$, and the final state of the transformation is

$$\rho^{\mathrm{tr}}(t|b,0) = \hat{\mathcal{U}}^{\dagger}(t,0)\rho^{\mathrm{tr}}(0|b,0)\hat{\mathcal{U}}(t,0). \tag{2.10}$$

3. An ideal measurement of the observable $\hat{A} = \sum_a a\hat{\Pi}_a$ is performed at time t and has outcome a. Similarly to the conditional probability, see Eq. (2.7), of "forward" process described in Sec. 2.1, the probability of observing the outcome a *given that* the first measurement of the time-reversed process had outcome b is given by

$$\begin{aligned} p^{\mathrm{tr}}(a,t|b,0) &= \mathrm{Tr}\left\{\hat{\Pi}_a\rho^{\mathrm{tr}}(t|b,0)\hat{\Pi}_a\right\} \\ &= \mathrm{Tr}\left\{\hat{\Pi}_a\hat{\mathcal{U}}^{\dagger}(t,0)\left(\frac{\hat{\tilde{\Pi}}_b\rho^{\mathrm{tr}}(0)\hat{\tilde{\Pi}}_b}{p^{\mathrm{tr}}(b,0)}\right)\hat{\mathcal{U}}(t,0)\hat{\Pi}_a\right\}. \end{aligned} \tag{2.11}$$

Therefore, the *joint* probability distribution in the time-reversed process is

$$p^{\mathrm{tr}}(a,t;b,0) = \mathrm{Tr}\left\{\hat{\Pi}_a\hat{\mathcal{U}}^{\dagger}(t,0)\hat{\tilde{\Pi}}_b\rho^{\mathrm{tr}}(0)\hat{\tilde{\Pi}}_b\hat{\mathcal{U}}(t,0)\hat{\Pi}_a\right\}. \tag{2.12}$$

We then compare the probability of the forward process Eq. (2.8) with the probability of the time-reversed process Eq. (2.12) using the entropy change

$$\sigma(b,t;a,0) \equiv \log\left(\frac{p(b,t;a,0)}{p^{\mathrm{tr}}(a,t;b,0)}\right). \tag{2.13}$$

To discuss the properties of this stochastic entropy change, we introduce the probabilities $p(\sigma)$ and $p^{\mathrm{tr}}(\sigma)$ of observing the entropy change σ in the forward and time-reversed process, respectively. These probabilities are given by

$$p(\sigma) = \sum_{b,a} p(b,t;a,0)\delta(\sigma - \sigma(b,t;a,0)), \tag{2.14a}$$

$$p^{\mathrm{tr}}(\sigma) = \sum_{a,b} p^{\mathrm{tr}}(a,t;b,0)\delta(\sigma - \sigma^{\mathrm{tr}}(a,t;b,0)), \tag{2.14b}$$

where $\sigma^{\mathrm{tr}}(a,t;b,0)$ is the entropy change in the time-reversed process. Note that, since the time-reversed of the time-reversed process corresponds to the forward one, the entropy change fulfils

$$\sigma^{\mathrm{tr}}(a,t;b,0) \equiv \log\left(\frac{p^{\mathrm{tr}}(a,t;b,0)}{p^{\mathrm{tr}^{\mathrm{tr}}}(b,t;a,0)}\right) = -\sigma(b,t;a,0). \tag{2.15}$$

Then, the probabilities in Eq. (2.14) obey

$$p(\sigma) = e^{\sigma} \sum_{b,a} p^{\rm tr}(a,t;b,0)\delta(\sigma - \sigma(b,t;a,0)) \quad \Rightarrow \quad \frac{p(\sigma)}{p^{\rm tr}(-\sigma)} = e^{\sigma}, \tag{2.16}$$

which is referred to as *detailed fluctuation theorem* [51]. From this result it is immediate to see that the entropy change also obeys the *integral fluctuation theorem*

$$\langle e^{-\sigma} \rangle = \sum_{a,b} p^{\rm tr}(a,t;b,0) = 1. \tag{2.17}$$

Interestingly, using Jensen inequality on Eq. (2.17), one also finds the second law $\langle \sigma \rangle \geq 0$, meaning that, on average, the entropy change is positive. Note that, to derive the detailed fluctuation theorem of Eq. (2.16) we did not use the protocol underlying the time-reversed process, but only the definition of the entropy change Eq. (2.13) and its anti-symmetry property Eq. (2.15). The independence of Eq. (2.16) from the specific details of the "opposite" process makes the detailed fluctuation theorem a rather general result. This generality is reflected in the fact that the fluctuation theorems Eqs. (2.16, 2.17) are *informational* properties of the entropy change defined in Eq. (2.13). For all these relations to be of use, we need the entropy change to be expressed in terms of physical and measurable quantites.

The choice of the time-reversed process helps towards this direction. Indeed, when the measurement projectors are one-dimensional, i.e. $\hat{\Pi}_a = |a\rangle\langle a|$ and $\hat{\tilde{\Pi}}_b = |\tilde{b}\rangle\langle\tilde{b}|$, the joint probability distributions of forward and time-reversed process become

$$p(b,t;a,0) = |\, \langle \tilde{b}|\hat{\mathcal{U}}(t,0)|a\rangle \,|^2 p(a,0), \tag{2.18a}$$

$$p^{\rm tr}(a,t;b,0) = |\, \langle a|\hat{\mathcal{U}}^{\dagger}(t,0)|\tilde{b}\rangle \,|^2 p^{\rm tr}(b,0). \tag{2.18b}$$

Then, then entropy change does not depend any longer on the unitary dynamics of the system, but only on the initial states of forward, i.e. $\rho(0)$, and time-reversed process, i.e. $\rho^{\rm tr}(0)$, namely

$$\sigma(b,t;a,0) = \log\left(\frac{p(a,0)}{p^{\rm tr}(b,0)}\right) = \log\left(\frac{\langle a|\rho(0)|a\rangle}{\langle\tilde{b}|\rho^{\rm tr}(0)|\tilde{b}\rangle}\right). \tag{2.19}$$

While the initial state of the forward process $\rho(0)$ is determined by the specific system and process considered, the initial state of the time-reversed process $\rho^{\rm tr}(0)$ can be *arbitrary* and still result in the detailed fluctuation theorem Eq. (2.16). Then, different choices of $\rho^{\rm tr}(0)$ lead to different entropy changes, and reflect what can and cannot be accessed through measurements [98, 99].

As a relevant thermodynamic example, let's consider a bipartite system, where the left (L) and right (R) subsystems are initially prepared in Gibbs states at different inverse temperatures $\beta_{\rm L/R} = (k_{\rm B}T_{\rm L/R})^{-1}$ and chemical potentials $\mu_{\rm L/R}$ [100].

Thus the initial state reads

$$\rho(0) = \tau_{\mathrm{L}} \otimes \tau_{\mathrm{R}} = \frac{e^{-\beta_{\mathrm{L}}(\hat{H}_{\mathrm{L}} - \mu_{\mathrm{L}}\hat{N}_L)}}{Z_{\mathrm{L}}} \otimes \frac{e^{-\beta_{\mathrm{R}}(\hat{H}_{\mathrm{R}} - \mu_{\mathrm{R}}\hat{N}_R)}}{Z_{\mathrm{R}}}, \tag{2.20}$$

where $\hat{H}_{\mathrm{L/R}}$ and $\hat{N}_{\mathrm{L/R}}$ are the Hamiltonians and number operators of the L/R subsystems. Here, for simplicity, we assume that $[\hat{H}_{\mathrm{L/R}}, \hat{N}_{\mathrm{L/R}}] = 0$. This also allows us to consider as measurements the joint measurements of energy and particle number of both subsystems, namely $a \to (E_{\mathrm{L},a}, N_{\mathrm{L},a}, E_{\mathrm{R},a}, N_{\mathrm{R},a})$ and $b \to (E_{\mathrm{L},b}, N_{\mathrm{L},b}, E_{\mathrm{R},b}, N_{\mathrm{R},b})$. Finally, as the initial state of the time-reversed protocol, we consider the same state as the forward process $\rho^{\mathrm{tr}}(0) = \rho(0)$, see Eq. (2.20). Then, the stochastic entropy change is given by

$$\sigma(b,t;a,0) = \beta_{\mathrm{L}}\left(\Delta E_{\mathrm{L}} - \mu_{\mathrm{L}}\Delta N_{\mathrm{L}}\right) + \beta_{\mathrm{R}}\left(\Delta E_{\mathrm{R}} - \mu_{\mathrm{R}}\Delta N_{\mathrm{R}}\right) \tag{2.21}$$

where $\Delta E_{\mathrm{L/R}} = E_{\mathrm{L/R},b} - E_{\mathrm{L/R},a}$ and $\Delta N_{\mathrm{L/R}} = N_{\mathrm{L/R},b} - N_{\mathrm{L/R},a}$ are the stochastic energy and particle number change in the process, respectively. Additionally, if the unitary transformation preserves both total energy, $[\hat{\mathcal{U}}(t,0), \hat{H}_{\mathrm{L}} + \hat{H}_{\mathrm{R}}] = 0$, and particle number, $[\hat{\mathcal{U}}(t,0), \hat{N}_{\mathrm{L}} + \hat{N}_{\mathrm{R}}] = 0$, we write Eq. (2.21) as

$$\sigma(b,t;a,0) = \left(\beta_{\mathrm{L}} - \beta_{\mathrm{R}}\right)\Delta E_{\mathrm{L}} + \left(\beta_{\mathrm{R}}\mu_{\mathrm{R}} - \beta_{\mathrm{L}}\mu_{\mathrm{L}}\right)\Delta N_{\mathrm{L}} \tag{2.22}$$

since $\Delta E_{\mathrm{L}} + \Delta E_{\mathrm{R}} = 0 = \Delta N_{\mathrm{L}} + \Delta N_{\mathrm{R}}$. Furthermore, defining the stochastic heat change $\Delta \mathcal{Q}_{\mathrm{L}} \equiv \Delta E_{\mathrm{L}} - \mu_{\mathrm{L}}\Delta N_{\mathrm{L}}$ we see that the average entropy change reads

$$\langle \sigma \rangle = \left(\beta_{\mathrm{L}} - \beta_{\mathrm{R}}\right)\langle \Delta \mathcal{Q}_{\mathrm{L}} \rangle \geq 0. \tag{2.23}$$

This confirms our classical thermodynamics intuition: Heat flows into L subsystem (on average), i.e. $\langle \Delta \mathcal{Q}_{\mathrm{L}} \rangle \geq 0$, only when the L subsystem is colder than the R one, i.e. $\beta_{\mathrm{L}} \geq \beta_{\mathrm{R}}$.

2.3 Fluctuation-dissipation theorem

In the previous section we discussed general properties of the probability distribution in the fluctuation theorems. However, it is often easier to access the (typically first few) moments of a measured observable Q. Then, it is interesting to know how the fluctuation theorems affect the moments. From a theorerical perspective, to calculate the moments of a stochastic variable Q it is often useful to consider the moment generating function $G_Q(\lambda)$ [101], defined as

$$G_Q(\lambda) \equiv \langle e^{i\lambda Q} \rangle. \tag{2.24}$$

Indeed, the n-th moment of Q is obtained from the generating function by evaluating its n-th derivative at $\lambda = 0$, namely

$$\langle Q^n \rangle = (-i)^n \left. \frac{\partial^n G_Q}{\partial \lambda^n} \right|_{\lambda=0}. \tag{2.25}$$

We now study how the generating function behaves in the two-point measurement scheme described in Sec. 2.1 to find how the fluctuation theorems discussed in Sec. 2.2 affect the moments of Q. We therefore focus on stochastic variables in the two-point measurement scheme $Q(b,t;a,0)$ that are anti-symmetric under time-reversal, i.e. $Q(b,t;a,0) = -Q^{\mathrm{tr}}(a,t;b,0)$. Using the definition of entropy change Eq. (2.13) we find

$$\begin{aligned} G_Q(\lambda) &= \sum_{b,a} e^{i\lambda Q(b,t;a,0)} p(b,t;a,0) \\ &= \sum_{b,a} e^{i\lambda Q(b,t;a,0)+\sigma(b,t;a,0)} p^{\mathrm{tr}}(a,t;b,0) \\ &= \sum_{b,a} e^{-i\lambda Q^{\mathrm{tr}}(a,t;b,0)-\sigma^{\mathrm{tr}}(a,t;b,0)} p^{\mathrm{tr}}(a,t;b,0) = \langle e^{-i\lambda Q-\sigma}\rangle_{\mathrm{tr}}, \end{aligned} \tag{2.26}$$

where once again we relate averages in the forward process with averages in the time-reversed process, here denoted with $\langle\bullet\rangle_{\mathrm{tr}}$. The property in Eq. (2.26) becomes particularly useful when the stochastic entropy change can be written as

$$\sigma = \sum_x \mathcal{A}_x Q_x = \vec{\mathcal{A}}\cdot\vec{Q}, \tag{2.27}$$

where $\mathcal{A}_x$ are called affinities or thermodynamic forces, and Q_x are the corresponding extensive quantities. For instance, this is the case in Eq. (2.22), where the entropy change is given in terms of the stochastic energy and particle number change. In this case, the corresponding affinities and extensive quantities are

$$\begin{array}{lll} \text{Energy change:} & \mathcal{A}_{\mathrm{e}} = \beta_{\mathrm{L}} - \beta_{\mathrm{R}} & Q_{\mathrm{e}} = \Delta E_{\mathrm{L}}, \\ \text{Particle number change:} & \mathcal{A}_{\mathrm{n}} = \beta_{\mathrm{R}}\mu_{\mathrm{R}} - \beta_{\mathrm{L}}\mu_{\mathrm{L}} & Q_{\mathrm{p}} = \Delta N_{\mathrm{L}}. \end{array} \tag{2.28}$$

Note that the affinities $\vec{\mathcal{A}}$ are *not* stochastic, but consist of biases driving the system out of equilibrium. In particular, for $\vec{\mathcal{A}} = 0$, the system is in thermodynamic equilibrium. Combining Eq. (2.26) and Eq. (2.27), the moment generating function of the stochastic variables $\vec{Q}$ entering the entropy production in Eq. (2.27) fulfils

$$G_{\vec{Q}}(\vec{\lambda},\vec{\mathcal{A}}) \equiv \langle e^{i\vec{\lambda}\cdot\vec{Q}}\rangle = G^{\mathrm{tr}}_{\vec{Q}}(i\vec{\mathcal{A}}-\vec{\lambda},\vec{\mathcal{A}}) \tag{2.29}$$

where we keep track of the dependence on the affinities $\vec{\mathcal{A}}$ of the generating functions. The relation in Eq. (2.29) highlights how the dissipation induced by the affinities $\vec{\mathcal{A}}$ links the forward and time-reversed processes [48, 51, 102].

Furthermore, Eq. (2.29) becomes particularly useful when the forward and time-reversed probabilities as well as the extensive quantities $\vec{Q}$ entering the entropy change satisfy

$$p(b,t;a,0) = p^{\mathrm{tr}}(b,t;a,0), \qquad Q(b,t;a,0) = Q^{\mathrm{tr}}(b,t;a,0). \tag{2.30}$$

This is the case in nondriven systems in which the forward and time-reversed processes have the same initial state, $\rho(0) = \rho^{\mathrm{tr}}(0)$, and the same observable is measured twice in the two-point measurement scheme. Then, the generating function is invariant under time-reversal,

$$G_{\vec{Q}}(\vec{\lambda}, \vec{\mathcal{A}}) = G^{\mathrm{tr}}_{\vec{Q}}(\vec{\lambda}, \vec{\mathcal{A}}), \tag{2.31}$$

and Eq. (2.29) reduces to

$$G_{\vec{Q}}(\vec{\lambda}, \vec{\mathcal{A}}) = G_{\vec{Q}}(i\vec{\mathcal{A}} - \vec{\lambda}, \vec{\mathcal{A}}). \tag{2.32}$$

Crucially, this is a symmetry on the generating function of the forward process alone. It allows us to establish relations between the moments $\vec{Q}$ and their response coefficients to the affinities. Indeed, on the one hand, we perform a series expansion of the averages $\langle Q_x \rangle$ around the equilibrium point $\vec{\mathcal{A}} = 0$ as

$$\langle Q_x \rangle = \langle Q_x \rangle|_{\vec{\mathcal{A}}=0} + \sum_y L_{xy}\mathcal{A}_y + \mathcal{O}(\mathcal{A}^2) \tag{2.33}$$

where L_{xy} are the linear-response coefficients around equilibrium.

$$L_{xy} \equiv \left.\frac{\partial \langle Q_x \rangle}{\partial \mathcal{A}_y}\right|_{\vec{\mathcal{A}}=0}. \tag{2.34}$$

On the other hand, we use the relation between the moments and the generating function Eq. (2.25) and the symmetry Eq. (2.32) to expand the averages $\langle Q_x \rangle$ in a series expansion around $\vec{\mathcal{A}} = 0$ starting from the generating function. Concretely, we have

$$\begin{aligned}
\langle Q_x \rangle &= -i \left.\frac{\partial G_{\vec{Q}}}{\partial \lambda_x}\right|_{\vec{\lambda}=0} = i \left.\frac{\partial G_{\vec{Q}}}{\partial \lambda_x}\right|_{\vec{\lambda}=i\vec{\mathcal{A}}} \\
&= i \left.\frac{\partial G_{\vec{Q}}}{\partial \lambda_x}\right|_{\vec{\lambda}=\vec{\mathcal{A}}=0} + \sum_y \left(- \left.\frac{\partial^2 G_{\vec{Q}}}{\partial \lambda_x \partial \lambda_y}\right|_{\vec{\lambda}=\vec{\mathcal{A}}=0} + i \left.\frac{\partial^2 G_{\vec{Q}}}{\partial \lambda_x \partial \mathcal{A}_y}\right|_{\vec{\lambda}=\vec{\mathcal{A}}=0} \right) \mathcal{A}_y + \mathcal{O}(\mathcal{A}^2) \\
&= - \langle Q_x \rangle|_{\vec{\mathcal{A}}=0} + \sum_y \left(\langle Q_x Q_y \rangle|_{\vec{\mathcal{A}}=0} - L_{xy} \right) \mathcal{A}_y + \mathcal{O}(\mathcal{A}^2),
\end{aligned} \tag{2.35}$$

where we recognized the second moment $\langle Q_x Q_y \rangle$ and the linear response coefficient L_{xy}. Comparing the different expansions Eq. (2.33) and Eq. (2.35) term by term we find

$$\langle Q_x \rangle|_{\vec{\mathcal{A}}=0} = 0, \tag{2.36a}$$

$$\langle Q_x Q_y \rangle|_{\vec{\mathcal{A}}=0} = 2L_{xy}, \tag{2.36b}$$

for the first two terms. Unsuprisingly, Eq. (2.36a) tells us that at equilibrium there is no average change in the extensive quantities Q_x. However, Eq. (2.36b)

tells us that the *correlations* in these extensive quantities are proportional to the linear response coefficient. This statement is the celebrated fluctuation-dissipation theorem [42, 44]. Here, the "fluctuation" corresponds to $\langle Q_x Q_y \rangle|_{\vec{\mathcal{A}}=0}$, while the linear-response coefficient is connected to the dissipation happening in the system. Indeed, from Eq. (2.36b) one can directly relate the right-hand side of Eq. (2.36b) to the average entropy change

$$\sum_{x,y} \langle Q_x Q_y \rangle|_{\vec{\mathcal{A}}=0} \mathcal{A}_x \mathcal{A}_y = 2 \sum_{x,y} \mathcal{A}_x L_{xy} \mathcal{A}_y \approx 2 \sum_{x} \mathcal{A}_x \langle Q_x \rangle = 2\langle \sigma \rangle. \tag{2.37}$$

Note that, while in Eq. (2.36) we only showed how the first two moments of $\vec{Q}$ are connected to the response coefficients, one can continue the expansions in Eqs. (2.33, 2.35) to arbitrary orders and establish the so-called generalized Green-Kubo relations between higher moments and higher response coefficients [48, 50, 51]. We also stress that, since the expansions (2.33, 2.35) are centered around equilibrium, both moments and response coefficients are evaluated at the equilibrium point. Therefore, the out-of-equilibrium correlations do generally not obey the fluctuation-dissipation theorem.

Example:
Consider the bipartite system discussed in Sec. 2.2, in which the stochastic entropy change is given in Eq. (2.21). For simplicity, consider the case in which there is no temperure bias, such that we can describe the whole system with a single inverse temperature $\beta \equiv \beta_{\mathrm{L}} = \beta_{\mathrm{R}}$. Instead, the chemical potential difference $\Delta\mu \equiv \mu_{\mathrm{R}} - \mu_{\mathrm{L}}$ is nonzero. The affinity associated to the particle-number change $Q_{\mathrm{p}} = \Delta N_{\mathrm{L}}$ then reads $\mathcal{A}_{\mathrm{p}} = \beta\Delta\mu$, and the fluctuation-dissipation theorem in Eq. (2.36b) yields

$$\langle \Delta N_{\mathrm{L}}^2 \rangle\Big|_{\Delta\mu=0} = 2 \left.\frac{\partial \langle \Delta N_{\mathrm{L}} \rangle}{\partial \beta \Delta\mu}\right|_{\Delta\mu=0} = 2k_{\mathrm{B}}T \left.\frac{\partial \langle \Delta N_{\mathrm{L}} \rangle}{\partial \Delta\mu}\right|_{\Delta\mu=0}$$

where $\beta = (k_{\mathrm{B}}T)^{-1}$. In particular, if we are interested in an electronic system, the chemical potential difference is typically written in terms of the voltage bias V as $\Delta\mu = qV$, where q is the electron charge. Additionally, in the long-time limit $t \to \infty$, the average charge current $\langle I \rangle$ and its zero-frequency noise S^I are given by

$$\langle I \rangle = \frac{q\langle \Delta N_{\mathrm{L}} \rangle}{t}, \quad S^I = \frac{q^2 \langle \Delta N_{\mathrm{L}}^2 \rangle}{t}.$$

Then, the fluctuation-dissipation theorem gives the Johnson-Nyquist noise [40, 41]

$$S^I\big|_{V=0} = 2\frac{k_{\mathrm{B}}T}{R},$$

where the resistance R is given by $1/R \equiv \left.\frac{\partial \langle I \rangle}{\partial V}\right|_{V=0}$.

2.4 Trade-off relations

In the previous section we have presented the fluctuation-dissipation theorem, according to which the fluctuations at equilibrium are determined by the response coefficients. However, as discussed in Sec. 1.2, many devices operate *out of equilibrium*, and, at the nanoscale, fluctuations have a sizable impact on the performance of the device. Therefore, to understand the precision of these devices we need to evaluate the fluctuations in an out-of-equilibrium condition. Then, the simple relation between fluctuations and response of Eq. (2.36b) does not generally hold [60, 61]. However, it is still possible to estimate *how precise* these devices can possibly be by means of trade-off relations [103]. These kind of relations put an upper bound on the ratio between the average and the standard deviation of an observable. In this section, we present two topical trade-off relations: the thermodynamic uncertainty relation (TUR) [11–19] and the kinetic uncertainty relation (KUR) [20–27]. Both TUR and KUR were first derived in classical Markovian systems, and, since then, they have been and are being investigated in quantum or non-Markovian system. While both relations give an upper limit on the precision, in the thermodynamic uncertainty relation, the maximum attainable precision is given by the *dissipation*, quantified by the average entropy production. Instead, in the kinetic uncertainty relation, the upper limit on the precision is given by the *activity*, quantified by the average number of transitions. This difference makes the two relations complement each other close to and far from equilibrium. Indeed, close to equilibrium, the average dissipation is small while the activity is generally not. Thus, close to equilibrium the TUR provides a stronger constraint on the precision than the KUR. Conversely, far from equilibrium, the average dissipation is typically much larger than the activity, thereby making the KUR a stronger constraint on the precision than the TUR. This interplay between dissipation and activity has also been combined in the so-called thermokinetic uncertainty relation, which also encompasses the intermediate out-of-equilibrium regimes [104–106].

2.4.1 Thermodynamic uncertainty relation

First, we derive the TUR in the two-point measurement scheme in a purely mathematical way: Instead of using the entropy change of Eq. (2.13), we construct the proof by defining a suitable stochastic entropy change, and only afterwards we discuss the connections of this entropy to other definitions of entropy.

To begin with, we consider a "current-like" observable Q of the initial measurement outcome a and the final outcome b which is anti-symmetric with respect to the outcome order, namely

$$Q(b,t;a,0) = -Q(a,t;b,0). \tag{2.38}$$

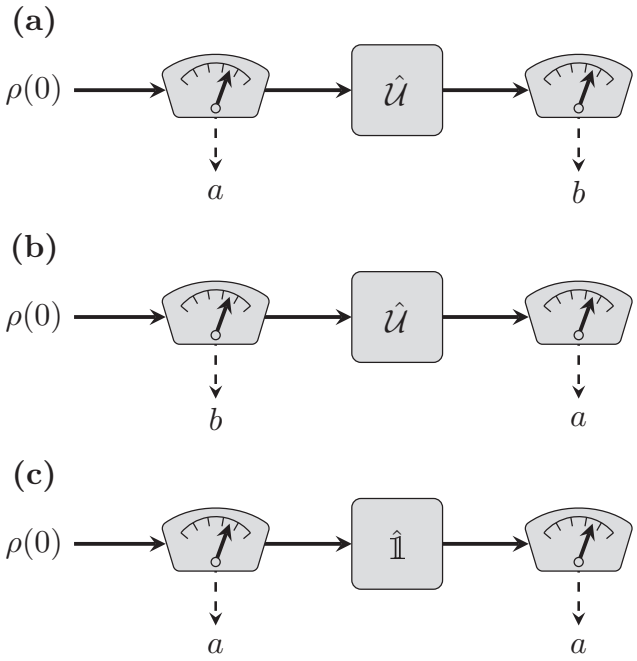

Figure 2.2: (a) *Forward process with oucomes* a, b.**(b)** *"Opposite" process. The initial state* $\rho(0)$ *undergoes the same series of measurements and unitary transformations as in the forward process, but the order of the measurement outcomes* b, a *is inverted.* **(c)** *Interrupted process in which the unitary transformation is replaced with the identity, and the measurements have the same outcome* a.

Example:
If the two measurement of the scheme measure the same operator $\hat{A} = \sum_a \lambda_a |a\rangle\langle a|$, then the change in the observed eigenvalue is a "current-like" observable,

$$Q(b, t; a, 0) = \lambda_b - \lambda_a = -Q(a, t; b, 0).$$

Given a total ordering " $\succ$ " on the outcome space $\Omega \ni a, b$, we can partition such a space according to whether the final outcome is equal, larger, or smaller than the initial outcome. This is done by defining the spaces

$$D_0 \equiv \{(a, a) | a \in \Omega\}, \quad D_{\gtrless} \equiv \left\{(b, a) \in \Omega^2 | b \gtrless a\right\}, \tag{2.39}$$

which satisfy $D_0 \cup D_\succ \cup D_\prec = \Omega^2$ and have the property

$$(a, b) \in D_\succ \Leftrightarrow (b, a) \in D_\prec.$$

Note that, because Q is anti-symmetric, it vanishes when evaluated on any element of D_0. We use the decomposition of the outcome space Ω^2 of the two measurements

together with the anti-simmetry of Q to write the first two moments of Q as

$$\begin{aligned}\langle Q\rangle &= \sum_{(b,a)\in\Omega^2} Q(b,t;a,0)p(b,t;a,0)\\ &= \sum_{(b,a)\in D_\succ} Q(b,t;a,0)\left[p(b,t;a,0)-p(a,t;b,0)\right], \qquad (2.40a)\\ \langle Q^2\rangle &= \sum_{(b,a)\in\Omega^2} [Q(b,t;a,0)]^2 p(b,t;a,0)\\ &= \sum_{(b,a)\in D_\succ} [Q(b,t;a,0)]^2\left[p(b,t;a,0)+p(a,t;b,0)\right], \qquad (2.40b)\end{aligned}$$

where we restricted the sum to the elements of $D_\succ$. Note that now the probability of the forward process sketched in 2.2(a) $p(b,t;a,0)$ appears together with the probability $p(a,t;b,0)$ which differs *only* in the order of the outcome, as depicted in 2.2(b). In particular, this latter probability is generally *not* the probability of the time-reversed process. The sum of the probabilities in Eq. (2.40b) suggests us to consider a probability distribution $w(b,a)$ defined on $D_0 \cup D_\succ$ alone as

$$w(b,a) \equiv \begin{cases} p(b,t;a,0) & \text{if} \quad (b,a)\in D_0 \\ p(b,t;a,0)+p(a,t;b,0) & \text{if} \quad (b,a)\in D_\succ \end{cases}. \qquad (2.41)$$

Essentially, while the probability p distinguishes between the order of the outcomes, w does not. Furthermore, we can write the first two moments of Q of Eq. (2.40) as averages with respect to the probability distribution w, here denoted with $\langle\bullet\rangle_w$, namely

$$\langle Q\rangle = \langle Q\tanh\left(\frac{\tilde\sigma}{2}\right)\rangle_w, \qquad (2.42a)$$

$$\langle Q^2\rangle = \langle Q^2\rangle_w, \qquad (2.42b)$$

where we introduced the entropy change $\tilde\sigma$, defined through

$$e^{\tilde\sigma} \equiv \frac{p(b,t;a,0)}{p(a,t;b,0)} \quad \to \quad \tilde\sigma(b,a) \equiv \log\left(\frac{p(b,t;a,0)}{p(a,t;b,0)}\right). \qquad (2.43)$$

Note that this entropy change $\tilde\sigma$ is generally different from the one in Eq. (2.13) because here we are not considering the time-reversed process. Instead, here the "opposite" process follows the same protocol as the forward process, but the outcomes of the measurements have opposite order. From the definition Eq. (2.43) it is immediate to see that $\tilde\sigma$ fulfils the integral fluctuation theorem

$$\langle e^{-\tilde\sigma}\rangle = 1 \quad \Rightarrow \quad \langle\tilde\sigma\rangle \geq 0, \qquad (2.44)$$

and is therefore positive on average. Furthermore, $\tilde\sigma$ is anti-symmetric

$$\tilde\sigma(b,a) = -\tilde\sigma(a,b), \qquad (2.45)$$

meaning that one can apply Eqs. (2.40, 2.42) to any odd function of $\tilde{\sigma}$.

Now that most definitions are in place, we establish the inequality at the core of the thermodynamic uncertainty relation. We start using Eq. (2.42a) to write the squared average $\langle Q\rangle^2$ as an average over the probability w. Then, we use Cauchy-Schwarz inequality,

$$\langle Q\rangle^2 = \langle Q \tanh\left(\frac{\tilde{\sigma}}{2}\right)\rangle_w^2 \leq \langle Q^2\rangle_w \langle \tanh^2\left(\frac{\tilde{\sigma}}{2}\right)\rangle_w = \langle Q^2\rangle \langle \tanh^2\left(\frac{\tilde{\sigma}}{2}\right)\rangle_w, \tag{2.46}$$

where in the last equality we used Eq. (2.42b). Furthermore, since $\tilde{\sigma}$ is anti-symmetric, from Eq. (2.42a) we also have

$$\langle \tanh\left(\frac{\tilde{\sigma}}{2}\right)\rangle = \langle \tanh^2\left(\frac{\tilde{\sigma}}{2}\right)\rangle_w. \tag{2.47}$$

Then, the trade-off relation setting an upper limit to the signal-to-noise ratio of the observable Q reads

$$\frac{\langle Q\rangle^2}{\mathrm{Var}[Q]} \leq \frac{\langle \tanh\left(\frac{\tilde{\sigma}}{2}\right)\rangle}{1-\langle \tanh\left(\frac{\tilde{\sigma}}{2}\right)\rangle}. \tag{2.48}$$

Here, the upper bound on the right-hand side is still rather complicated as it involves the average of functions of the entropy change. A simpler constraint is obtained *close to equilibrium*, i.e. when $\tilde{\sigma} \ll 1$. Then, Eq. (2.48) reduces to

$$\frac{\langle Q\rangle^2}{\mathrm{Var}[Q]} \leq \frac{\langle \tilde{\sigma}\rangle}{2}, \tag{2.49}$$

which was first proven for classical Markovian systems [11]. Therefore, close to equilibrium, the average entropy change $\langle\tilde{\sigma}\rangle$ sets a fundamental constraint on the "current-like" observables Q. In the general case in which $\tilde{\sigma} \not\ll 1$, it is still possible to write the upper limit on the precision as a function of the average entropy change as

$$\frac{\langle Q\rangle^2}{\mathrm{Var}[Q]} \leq \sinh^2\left[\frac{h(\langle\tilde{\sigma}\rangle)}{2}\right], \tag{2.50}$$

where $h(x)$ is the inverse function of $x\tanh(x/2)$ [107]. However, as mentioned before, the entropy change $\tilde{\sigma}$ entering Eqs. (2.48, 2.49, 2.50), is generally different from the entropy change defined in Eq. (2.13) by comparing the forward process with its time-reversed. An important case in which these two definitions of entropy change coincide is the one of processes invariant under time reversal. This symmetry is met when Eq. (2.30) is fulfilled, which then guarantees that the two definition of entropy change, Eq. (2.13) and Eq. (2.43), coincide. Then, one can indeed replace $\tilde{\sigma} \to \sigma$ in the TURs Eqs. (2.48, 2.49, 2.50). In this case, the TUR gives a fundamental constraint on the precision of "current-like" observables in terms of the dissipation incurred in the process. However, if the system is *not*

invariant under time reversal, which is for instance the case in the presence of feedback, then the replacement $\tilde{\sigma} \to \sigma$ cannot be done. In this case, the TUR formulations with the entropy change σ in Eq. (2.13) need to include combinations of averages on the forward and the time-reversed process [16].

Here the discussion was limited to the two-point measurement scheme. However, both classical and quantum Markovian dynamics are characterized by trajectories describing the evolution of the state in time. To treat these cases, one needs to consider a multi-measurement process, where an arbitrary number n of measurement takes place. Then, the trajectories are determined by the sequence of outcomes of such measurements, and the same procedure discussed here can be applied, see App. A.

2.4.2 Kinetic uncertainty relation

Similarly to the TUR, the kinetic uncertainty relation (KUR) emerges when we compare the probability of the forward process with a different, but similar, probability distribution. However, the comparison needed to find the KUR is *different* from the one used in Sec. 2.4.1. Indeed, for the KUR, we begin by considering the difference between the average values of the observable Q in the arbitrary probability distributions p and w on the same outcome space $\Omega \ni \omega$, namely

$$\langle Q\rangle - \langle Q\rangle_w = \int_\Omega d\omega Q(\omega)[p(\omega) - w(\omega)] = \int_\Omega d\omega [Q(\omega) - \langle Q\rangle][p(\omega) - w(\omega)]. \quad (2.51)$$

By means of Cauchy-Schwarz inequality, this difference in average Q is limited by

$$|\langle Q\rangle - \langle Q\rangle_w|^2 \leq \mathrm{Var}[Q] \int_\Omega d\omega \left(1 - \frac{w(\omega)}{p(\omega)}\right)^2 p(\omega). \quad (2.52)$$

The KUR was first derived for Markov jump systems in continuous time using Eq. (2.52) [20]. In particular, the probability distribution p describing the system is compared with the probability distribution w obtained by rescaling all the transition rates W_{ij} between states i, j of the process with a continuous parameter α, namely $W_{ij} \to (1+\alpha)W_{ij}$ [20, 108]. Then, in the limit $\alpha \to 0$, in which the original probability distribution p and the rescaled one w become infinitesimely close, Eq. (2.52) leads to

$$\frac{\left(t\langle \dot{Q}\rangle\right)^2}{\mathrm{Var}[Q]} \leq \langle K\rangle \equiv \sum_{i,j\neq i} \langle n_{ij}\rangle, \quad (2.53)$$

which is the KUR. Similarly to the TUR in Eq. (2.49), Eq. (2.53) provides an upper limit to the signal-to-noise ratio of the observable Q. The crucial difference is that the upper limit is not given by the average entropy production, but by the *activity* $\langle K\rangle$, which quantifies the average number of jumps in the time t, $\langle n_{ij}\rangle$,

between any different states i, j. In the long-time limit, where the system reaches its steady-state, the activity fulfils

$$\frac{\langle K \rangle}{t} \overset{t\to\infty}{\to} \sum_{i,j\neq i} W_{ij} p_j^{\rm ss}, \tag{2.54}$$

where $p_j^{\rm ss}$ is the steady-state probability of the system being in state j.

Generalizations of Eq. (2.53) to quantum Markovian dynamics have been established using the same rescaling technique of the rates. In the quantum case, the presence of coherent dynamics allows to achieve higher precision [22, 25, 27]. However, finding an equivalent of Eq. (2.53) in the two-point measurement scheme described in Sec. 2.1 is not straightforward because the discrete nature of the setup clashes with the (continuous) rescaling technique. Here, we attempt to establish a constraint in which, in the same spirit as the KUR in Eq. (2.53), the precision is limited by how often transitions happen. We start by comparing the two-point probability $p(b, t; a, 0)$ with the probability

$$w(b, t; a, 0) = \delta_{ab} p(a, 0) \tag{2.55}$$

corresponding to a process in which the unitary transformation between the two measurements is replaced by the identity transformation, such that both measurements have the same outcome, see 2.2(c). In contrast, the probability distribution $p(b, t; a, 0)$ generally contains transitions between different measurement outcomes. The difference between the average values of an observable Q in the two probability distributions at the left-hand side of Eq. (2.52) then reads

$$\langle Q \rangle - \langle Q \rangle_w = \sum_{b,a} [Q(b, t; a, 0) - Q(a, t; a, 0)] p(b, t; a, 0) = \langle \delta Q \rangle \tag{2.56}$$

where we introduced the change in Q due to the transition $a \to b$,

$$\delta Q(b, t; a, 0) \equiv Q(b, t; a, 0) - Q(a, t; a, 0). \tag{2.57}$$

The right-hand side of Eq. (2.52) contains the average

$$\begin{aligned} \langle \left(1 - \frac{w}{p}\right)^2 \rangle &= \sum_{b,a} \left(1 - \frac{\delta_{ba} p(a, 0)}{p(b, t; a, 0)}\right)^2 p(b, t; a, 0) \\ &= \sum_{b,a} \left(1 - \frac{\delta_{ba}}{p(b, t|a, 0)}\right)^2 p(b, t; a, 0) \\ &= \sum_{a,b\neq a} p(b, t; a, 0) + \sum_a \left(1 - \frac{1}{p(a, t|a, 0)}\right)^2 p(a, t; a, 0), \end{aligned} \tag{2.58}$$

in which we separated the contribution in which a transition happens, $a \neq b$, from the one in which the measurement yields the same outcome, $a = b$. We now

introduce the probability $\mathcal{K}(a)$ of having a transition from the initial outcome a to any other outcome $b \neq a$, namely

$$\mathcal{K}(a) \equiv 1 - p(a,t|a,0) = \sum_{b\neq a} p(b,t|a,0). \tag{2.59}$$

In terms of this probability, Eq. (2.58) becomes

$$\begin{aligned} \langle \left(1 - \frac{w}{p}\right)^2 \rangle &= \sum_a \left[\mathcal{K}(a) + \frac{\mathcal{K}^2(a)}{1-\mathcal{K}(a)}\right] p(a,0) \\ &= \sum_a \frac{\mathcal{K}(a)}{1-\mathcal{K}(a)} p(a,0). \end{aligned} \tag{2.60}$$

Then, from inequality (2.52) we find

$$\frac{\langle \delta Q \rangle^2}{\mathrm{Var}[Q]} \leq \sum_a \frac{\mathcal{K}(a)}{1-\mathcal{K}(a)} p(a,0). \tag{2.61}$$

Note that, if the observable Q vanishes on the realizations in which no transition occur, then $\delta Q = Q$, and Eq. (2.61) provides a limit on the precision of Q. Here, the maximum attainable precision is given in terms of the probability $\mathcal{K}(a)$ of experiencing a transition from the outcome a. Interestingly, a similar probability has recently been used to limit the precision in quantum thermal machines [109, 110]. Furthermore, when the transition probability is small, $\mathcal{K}(a) \ll 1$, we can approximate Eq. (2.61) as

$$\frac{\langle \delta Q \rangle^2}{\mathrm{Var}[Q]} \leq \sum_a \mathcal{K}(a) p(a,0) = \mathcal{K}, \tag{2.62}$$

where $\mathcal{K} \equiv \sum_{a,b\neq a} p(b,t;a,0)$ is the probability of a transition happening. Here, the similarity with the KUR is more clear. Indeed, in Eq. (2.53) the upper limit on the precision is given by the number of jumps between any two different states, and in Eq. (2.62) is given by the probability of a transition between any two different outcomes. In this sense, both Eq. (2.53) and Eq. (2.62) provide a limit on the precision which is given how "active" a system is. However, they are not equivalent because the KUR of Eq. (2.53) relies on a state trajectory in the full time interval of the process, whereas the constraint of Eq. (2.61) is based on a state trajectory that consists of only two points. To see whether a connection between the two can be established, extending Eq. (2.61) to the multi-measurement process discussed in App. A is necessary.

2.5 Two-point measurement and transport

In this section we discussed the two-point measurement scheme as a way to access the statistics of a quantum process. By comparing different variations of

such processes, e.g. the forward and the time-reversed ones, fluctuation theorems are established. These results are then used to prove the fluctuation-dissipation theorems and trade-off relations on the precision.

In the following chapter, we use the two-point measurement scheme as a lens through which we describe quantum transport setups. In the appended papers, the out-of-equilibrium fluctuations in such transport setups are studied, but they are not discussed from the two-point measurement point of view. In this thesis, we instead show how the same statistics is obtained from the two-point measurement framework. This connection between two-point measurement scheme and quantum transport allows us to borrow some of the ideas and techiques discussed in this section and apply them to transport. For instance, Papers I-IV are based on the comparison between two variations of the same process. However, instead of comparing the forward and the time-reversed process, we compare a process that starts in a state where a temperature bias is present to the same process starting from the state in which the temperature bias is absent. This results in constraints between the noise and the current that complement the fluctuation-dissipation theorem discussed in Sec. 2.3 to out-of-equilibrium regimes. Furthermore, in Paper V we establish trade-off relations between entropy production and noise. Later, in Paper VI, we used the results of Paper V to establish a limit on the precision of currents in a quantum transport setup. Here, the maximum attainable precision is determined by the particle current noise. Intuitively, the particle current noise accounts for the transitions in the number of transferred particles. For this reason, it plays a similar role to the activity discussed for the KUR in Sec. 2.4.2 in a quantum transport setup.

3 Statistics in quantum transport

This chapter is dedicated to the theoretical frameworks used in the appended papers to describe transport, namely scattering theory and the perturbative approach. These frameworks have been used extensively in the field of quantum transport, where a lot of emphasis is placed on the current operator. In this chapter, we provide equivalent formulations of such frameworks focusing instead on the outcomes of a two-point measurement scheme, thereby bridging the formalism described in Sec. 2 with the ones of quantum transport.

First, in Sec. 3.1, we provide an alternative description of the scattering theory introduced by Landauer and Büttiker in Refs. [111–113]. This approach relies on large coherence length (compared to the size of the device), and weak particle-particle interaction. These assumptions allow to consider single-particle wavefunctions propagating on a potential landscape, meaning that the full unitary evolution of the system can be "broken down" in a composition of single-particle evolutions. Typically, this framework is formulated in second quantization, and the average and correlations between current operators are calculated from the expectation values of the field operators describing incident particle fluxes. We refer to this approach as the "traditional" approach from now on. Here, instead, we first obtain the density matrix of the system, and then use it to calculate the conditional probabilities of finding n particles in the final state *given* a specific initial state. These probabilities are then used to calculate the average and the variance of the *change of particle number*, leading to the same results as the traditional approach. Even though this approach gets to the same results in a more complicated way, it also allows us to look into the entropy production at different stages of the process, which is typically hard to describe within the traditional approach, but highly relevant in the context of quantum thermodynamics.

In Sec. 3.2, we describe a different, yet common, theoretical approach to quantum transport, namely a perturbative approach for weak coupling. Again, we describe it through the lens of the two-point measurement scheme. This approach relies on having a weak coupling, which allows for a perturbative expansion. This means that the full unitary evolution of the system can be approximated up to the lowest order in the coupling strength. In contrast with scattering theory, where the coupling can be strong but particle-particle interactions are negligible, here the particle-particle interactions can be strong. Similarly to Sec. 3.1, we first calculate the transition probabilities conditioned on an initial state and then study the statistics of the change in an observable.

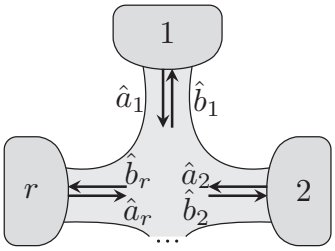

Figure 3.1: *Sketch of r leads connecting r reservoirs (labeled $1, 2, \ldots, r$) to a central scatterer. The coherent scattering of incoming particle fluxes in the leads, described by the field operators $\hat{a}_\alpha$, maps them into outgoing particle fluxes, described by the field operators $\hat{b}_\alpha$.*

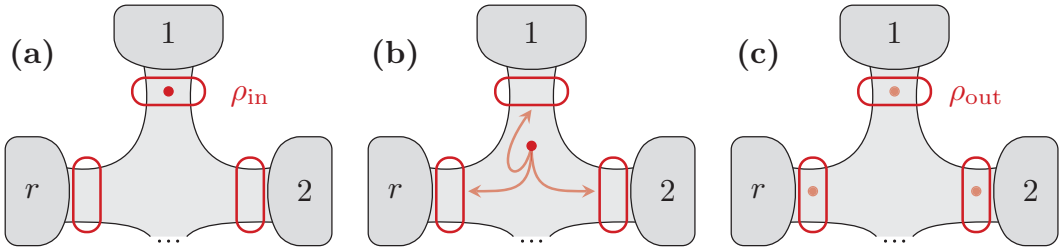

Figure 3.2: *Single-shot description of a scattering event. The incoming particles in the leads, highlighted by the red boxes, described by the state ρ_{in}* **(a)** *enter the central conductor where they scatter coherently* **(b)**. *After the scattering event, the outgoing particles in the leads are described by the state ρ_{out}* **(c)**.

3.1 Scattering theory revisited

The setup of scattering theory consists of r leads (labeled with greek letters $\alpha, \beta, \ldots$) connected to a central conductor, where the scattering process takes place. Furthermore, lead α supports M_α different transport channels (labeled with roman letters $i, j, \ldots$).

In the stationary case, an incoming particle to the scattering region at energy E is eventually scattered into an outgoing particle at the same energy. In the field-theoretical approach to scattering theory, one associates the field operators $\hat{a}_{\alpha i}(E)$ and $\hat{b}_{\alpha i}(E)$ to the incoming and outgoing particle fluxes in lead α and channel i, respectively, see Fig. 3.1. Then, the scattering process relates such field operators through

$$\hat{b}_{\alpha i}(E) = \sum_{\beta j} s_{\alpha i,\beta j}(E)\hat{a}_{\beta j}(E), \tag{3.1}$$

where $s(E)$ is a unitary matrix referred to as *scattering matrix*. This matrix describes the evolution of a single-particle state. With these key ingredients one can calculate the average of the current operator and its correlations. Note that these ingredients do not include the density matrix of the system, which is somehow hidden in the traditional approach. Here, we want to explicitely show how the

density matrix enters these calculations, and also use it to understand entropy production in these coherent systems. To this end, instead of focusing on the fields of incoming and outgoing particle fluxes, we focus on the state of the particles in the leads before and after the scattering process. We consider the Fock space of particles in the leads at a *specific energy* E, which, from now onward, is not specified unless needed. Calling the empty state, namely the state with no particles,

$$|\varnothing\rangle \equiv |\underbrace{0\cdots0}_{M_1}\cdots\underbrace{0\cdots0}_{M_r}\rangle\,, \tag{3.2}$$

we write all other states through the application of the creation operators $\hat{c}^\dagger_{\alpha i}$

$$\left([\hat{c}^\dagger_{\alpha_1 i_1}]^{n_{\alpha_1 i_1}}\cdots[\hat{c}^\dagger_{\alpha_k i_k}]^{n_{\alpha_k i_k}}\right)|\varnothing\rangle = |0\cdots0 n_{\alpha_1 i_1}\cdots n_{\alpha_k i_k}0\cdots0\rangle\,. \tag{3.3}$$

Here, we distinguish the operators $\hat{c}_{\alpha i}$ from the previously discussed $\hat{a}_{\alpha i}, \hat{b}_{\alpha i}$ because the former describe annihilation of particles, while the latter describe annihilation of particle fluxes.

Note that, if the considered particles are fermions, then $n_{\alpha_k i_k} \in \{0,1\}$, whereas they can be any natural number for bosons. Furthermore, the states in Eq. (3.3) are not normalized (for bosons), but have norm

$$\langle 0\cdots0 n_{\alpha_1 i_1}\cdots n_{\alpha_k i_k}0\cdots0|0\cdots0 n_{\alpha_1 i_1}\cdots n_{\alpha_k i_k}0\cdots0\rangle = (n_{\alpha_1 i_1}!)\cdots(n_{\alpha_k i_k}!). \tag{3.4}$$

Now that we have specified a basis, we can write any possible density matrix of the leads. In Sec. 3.1.1, we will see that the density matrix contains too much information when it comes to calculating the particle current and its noise. However, in Sec. 3.1.2 this additional information is instrumental for understanding the correlation entropy produced by the scattering event, and how this relates to the thermodynamic entropy production.

Example:
For two single-channel fermionic leads, i.e. $r = 2$ and $M_1 = M_2 = 1$, we can drop the channel index and write the basis of the Fock space as

$$|\varnothing\rangle = |00\rangle\,,\quad c_1^\dagger|\varnothing\rangle = |10\rangle\,,\quad c_2^\dagger|\varnothing\rangle = |01\rangle\,,\quad c_1^\dagger c_2^\dagger|\varnothing\rangle = -c_2^\dagger c_1^\dagger|\varnothing\rangle = |11\rangle\,,$$

where the basis states correspond to the following sketches.

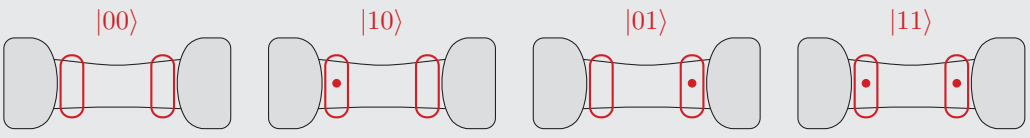

Crucially, the scattering process transforms an initial density matrix ρ_{in}, which describes the state of the incoming particles in the leads, into a final density

matrix ρ_{out}, which describes the state of the outgoing particles in the leads, as depicted in Fig. 3.2. Analogously to Eq. (3.1), the scattering process evolves the state by mapping the creation operators into the linear superposition,

$$\hat{c}^\dagger_{\alpha i} \to \sum_{\beta j} s_{\beta j,\alpha i} \hat{c}^\dagger_{\beta j} \tag{3.5}$$

determined by the scattering matrix. Intuitively, Eq. (3.5) describes a particle in αi evolving into a superposition over all other leads and channels, whose amplitudes are determined by the scattering matrix. The single-particle evolution of Eq. (3.5) is then used to evolve any multi-particle state through

$$\prod_x [\hat{c}^\dagger_{\alpha_x i_x}]^{n_x} |\varnothing\rangle \to \prod_x \left[\sum_{\beta j} s_{\beta j,\alpha_x i_x} \hat{c}^\dagger_{\beta j}\right]^{n_x} |\varnothing\rangle \,. \tag{3.6}$$

Example:
For two single-channel fermionic leads, the empty state is left unchanged,

$$|00\rangle \to |00\rangle \,,$$

as there are no fermions to scatter. The remaining basis vectors evolve according to

$$|10\rangle \to s_{11} |10\rangle + s_{21} |01\rangle \,, \quad |01\rangle \to s_{12} |10\rangle + s_{22} |01\rangle \,, \quad |11\rangle \to \det(s) |11\rangle \,,$$

where the unitarity of s guarantees the normalization. These evolutions can also be represented as the following sketches, where the solid (dashed) arrows represent transmission (reflection) processes.

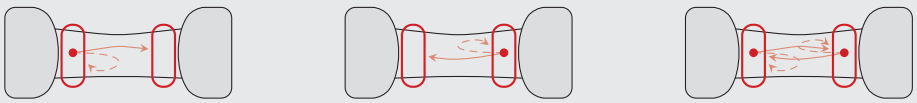

Therefore, given any initial state ρ_{in}, we can calculate the final state ρ_{out} by means of Eq. (3.6). The initial states that we consider here are diagonal in the number basis and uncorrelated between different channels. This assumption is in particular verified when each lead is connected to a thermal reservoir of temperature T_α and chemical potential μ_α. These reservoirs "prepare" the initial state by (probabilistically) injecting particles into the leads. In this case of thermal reservoirs, the average occupation number $f_\alpha(E)$ of the reservoir fully determines the distribution of the initial state and is given by the Fermi or Bose distribution

$$f_\alpha(E) = \frac{1}{\exp\left[\frac{E-\mu_\alpha}{k_B T_\alpha}\right] \pm 1} \tag{3.7}$$

for fermions (upper sign) and bosons (lower sign), respectively. In particular, for fermions each channel of lead α is occupied with probability f_α, and is empty with probability $1-f_\alpha$. Instead, for bosons the probability of having n particles in a channel of lead α is proportional to $\exp\left[-n\frac{E-\mu_\alpha}{k_\mathrm{B}T_\alpha}\right] = \left[\frac{f_\alpha}{1+f_\alpha}\right]^n$. These simple initial states make the calculatiions of the particle current and its noise easier, as we will show in Sec. 3.1.1.

Example:
For two single-channel fermionic leads connected to reservoirs described by the average occupation $f_\alpha \in [0,1]$, the initial state is a mixture of the possible number basis states weighted by the joint probabilities, i.e.

$$\rho_\mathrm{in} = f_1^- f_2^- \,|00\rangle\langle 00| + f_1 f_2^- \,|10\rangle\langle 10| + f_1^- f_2 \,|01\rangle\langle 01| + f_1 f_2 \,|11\rangle\langle 11|\,,$$

where $f_\alpha^- \equiv 1-f_\alpha$. By evolving the initial state one finds the final state

$$\rho_\mathrm{out} = \left(\begin{array}{c|cc|c} f_1^- f_2^- & 0 & 0 & 0 \\ \hline 0 & f_1 f_2^- |s_{11}|^2 + f_2 f_1^- |s_{12}|^2 & f_1 f_2^- s_{11}s_{21}^* + f_2 f_1^- s_{12}s_{22}^* & 0 \\ 0 & f_1 f_2^- s_{11}^* s_{21} + f_2 f_1^- s_{12}^* s_{22} & f_1 f_2^- |s_{21}|^2 + f_2 f_1^- |s_{22}|^2 & 0 \\ \hline 0 & 0 & 0 & f_1 f_2 \end{array}\right),$$

where we highlighted the block structure corresponding to different amounts of total number of particles.

Even with these assumptions on the initial states, the full density matrix contains too much information if one is interested in properties of a single lead like, for instance, the particle current flowing in a lead γ. It is therefore convenient to consider the marginal state on such a lead. In particular, given an initial state with k particles in the leads $\overrightarrow{\alpha i} \equiv (\alpha_1 i_1, \cdots, \alpha_k i_k)$, the final state *conditioned* on such an initial state $\overrightarrow{\alpha i}$, $\rho_{\mathrm{out}|\overrightarrow{\alpha i}}$, is obtained according to Eq. (3.6),

$$|\overrightarrow{\alpha i}\rangle\langle\overrightarrow{\alpha i}| \equiv \left(\hat{c}^\dagger_{\alpha_1 i_1} \cdots \hat{c}^\dagger_{\alpha_k i_k}\right) |\varnothing\rangle\langle\varnothing| \left(\hat{c}_{\alpha_k i_k} \cdots \hat{c}_{\alpha_1 i_1}\right) \to \rho_{\mathrm{out}|\overrightarrow{\alpha i}}. \tag{3.8}$$

Then, we need to reduce this state $\rho_{\mathrm{out}|\overrightarrow{\alpha i}}$ to lead γ. The marginal state on lead γ is obtained by tracing out all other leads, namely

$$\rho_{\gamma|\overrightarrow{\alpha i}} \equiv \mathrm{Tr}_{\overline{\gamma}}\left\{\rho_{\mathrm{out}|\overrightarrow{\alpha i}}\right\}, \tag{3.9}$$

where $\overline{\gamma}$ represents the complement to γ. Particle number conservation of the scattering evolution makes this reduced density matrix have a block-diagonal structure in the Fock subspaces, i.e.

$$\rho_{\gamma|\overrightarrow{\alpha i}} = \begin{pmatrix} \rho_{\gamma,0|\overrightarrow{\alpha i}} & 0 & \cdots \\ 0 & \rho_{\gamma,1|\overrightarrow{\alpha i}} & \cdots \\ \vdots & \vdots & \ddots \end{pmatrix}, \tag{3.10}$$

where $\rho_{\gamma,n|\overrightarrow{\alpha i}}$ is the block in the subspace with n particles. If one is interested in the correlations that the scattering event generates between different channels, then all the entries of these block-matrices carry relevant information. However, if one is interested in the particle current, only the probability $p_{n|\overrightarrow{\alpha i}}$ of finding n particles in the final state given the initial state $\overrightarrow{\alpha i}$ matters. This probability is simply given by the trace of the corresponding matrix block, i.e.

$$p_{n|\overrightarrow{\alpha i}} = \mathrm{Tr}\left\{\rho_{\gamma,n|\overrightarrow{\alpha i}}\right\}. \tag{3.11}$$

The difference between fermionic and bosonic statistics is reflected in this conditional probability, which reads

$$\begin{aligned} p_{n|\overrightarrow{\alpha i}} = \frac{1}{\langle\overrightarrow{\alpha i}|\overrightarrow{\alpha i}\rangle\, k!}\binom{k}{n}\sum_{\sigma,\sigma'\in\mathcal{S}_k}\Bigg\{(\mp 1)^{\sigma+\sigma'}\left[\prod_{\xi=1}^{n}\left(\sum_l s_{\gamma l,\sigma(\alpha_\xi i_\xi)}s^*_{\gamma l,\sigma'(\alpha_\xi i_\xi)}\right)\right]\times \\ \times\left[\prod_{\xi=n+1}^{k}\left(\delta_{\sigma(\alpha_\xi i_\xi)\sigma'(\alpha_\xi i_\xi)} - \sum_l s_{\gamma l,\sigma(\alpha_\xi i_\xi)}s^*_{\gamma l,\sigma'(\alpha_\xi i_\xi)}\right)\right]\Bigg\}, \end{aligned} \tag{3.12}$$

where the upper/lower sign refers to fermions/bosons. A detailed derivation of Eq. (3.12) is found in App. B. Here, $\mathcal{S}_k$ is the group of permutation of k elements, and $(-1)^\sigma$ indicates the sign of the permutation σ. In Eq. (3.12) the first product represents the distribution of n of the initial k particles in any channel l of lead γ, whereas the second product represents the distribution of the remaining $k-n$ particles in any other lead. In the last product, the unitarity of the scattering matrix s was used. The prefactor $\langle\overrightarrow{\alpha i}|\overrightarrow{\alpha i}\rangle^{-1}$ is needed to normalize the initial state (in the bosonic case, since it is always 1 in the fermionic case), while $\frac{1}{k!}\binom{k}{n}$ removes the double-counting encountered when we permute the n particles that ended up in lead γ or the $k-n$ particles in the remaining leads.

To calculate expectation values over the conditional probability Eq. (3.12) it is convenient to exploit the recursive relation

$$p_{n|\overrightarrow{\alpha i}} = \frac{1}{k-n}\sum_{x=1}^{k} p_{n|\overrightarrow{\alpha i}\setminus\{\alpha_x i_x\}} - \frac{n+1}{k-n}p_{n+1|\overrightarrow{\alpha i}}, \qquad \text{for} \quad n<k, \tag{3.13}$$

fulfilled by both fermions and bosons. The derivation of Eq. (3.13) and its use in calculating the average number and variance of transferred particles is found in App. B. Note that this relation is recursive both in the number n of particles in lead γ after the scattering process, and in the number k of particles in the initial state. Indeed, Eq. (3.13) contains the probability $p_{n+1|\overrightarrow{\alpha i}}$ of ending up with $n+1$ particles after the scattering process given the same initial state. Furthermore, it also contains the probability $p_{n|\overrightarrow{\alpha i}\setminus\{\alpha_x i_x\}}$ which is conditioned on the initial state $\overrightarrow{\alpha i}\setminus\{\alpha_x i_x\} = (\alpha_1 i_1, \cdots, \alpha_{x-1} i_{x-1}, \alpha_{x+1} i_{x+1}, \cdots, \alpha_k i_k)$ obtained by

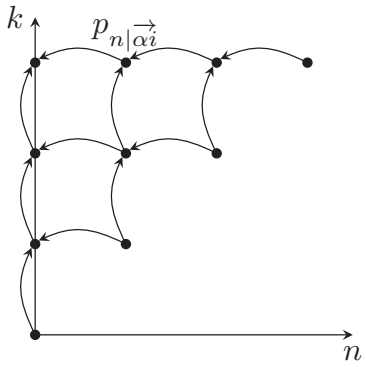

Figure 3.3: *Schematic representation of the recursive relation Eq. (3.13) for the probability $p_{n|\overrightarrow{\alpha i}}$ of ending with n particles given the initial state $\overrightarrow{\alpha i}$ containing k particles. Particle number conservation implies that for $n > k$ the probability vanishes. For $n < k$, $p_{n|\overrightarrow{\alpha i}}$ is determined by the "adjacent" probabilities $p_{n+1|\overrightarrow{\alpha i}}$ and by $p_{n|\overrightarrow{\beta j}}$, with $\overrightarrow{\beta j}$ containing $k-1$ particles, as indicated by the arrows. The boundary condition of the recursive relation is set by the probabilities on the diagonal, i.e. $n = k$.*

removing one of the initial particles. Therefore, the initial state of this conditional probability has $k-1$ particles. This means that, if one knows the conditional probability $p_{m|\overrightarrow{\beta j}}$ for all m and for all initial states $\overrightarrow{\beta j}$ with $k-1$ particles, and the probability $p_{k|\overrightarrow{\alpha i}}$ conditioned on the initial state $\overrightarrow{\alpha i}$ with k particles, then we can recursively calculate all the conditional probabilities $p_{n|\overrightarrow{\alpha i}}$. The recursive procedure is schematically depicted in Fig. 3.3, and turns out to be particularly useful to calculate the expectation values of quantities like, for instance, the change in particle number induced by the scattering process and its variance, as shown in App. B.

3.1.1 Current and noise

Now that we have the probabilities of having n scattered particles in a specific lead γ, we can study the statistics of the net amount of particles flowing into one lead by studying the change in the lead particle number before and after the scattering process. To access this change it is natural to measure the particle number before and after the scattering process. This corresponds to a two-point measurement scheme with the following protocol:

1. We measure the particle number in a given lead γ, i.e. the observable $\hat{N}_\gamma = \sum_i \hat{c}^\dagger_{\gamma i}\hat{c}_{\gamma i}$, on the initial state ρ_{in}. We call $N_{\text{in},\gamma}$ the outcome of the measurement occuring with probability $P(N_{\text{in},\gamma})$ and label $\rho_{\text{in}|N_{\text{in},\gamma}}$ the corresponding state conditioned on the outcome of the measurement.

2. The system undergoes the scattering process, which transforms the initial

state $\rho_{\text{in}|N_{\text{in},\gamma}}$ into the output state $\rho_{\text{out}|N_{\text{in},\gamma}}$ according to Eq. (3.6).

3. We measure again the particle number $\hat{N}_\gamma$ in lead γ on the scattered state $\rho_{\text{out}|N_{\text{in},\gamma}}$. We call $N_{\text{out},\gamma}$ the outcome of the measurement occuring with probability $P(N_{\text{out},\gamma}|N_{\text{in},\gamma})$.

We are then interested in the statistics of the stochastic variable $Q_\gamma \equiv N_{\text{out},\gamma} - N_{\text{in},\gamma}$, which counts the net amount of particles flowing into lead γ on a single realization of the protocol. In general, the average of Q_γ is given by

$$\langle Q_\gamma \rangle = \sum_{N_{\text{out},\gamma}, N_{\text{in},\gamma}} (N_{\text{out},\gamma} - N_{\text{in},\gamma}) P(N_{\text{out},\gamma}|N_{\text{in},\gamma}) P(N_{\text{in},\gamma}), \tag{3.14}$$

and its variance by

$$\text{Var}\,[Q_\gamma] = \sum_{N_{\text{out},\gamma}, N_{\text{in},\gamma}} (N_{\text{out},\gamma} - N_{\text{in},\gamma})^2 P(N_{\text{out},\gamma}|N_{\text{in},\gamma}) P(N_{\text{in},\gamma}) - \langle Q_\gamma \rangle^2. \tag{3.15}$$

Then, given any initial state ρ_{in}, we can apply the two-point measurement protocol combined with the scattering evolution to find the statistics of the observable Q_γ As mentioned previously, a relevant choice of initial state is given by the states "prepared" by thermal reservoirs, which randomly inject uncorrelated particles in the leads. These initial states take the form

$$\rho_{\text{in}} = \bigotimes_{\beta j} \left(\sum_{n_{\beta j}} p_{n_{\beta j}} \frac{|n_{\beta j}\rangle\langle n_{\beta j}|}{\langle n_{\beta j}|n_{\beta j}\rangle} \right) \tag{3.16}$$

where the tensor product spans over the different leads and channels. Here, $p_{n_{\beta j}}$ is the probability of injecting $n_{\beta j}$ particles in lead β, channel j. Clearly, for fermions we have only two possible values of $n_{\beta j}$, namely $n_{\beta j} \in \{0, 1\}$, whereas for bosons any possible natural number is admissible, $n_{\beta j} \in \mathbb{N}$. We furthermore consider the case in which the injection probability $p_{n_{\beta j}}$ does not depend on the specific channel in the lead. For fermions, the probability of injecting one particle corresponds to the average occupation of the reservoir at the energy E that we are considering, given by $f_\beta(E) \in [0, 1]$, namely

$$p_{n_{\beta j}=1} = f_\beta(E). \tag{3.17}$$

The probability of injecting zero particles is then given by $p_{n_{\beta j}=0} = 1 - f_\beta(E)$. In the thermal case, the average particle number $f_\beta(E)$ over different energies is given by the Fermi distribution of Eq. (3.7) (upper sign). Instead, for bosons the probability of injecting $n_{\beta j}$ is related to the average particle number $f_\beta(E) \geq 0$ through

$$p_{n_{\beta j}} = \frac{1}{1 + f_\beta(E)} \left[\frac{f_\beta(E)}{1 + f_\beta(E)} \right]^{n_{\beta j}}. \tag{3.18}$$

This exponential behaviour with respect to the particle number is understood by considering, at the chosen energy E, a thermal reservoir with temperature $T_\beta(E)$ and chemical potential $\mu_\beta(E)$ which are specific to that energy. In turn, this means that particles in each energy interval dE interact with different thermal reservoirs, and across different energies the average occupation number $f(E)$ is generally nonthermal. However, if these intensive parameters of the reservoir are energy-independent, then $f_\beta(E)$ is given by the Bose distribution of Eq. (3.7) (lower sign). Note that, given the initial occupation probabilities Eqs. (3.17, 3.18), the variance of the initial particle number is given in terms of the average number of particles $f_\beta(E)$ through

$$\mathrm{Var}[n_{\beta j}] = f_\beta(E)[1 \mp f_\beta(E)], \tag{3.19}$$

where the upper/lower sign refers to fermions/bosons.

With these assumptions on the initial state, we can calculate the average and the variance of the number of transferred particles Q_γ, see App. B for the detailed derivations. Here, it is convenient to write the results in terms of the scattering submatrices $t_{\alpha\beta}$ which map the M_β channels of lead β into the M_α channels of lead α according to $[t_{\alpha\beta}]_{ij} = s_{\alpha i,\beta j}$. In particular, the scattering matrix s is written in terms of the submatrices $t_{\alpha\beta}$ with the following block structure

$$s = \begin{pmatrix} t_{11} & t_{12} & \cdots & t_{1r} \\ t_{21} & t_{22} & \cdots & t_{2r} \\ \vdots & \vdots & \ddots & \vdots \\ t_{r1} & t_{r2} & \cdots & t_{rr} \end{pmatrix}. \tag{3.20}$$

Indeed, in terms of the submatrices $t_{\alpha\beta}$, the average number of transferred particles reads

$$\langle Q_\gamma \rangle = \sum_\alpha \mathrm{Tr}\left\{ t_{\gamma\alpha} t_{\gamma\alpha}^\dagger \right\} (f_\alpha - f_\gamma) \tag{3.21}$$

for both fermions and bosons. Instead, the variance of the transferred particle number displays a difference between them beyond the difference in the average occupation number, namely

$$\begin{aligned} \mathrm{Var}[Q_\gamma] = &\sum_{\alpha\neq\gamma} \mathrm{Tr}\left\{ t_{\gamma\alpha} t_{\gamma\alpha}^\dagger \right\} [f_\alpha(1 \mp f_\gamma) + f_\gamma(1 \mp f_\alpha)] + \\ &\mp \sum_{\alpha\beta} \mathrm{Tr}\left\{ t_{\gamma\alpha} t_{\gamma\alpha}^\dagger t_{\gamma\beta} t_{\gamma\beta}^\dagger \right\} [f_\alpha - f_\gamma][f_\beta - f_\gamma]. \end{aligned} \tag{3.22}$$

Here, the different signs for fermions and bosons (upper and lower, respectively) emerge not only because of the different sign in the variance of the initial particle number, see Eq. (3.19), but also because of the difference in the exchange statistics during the scattering process, see Eq. (3.12). In particular, the sign of the last contribution in Eq. (3.22) reflects the anti-bunching and bunching of fermionic and bosonic particles, respectively.

This description essentially focuses on "single-shot" scattering events, where an initial state is prepared and then scattered. To finally complete the connection to Landauer-Büttiker scattering theory we need to find the average current and its noise from this single-shot description. Here, it is important to note that the lack of particle-particle interaction guarantees the independence between different scattering events. Therefore, it is sufficient to know *how many* of such events occur in a unit time. We now assume that all the particles in the infinitesimal energy interval $[E, E + dE]$ around the energy E that we are focusing on move with velocity $v(E)$. Then, the charge current is the energy interval is $d\mathcal{I}_\gamma = qv(E)Q_\gamma(E)g(E)dE$, with $g(E)$ being the density of states. In the one-dimensional leads the density of states is $g(E) = [hv(E)]^{-1}$ [114]. This makes the charge current in the infinitesimal energy interval take the simple form

$$d\mathcal{I}_\gamma(E) = \frac{q}{h} Q_\gamma(E) dE. \tag{3.23}$$

The total current $\mathcal{I}_\gamma$ is then obtained by integrating over the energy, and its average value reads

$$I_\gamma \equiv \langle \mathcal{I}_\gamma \rangle = \frac{q}{h} \int dE \langle Q_\gamma \rangle = \frac{q}{h} \int dE \sum_\alpha \mathrm{Tr} \left\{ t_{\gamma\alpha} t_{\gamma\alpha}^\dagger \right\} (f_\alpha - f_\gamma), \tag{3.24}$$

which is the Landauer-Büttiker formula. Here, the trace $\mathrm{Tr}\left\{t_{\alpha\gamma} t_{\alpha\gamma}^\dagger\right\}$ is the transmission from lead α to lead γ accounting for all possible channels. In the single-channel case this transmission is simply the probability of being transmitted from α to γ.

Furthermore, the statistical independence between different scattering events allows to write the zero-frequency noise of the charge current in terms of the variance of the transferred particle number through

$$S_{\gamma\gamma}^I = \frac{q^2}{h} \int dE \mathrm{Var}[Q_\gamma], \tag{3.25}$$

as detailed in App. C. Again, as expected, this coincides with the zero-frequency noise obtained with the traditional approach [114].

The same procedure can be applied to the transport of a possibly energy-dependent observable X trasferred by the particles, as is the case for energy and heat currents. To do so, we just need to replace the charge q with the energy-dependent quantity $x(E)$ carried by each particle under the integration signs. Then, the average current of X and its noise read

$$I_\gamma^{(X)} = \frac{1}{h} \int dE x(E) \langle Q_\gamma \rangle, \tag{3.26a}$$

$$S_{\gamma\gamma}^{(X)} = \frac{1}{h} \int dE [x(E)]^2 \mathrm{Var}[Q_\gamma]. \tag{3.26b}$$

Classical and quantum noise contributions

Clearly, the noise is more cumbersome to work with compared to the average currents. To simplify the treatment of the zero-frequency noise, we split it into two terms, a "classical" and a "quantum" contribution, given by

$$S_{\gamma\gamma}^{(X),\mathrm{cl}} = \frac{1}{h}\sum_{\alpha\neq\gamma}\int dE[x(E)]^2 \mathrm{Tr}\left\{t_{\gamma\alpha}t_{\gamma\alpha}^\dagger\right\}\left[f_\alpha(1\mp f_\gamma)+f_\gamma(1\mp f_\alpha)\right], \tag{3.27a}$$

$$S_{\gamma\gamma}^{(X),\mathrm{qu}} = \mp\frac{1}{h}\sum_{\alpha\beta}\int dE[x(E)]^2 \mathrm{Tr}\left\{t_{\gamma\alpha}t_{\gamma\alpha}^\dagger t_{\gamma\beta}t_{\gamma\beta}^\dagger\right\}\left[f_\alpha - f_\gamma\right]\left[f_\beta - f_\gamma\right], \tag{3.27b}$$

respectively. The classical contribution is quadratic in the scattering matrix elements, and is therefore linear in the transmission probability between different leads. Instead, the quantum contribution is quadratic in the transmission probability. This means that, in the tunneling regime, i.e. when the transmission probability is small, the classical contribution to the noise approximates the full noise well. Furthermore, the quantum contribution is negligible compared to the classical one also close to equilibrium, i.e. when $f_\alpha \approx f_\beta$, even far from the tunneling regime. Indeed, at equilibrium the noise is given by the classical contribution only, which also fulfils the fluctuation-dissipation theorem discussed in Sec. 2.3. When both the tunneling regime and the close to equilibrium condition are *not* fulfilled, the quantum contribution of Eq. (3.27b) to the noise needs to be accounted for. This strongly-coupled, out-of-equilibrium condition is interesting when studying the effect of quantum phenomena (in this case particle intereference) on the performance of thermal machines. In particular, the noise, and therefore the precision, of such machines is affected significantly. Within this context, Papers III, V, VI provide constraint on such out-of-equilibrium noise which also include the quantum noise contribution Eq. (3.27b), thereby establishing limits on the current precision in devices described by scattering theory. Furthermore, from Eq. (3.27b) we already see a crucial difference between fermions and bosons: The quantum contribution to the noise is negative for fermions and positive for bosons. This reflects the anti-bunching/bunching properties of the particles. Indeed, the integrand in Eq. (3.27b) emerges from the exchange statistics in scattering processes with two particles.

Note that, while the distinction between classical and quantum contribution to the noise is appealing from both a technical and a conceptual point of view, it is by no means the only way to split the noise in multiple contributions. Indeed, depending on the context and the system considered, splitting the noise in different contributions, as, for instance, thermal and shot noise, may be more useful. This is indeed the case in Papers I-III. However, only the full noise can typically be accessed experimentally, so it is important to note that statements on a single contribution may not apply to the full noise unless that contribution dominates over the other.

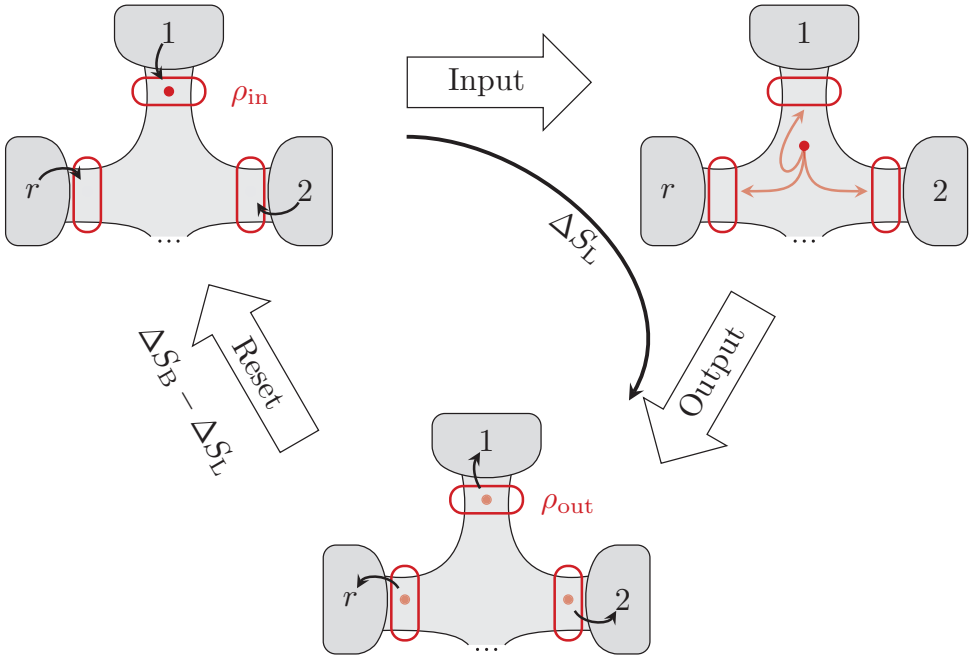

Figure 3.4: *The input state ρ_{in} is prepared by the baths $1, 2, \cdots, r$ and enters the central conductor, where the scattering process happens. After the scattering, the output state ρ_{out} is established in the leads, where it then couples to the baths. The baths reset the output state into the input state to close the cycle. In the scattering process the entropy ΔS_L is produced in the leads. In the reset process the entropy $-\Delta S_L$ is produced in the leads, and the entropy ΔS_B is generated in the baths.*

3.1.2 Entropy production and fluctuations

Now that we have access to the input and output density matrices, we can study how the von Neumann entropy of such states behaves, and how this entropy change relates to the thermodynamic entropy production in the baths. Since the scattering evolution between initial and final states is unitary, the von Neumann entropy of the input state ρ_{in} and output state ρ_{out} coincide, i.e.

$$S_{\text{vN}}[\rho_{\text{in}}] = S_{\text{vN}}[\rho_{\text{out}}]. \tag{3.28}$$

However, the scattering process creates correlations between different leads. This means that, if one focuses on the marginal state on one specific lead, say γ, i.e. $\rho_{\gamma,\text{in/out}} = \text{Tr}_{\bar{\gamma}}\{\rho_{\text{in/out}}\}$, the von Neumann entropies of input and output states are generally different

$$S_{\text{vN}}[\rho_{\gamma,\text{in}}] \neq S_{\text{vN}}[\rho_{\gamma,\text{out}}]. \tag{3.29}$$

Example:
For two single-channel fermionic leads, the marginal input state on the first lead

reads

$$\rho_{1,\mathrm{in}} = \begin{pmatrix} f_1^- & 0 \\ 0 & f_1 \end{pmatrix},$$

with $f_1^- = 1 - f_1$. Instead, after the scattering event, the marginal output state on the same lead reads

$$\rho_{1,\mathrm{out}} = \begin{pmatrix} (1-|s_{12}|^2)f_1^- + |s_{12}|^2 f_2^- & 0 \\ 0 & (1-|s_{12}|^2)f_1 + |s_{12}|^2 f_2 \end{pmatrix},$$

with $|s_{12}|^2 = |s_{21}|^2$ being the transmission probability. Clearly, for $|s_{12}|^2 \neq 0$ and $f_2 \neq f_1$, the states are different and have different von Neumann entropies.

On each lead the von Neumann entropy can either increase or decrease. However, if the initial state is a tensor product on the leads, i.e. $\rho_{\mathrm{in}} = \bigotimes_\alpha \rho_{\alpha,\mathrm{in}}$, the *total* entropy production ΔS_{L} accounting for all leads is always positive. Indeed, this entropy difference can be written in terms of a relative entropy $D[\rho||\sigma] \equiv \mathrm{Tr}\,\{\rho[\log\rho - \log\sigma]\}$ as

$$\frac{1}{k_{\mathrm{B}}}\Delta S_{\mathrm{L}} \equiv \sum_\gamma \left(S_{\mathrm{vN}}[\rho_{\gamma,\mathrm{out}}] - S_{\mathrm{vN}}[\rho_{\gamma,\mathrm{in}}]\right) = D[\rho_{\mathrm{out}}||\bigotimes_\gamma \rho_{\gamma,\mathrm{out}}] \geq 0, \tag{3.30}$$

where we used the conservation of entropy under the unitary transformation Eq. (3.28). While this entropy production gives us insights into the correlations created in the scattering process [115–117], it is completely oblivious to the thermodynamic entropy prodution in the baths. Indeed, while the effect of the baths enters this entropy productions through the input state, how the output state couples and induces dissipation in the baths is not included in the description.

Here, we clarify the difference and the connection between the entropy production in the leads and the one in the baths. Since each lead is coupled to a different bath, we focus on one specific lead and its bath, say γ. This also allows us to work only with the marginal state on such a lead because the remaining leads do not participate in the coupling. Furthermore, we assume the dissipation to the bath to happen far from the central conductor, such that the lead-bath coupling does not affect the coherent scattering evolution of the lead states [118–120], as depicted in Fig. 3.4. Note that this description is reminiscent of the Markovian embedding technique used to deal with systems strongly coupled to the reservoirs [121, 122].

We focus now on the lead-bath interaction happening after the scattering process took place which resets the lead state to the input state, as shown in Fig. 3.4. Calling $t = 0$ the starting time of the lead-bath coupling, we assume the state of lead (L) γ and the corresponding bath (B) to be uncorrelated at that time, i.e. $\rho_{\mathrm{LB},\gamma}(0) = \rho_{\mathrm{L},\gamma}(0) \otimes \rho_{\mathrm{B},\gamma}(0)$. Furthermore, since the coupling happens after the scattering process, the state of the lead at $t = 0$ corresponds to the output state of the scattering process, namely $\rho_{\mathrm{L},\gamma}(0) = \rho_{\gamma,\mathrm{out}}$. The lead-bath system evolves

unitarily under the Hamiltonian

$$\hat{H}(t) = \hat{H}_{\mathrm{L},\gamma} + \hat{H}_{\mathrm{B},\gamma} + \hat{V}_\gamma, \tag{3.31}$$

where $\hat{V}_\gamma$ is the weak (possibly time-dependent) coupling between lead and bath. Having an uncorrelated state at $t = 0$ in the lead-bath system allows to write the second law of thermodynamics as

$$k_{\mathrm{B}} D[\rho_{\mathrm{LB},\gamma}(t) || \rho_{\mathrm{L},\gamma}(t) \otimes \rho_{\mathrm{B},\gamma}(t)] = \Delta S_{\mathrm{L},\gamma}(t) + \Delta S_{\mathrm{B},\gamma}(t) \geq 0 \tag{3.32}$$

where $\Delta S_{\mathrm{L/B},\gamma}(t) \equiv k_{\mathrm{B}} \left(S_{\mathrm{vN}}[\rho_{\mathrm{L/B},\gamma}(t)] - S_{\mathrm{vN}}[\rho_{\mathrm{L/B},\gamma}(0)] \right)$ is the entropy difference of lead/bath [123]. When the bath is sufficiently large such that its state is weakly perturbed by the interaction with the lead, and when it is in a thermal state $\rho_{\mathrm{B},\gamma}(0) \propto \exp[-(\hat{H}_{\mathrm{B},\gamma} - \mu_\gamma \hat{N}_{\mathrm{B},\gamma})/k_{\mathrm{B}} T_\gamma]$, its entropy production obeys Clausius' relation,

$$\Delta S_{\mathrm{B},\gamma}(t) \approx \frac{\Delta \mathcal{Q}_{\mathrm{B},\gamma}(t)}{T_\gamma}, \tag{3.33}$$

connecting the entropy production to the absorbed heat $\Delta \mathcal{Q}_{\mathrm{B},\gamma}(t)$ and the bath temperature T_γ, as detailed in App. D.

To completely reset the state of the lead to the input state $\rho_{\gamma,\mathrm{in}}$ (which was initially prepared by the bath), we let the lead and the bath interact until the time τ at which the lead's state fully relaxes to $\rho_{\gamma,\mathrm{in}}$. Therefore, the entropy difference of the lead is exacly opposite to the one produced during the scattering process,

$$\frac{1}{k_{\mathrm{B}}} \Delta S_{\mathrm{L},\gamma}(\tau) = S_{\mathrm{vN}}[\rho_{\gamma,\mathrm{in}}] - S_{\mathrm{vN}}[\rho_{\gamma,\mathrm{out}}]. \tag{3.34}$$

This means that, in the full cycle made of scattering process and reset of the lead state, depicted in Fig. 3.4, the thermodynamic entropy production $\Delta\Sigma$ is only given by the entropy production in the baths $\Delta S_{\mathrm{B},\gamma}(\tau)$,

$$\Delta\Sigma = \sum_\gamma \left[\Delta S_{\mathrm{L},\gamma}(\tau) + \Delta S_{\mathrm{B},\gamma}(\tau) \right] + \Delta S_{\mathrm{L}} = \sum_\gamma \Delta S_{\mathrm{B},\gamma}(\tau) \equiv \Delta S_{\mathrm{B}}. \tag{3.35}$$

Note that, combining the inequalities of Eqs. (3.30, 3.32) we see that the thermodynamic entropy production $\Delta\Sigma$ also obeys the second law.

$$\Delta\Sigma = \Delta S_{\mathrm{B}} \geq \Delta S_{\mathrm{L}} \geq 0. \tag{3.36}$$

In our description of the scattering process we could focus on one specific energy E because particles at different energies do neither interact nor mix. If this property also applies to the coupling with the bath, we can extend this single-energy description. Then, the bath is described by the state

$$\rho_{\mathrm{B},\gamma}(0) = \frac{1}{Z_{\mathrm{B},\gamma}} \exp\left[-\frac{E - \mu_\gamma(E)}{k_{\mathrm{B}} T_\gamma(E)} \hat{N}_{\mathrm{B},\gamma} \right] \tag{3.37}$$

where $\hat{N}_{\mathrm{B},\gamma}$ is the number operator of the bath at the energy E, and $T_\gamma(E), \mu_\gamma(E)$ are the temperature and chemical potential, respectively. Note that the energy dependence of the intensive quantities $T_\gamma(E), \mu_\gamma(E)$ is equivalent to considering many baths with different temperatures and chemical potentials that connect to the leads only in narrow energy windows that do not overlap. Having focused only on the energy E, we write the entropy production in the bath in terms of the change in the bath particle number $\Delta\mathcal{N}_{\mathrm{B},\gamma} \equiv \mathrm{Tr}\left\{\hat{N}_{\mathrm{B},\gamma}[\rho_{\mathrm{B},\gamma}(t) - \rho_{\mathrm{B},\gamma}(0)]\right\}$ as

$$\frac{\Delta\mathcal{Q}_\gamma}{k_\mathrm{B}T_\gamma(E)} = \frac{E-\mu_\gamma(E)}{k_\mathrm{B}T_\gamma(E)}\Delta\mathcal{N}_{\mathrm{B},\gamma} = \log\left(\frac{1\mp f_\gamma(E)}{f_\gamma(E)}\right)\Delta\mathcal{N}_{\mathrm{B},\gamma}, \tag{3.38}$$

where we expressed the amount of heat transferred by each particle, $E-\mu_\gamma(E)$, in terms of the average occupation number $f_\gamma(E)$. Again, the upper/lower sign corresponds to fermionic/bosonic particles. Furthermore, assuming that particles are conserved during the lead-bath interaction, the change in the bath particle number satisfies $\Delta\mathcal{N}_{\mathrm{B},\gamma} + \Delta N_{\mathrm{L},\gamma} = 0$, where $\Delta N_{\mathrm{L},\gamma} \equiv \mathrm{Tr}\left\{\hat{N}_{\mathrm{L},\gamma}[\rho_{\mathrm{L},\gamma}(t) - \rho_{\mathrm{L},\gamma}(0)]\right\}$ is the change in the lead particle number. This leads to

$$\frac{\Delta\mathcal{Q}_\gamma}{k_\mathrm{B}T_\gamma(E)} = -\log\left(\frac{1\mp f_\gamma(E)}{f_\gamma(E)}\right)\Delta N_{\mathrm{L},\gamma} = \log\left(\frac{1\mp f_\gamma(E)}{f_\gamma(E)}\right)\langle Q_\gamma\rangle, \tag{3.39}$$

where we recognize that, since $\rho_{\mathrm{L},\gamma}(t) = \rho_{\gamma,\mathrm{in}}$, and $\rho_{\mathrm{L},\gamma}(0) = \rho_{\gamma,\mathrm{out}}$, the change in the lead particle number $\Delta N_{\mathrm{L},\gamma}$ in the interaction with the bath is the opposite of the average number of transferred particles $\langle Q_\gamma\rangle$ during the scattering process. This connection between the bath entropy production and the stochastic number of transferred particles Q_γ extends to each realization when we introduce the stochastic entropy production s_γ as

$$s_\gamma \equiv k_\mathrm{B}\log\left(\frac{1\mp f_\gamma(E)}{f_\gamma(E)}\right)Q_\gamma. \tag{3.40}$$

This allows us to study the fluctuations in the entropy production through Eq. (3.26), and was done, for instance, in Paper V.

To summarize, in this Section we discussed Landauer-Büttiker theory from an alternative point of view, in which the measurement of the particle number plays a crucial role in determining the fluctuations of the currents. Furthermore, with this approach we can distinguish between the entropy produced in the scattering and the one produced in the baths, as well as introduce a notion of stochastic entropy production. In this description, we considered ideal measurements of the particle numbers in the leads. These measurements did not destroy any coherence in the states because the latter were already (block-)diagonal in the particle number eigenspaces. This approach opens up for the possibility of having generalized measurements that are not ideal, or that affect the states in a non-trivial way. A possible playground in which the action of such generalized measurements

can be investigated are periodically driven coherent scatterers. Here, the driving establishes coherences between different energies. Thus, a measurement of, e.g., the energy of the state would affect the statistics of energy transport.

3.2 Perturbative approach to transport

In the previous section we described transport in a system with negligible particle-particle interaction, such that the unitary evolution of the system could be split into single-particle evolutions. Here instead we present a framework where particle-particle interactions can be sizable. However, this framework is limited to the weak coupling regime. In particular, the coupling strength is treated perturbatively, and transport quantities are calculated under this approximation.

The system is described by the Hamiltonian $\hat{H} = \hat{H}_0 + \hat{V}(t)$, where $\hat{H}_0$ is the arbitrary unperturbed Hamiltonian and $\hat{V}(t)$ is the weak coupling of the form

$$\hat{V}(t) = \hat{A}e^{-i\omega t} + \hat{A}^\dagger e^{i\omega t}, \tag{3.41}$$

where ω is the frequency of the external driving, as sketched in Fig. 3.5. Depending on the context, this frequency has different origins. For example, if one considers an atom coupled to a single bosonic mode, within the rotating wave approximation, the coupling takes the form of Eq. (3.41) with ω being the detuning between the cavity and atom frequencies. There, one typically applies a unitary transformation to move into the so-called rotating frame, where the unperturbed Hamiltonian $\hat{H}_0$ is modified and $\hat{V}(t)$ loses its time-dependence [124]. Amusingly, the opposite transformation is often sought after in tunnel-coupled electronic systems subject to a voltage bias. There, the unpertubed Hamiltonian $\hat{H}_0$ contains a term of the form $\mu\hat{N}$, with μ being the chemical potential and $\hat{N}$ being the number operator, while the tunnel coupling takes the form of Eq. (3.41) with $\omega = 0$. In such systems, one often applies a unitary transformation (sometimes called gauge transformation) to eliminate the chemical potential dependence in the unperturbed Hamiltonian to gain the frequency $\omega = \Delta\mu/\hbar$ in the tunnel coupling [58].

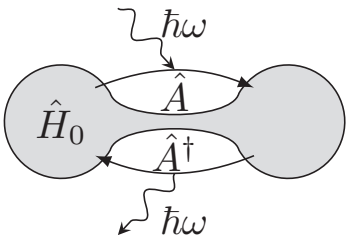

Figure 3.5: *Sketch of a system with unperturbed Hamiltonian $\hat{H}_0$ weakly driven with the coupling operators $\hat{A}, \hat{A}^\dagger$ while absorbing or emitting energy quanta $\hbar\omega$.*

3.2.1 Time evolution and transition rates

The full unitary evolution of the system from time 0 to time t is given by $\hat{\mathcal{U}}(t,0)$

$$\hat{\mathcal{U}}(t,0) = \mathcal{T}\left\{e^{-\frac{i}{\hbar}\int_0^t ds\left[\hat{H}_0+\hat{V}(t)\right]}\right\} \approx \hat{\mathcal{U}}_0(t,0) + \delta\hat{\mathcal{U}}(t,0) \tag{3.42}$$

where $\mathcal{T}\{\cdots\}$ is the time-ordering operation. We approximate this unitary evolution up to the first order contribution in the coupling $\hat{V}(t)$ using the terms

$$\hat{\mathcal{U}}_0(t,0) \equiv e^{-i\hat{H}_0 t/\hbar}, \tag{3.43a}$$

$$\delta\hat{\mathcal{U}}(t,0) \equiv -\frac{i}{\hbar}\int_0^t dx\; \hat{\mathcal{U}}_0(t,x)\hat{V}(x)\hat{\mathcal{U}}_0(x,0). \tag{3.43b}$$

From Eq. (3.43b), we already see how the coupling $\hat{V}(t)$ induces transitions in the system. In particular, since the coupling $\hat{V}(t)$ does not generally commute with the unperturbed Hamiltonian $\hat{H}_0$, transitions between the eigenstates $\{|a\rangle\}$ of the unperturbed Hamiltonian $\hat{H}_0$ will happen. Here, we are interested in the rates of such transitions. To this end, we employ the two-point measurement scheme described in Sec. 2.1. First, a measurement is done at $t = 0$ on the initial state $\rho(0)$ which has outcome a with probability

$$p(a,0) = \mathrm{Tr}\left\{|a\rangle\langle a|\,\rho(0)\right\}. \tag{3.44}$$

Then, we let the system evolve for time t and perform a second measurement. From now on we define $\epsilon_{ba} \equiv \epsilon_b - \epsilon_a$ the difference of two energy eigenenergies $\hat{H}_0|a\rangle = \epsilon_a|a\rangle$ and the matrix element $A_{ba} \equiv \langle b|\hat{A}|a\rangle$. The second measurement is then performed and has outcome b with probability

$$p(b,t|a,0) = |\,\langle b|\hat{\mathcal{U}}(t,0)|a\rangle\,|^2 \tag{3.45}$$

conditioned on the outcome of the first measurement. In the case $b \neq a$, we expand perturbatively the (conditioned) probability in Eq. (3.45) associated to the outcome b as

$$\begin{aligned} p(b,t|a,0) &\approx |\,\langle b|\hat{\mathcal{U}}_0(t,0) + \delta\hat{\mathcal{U}}(t,0)|a\rangle\,|^2 \\ &\approx \left|\delta_{ba} - i\left[A_{ba}\frac{e^{-i\omega t} - e^{-i\epsilon_{ba}t/\hbar}}{\epsilon_{ba}-\hbar\omega} + A^*_{ab}\frac{e^{i\omega t} - e^{-i\epsilon_{ba}t/\hbar}}{\epsilon_{ba}+\hbar\omega}\right]\right|^2 \\ &\approx |A_{ba}|^2\frac{2-2\cos\left[\left(\frac{\epsilon_{ba}}{\hbar}-\omega\right)t\right]}{(\epsilon_{ba}-\hbar\omega)^2} + |A_{ab}|^2\frac{2-2\cos\left[\left(\frac{\epsilon_{ba}}{\hbar}+\omega\right)t\right]}{(\epsilon_{ba}+\hbar\omega)^2}, \end{aligned} \tag{3.46}$$

where we assumed that the coupling operator $\hat{A}$ satisfies $A_{ab}A_{ba} = 0$ for all a, b. This means that only one of the transitions $|a\rangle \to |b\rangle$ and $|b\rangle \to |a\rangle$ is possible

with the absorption of one quantum $\hbar\omega$. Taking the time-derivative yields

$$\begin{aligned}\partial_t p(b,t|a,0) &\approx \frac{2}{\hbar}|A_{ba}|^2\frac{\sin\left[\left(\frac{\epsilon_{ba}}{\hbar}-\omega\right)t\right]}{\epsilon_{ba}-\hbar\omega}+\frac{2}{\hbar}|A_{ab}|^2\frac{\sin\left[\left(\frac{\epsilon_{ba}}{\hbar}+\omega\right)t\right]}{\epsilon_{ba}+\hbar\omega},\\ &\overset{t\to\infty}{\to} \frac{2\pi}{\hbar}|A_{ba}|^2\delta\left(\epsilon_{ba}-\hbar\omega\right)+\frac{2\pi}{\hbar}|A_{ab}|^2\delta\left(\epsilon_{ba}+\hbar\omega\right),\end{aligned} \tag{3.47}$$

where the long-time limit is taken while keeping $\frac{|A_{ba}|t}{\hbar} \ll 1$ such that the perturbative approach remains valid. Now, suppose witout loss of generality that $A_{ba} \neq 0$ and $A_{ab} = 0$, then only the first term in Eq. (3.47) does not vanish. In this case, the transition rate of the process $|a\rangle \to |b\rangle$ in which one quantum $\hbar\omega$ was *absorbed* reads

$$\Gamma_{a\to b} = \partial_t p(b,t|a,0)p(a) = \frac{2\pi}{\hbar}\delta(\epsilon_{ba}-\hbar\omega)|A_{ba}|^2 p_a. \tag{3.48}$$

Conversely, in the time-derivative of the conditional probability $p(a,t|b,0)$, only the second term in Eq. (3.47) contributes. Then, the transition of the process $|b\rangle \to |a\rangle$ in which one quantum $\hbar\omega$ was *emitted* reads

$$\Gamma_{a\leftarrow b} = \partial_t p(a,t|b,0)p(b) = \frac{2\pi}{\hbar}\delta(\epsilon_{ba}-\hbar\omega)|A_{ba}|^2 p_b. \tag{3.49}$$

Note that these transition rates satisfy

$$\frac{\Gamma_{a\to b}}{\Gamma_{a\leftarrow b}} = \frac{p_a}{p_b}. \tag{3.50}$$

A the special case is the one in which the system is prepared in a Gibbs state with inverse temperature $\beta \equiv (k_{\mathrm{B}}T)^{-1}$

$$\rho(0) = \tau = \frac{e^{-\beta\hat{H}_0}}{Z}, \tag{3.51}$$

where $Z = \mathrm{Tr}\left\{e^{-\beta\hat{H}_0}\right\}$ is the partition function. Indeed, for this thermal state, Eq. (3.50) loses the dependence on the initial and final states' energies, and reduces to the detailed balance condition

$$\frac{\Gamma_{a\to b}}{\Gamma_{a\leftarrow b}} = e^{-\beta(\epsilon_a-\epsilon_b)} = e^{\beta\hbar\omega} \tag{3.52}$$

because of the delta distribution in the transition rates, see Eqs. (3.48, 3.49). This property is used later in Sec. 3.2.2 to link the average current with its noise in systems without any temperature bias.

Indeed, the transition rates of Eqs. (3.48, 3.49) can be used to calculate transport properties. For instance, summing over all possible initial and final states

we find the spectral representation of absorption and emission rates [42]

$$\Gamma_{\rightarrow} = \sum_{a,b} \Gamma_{a\rightarrow b} = \sum_{a,b} \frac{2\pi}{\hbar} \delta(\epsilon_{ba} - \hbar\omega) |A_{ba}|^2 p_a, \tag{3.53a}$$

$$\Gamma_{\leftarrow} = \sum_{a,b} \Gamma_{a\leftarrow b} = \sum_{a,b} \frac{2\pi}{\hbar} \delta(\epsilon_{ba} - \hbar\omega) |A_{ba}|^2 p_b. \tag{3.53b}$$

3.2.2 Current and noise

It is also possible to consider not only the absorption and emission rates, but also the rate of change in an observable $\hat{O}$. Here we assume that such an observable $\hat{O}$ commutes with the unperturbed Hamiltonian $\hat{H}_0$, i.e. $[\hat{O}, \hat{H}_0] = 0$. This guarantees that $\{|a\rangle\}$ is also an eigenbasis of $\hat{O}$. We refer to the corresponding eigenvalues as $\{q_a\}$, i.e. $\hat{O}|a\rangle = q_a |a\rangle$. Then, we calculate the average current I associated to the change in $\hat{O}$ and its zero-frequency noise S^I. Specifically, we define for the transition $a \rightarrow b$ from the state $|a\rangle$ to the state $|b\rangle$ the stochastic variable $Q \equiv q_b - q_a$ accounting for the change in the observable $\hat{O}$. Then, taking the time-derivative of the average and variance of Q we have

$$I = \partial_t \langle Q \rangle = \sum_{a,b} (q_b - q_a)(\Gamma_{a\rightarrow b} - \Gamma_{a\leftarrow b}), \tag{3.54a}$$

$$S^I = \partial_t \mathrm{Var}[Q] \approx \sum_{a,b} (q_b - q_a)^2 (\Gamma_{a\rightarrow b} + \Gamma_{a\leftarrow b}). \tag{3.54b}$$

In the noise, the contribution of $\langle Q \rangle^2$ is neglected because it is at higher order in the coupling.

In the special case when the observable $\hat{O}$ fulfils the following commutation relation with the coupling operator $\hat{A}$

$$[\hat{O}, \hat{A}] = q\hat{A}, \tag{3.55}$$

the current and its noise can be simplified. Indeed, the commutation relation of Eq. (3.55) means that each transition induced by $\hat{A}$ transfers exactly the amount q of the observable.

Example:
Consider the tunneling Hamiltonian

$$\hat{V}(t) = g\left((\hat{a}^\dagger)^n \hat{b} e^{-i\omega t} + \hat{b}^\dagger (\hat{a})^n e^{i\omega t}\right),$$

with $\hat{a}, \hat{b}$ bosonic ladder operators. Then, the $\hat{A}$ operator is $\hat{A} = g(\hat{a}^\dagger)^n \hat{b}$. Let the considered observable be the number operator $\hat{O} = \hat{a}^\dagger \hat{a}$. Then, the commutator between the number operator and the $\hat{A}$ operator reads

$$[\hat{O}, \hat{A}] = g[\hat{a}^\dagger \hat{a}, (\hat{a}^\dagger)^n]\hat{b} = gn(\hat{a}^\dagger)^n \hat{b}$$

meaning that $q = n$ is the number of particles "a" created by removing a particle "b".
If instead the coupling is

$$\hat{V}(t) = g\left((\hat{a}^\dagger)^n \hat{b} + (\hat{a}^\dagger)^m \hat{c}\right) e^{-i\omega t} + \text{h.c.}$$

and the observable considered is again the particle number $\hat{O} = \hat{a}^\dagger \hat{a}$, then the commutator reads

$$[\hat{O}, \hat{A}] = g[\hat{a}^\dagger \hat{a}, (\hat{a}^\dagger)^n \hat{b} + (\hat{a}^\dagger)^m \hat{c}] = g\left(n(\hat{a}^\dagger)^n \hat{b} + m(\hat{a}^\dagger)^m \hat{c}\right) \neq q\hat{A}.$$

In this case the coupling operator contains two processes that generate a different number of particles, and the commutation relation of Eq. (3.55) no longer holds.

Then, the average current and its noise take on the simpler form

$$I = \sum_{a,b} q(\Gamma_{a\to b} - \Gamma_{a\leftarrow b}) = q\left(\Gamma_{\to} - \Gamma_{\leftarrow}\right), \tag{3.56a}$$

$$S^I = \sum_{a,b} q^2(\Gamma_{a\to b} + \Gamma_{a\leftarrow b}) = q^2\left(\Gamma_{\to} + \Gamma_{\leftarrow}\right), \tag{3.56b}$$

and become proportional to the difference and the sum of the absorption and emission rates, respectively. In this form it is easy to see that the noise is always super-Poissonian [125, 126], i.e. $S^I \geq |qI|$, since both absorption and emission rates are positive by definition. Furthermore, if the state is prepared in the Gibbs state Eq. (3.51) we can use the simplified detailed balance relation of Eq. (3.52) to relate the average current and its noise. Starting from Eq. (3.56b) we have [58, 59]

$$\begin{aligned} S^I &= q^2 \sum_{a,b} \Gamma_{a\to b}\left(1 + \frac{\Gamma_{a\leftarrow b}}{\Gamma_{a\to b}}\right) = q^2 \sum_{a,b} \Gamma_{a\to b}\left(1 + e^{-\beta\hbar\omega}\right) \\ &= q^2 \sum_{a,b} \Gamma_{a\to b}\left(1 - e^{-\beta\hbar\omega}\right) \coth\left(\frac{\beta\hbar\omega}{2}\right) = qI \coth\left(\frac{\beta\hbar\omega}{2}\right). \end{aligned} \tag{3.57}$$

This well known result relates the noise and the current even in the presence of an external drive, and has proven particularly useful in the context of electronic transport, where the driving frequency is associated to the voltage bias [58, 59, 125]. Indeed, the ω-dependence of Eq. (3.57) allows to explore two different regimes, and the transition between them. The first regime happens for small driving frequencies, i.e. $\beta\hbar\omega \ll 1$. Then, Eq. (3.57) reduces to the Johnson-Nyquist noise [40, 41] which we discussed in Sec. 2.3,

$$S^I \approx 2qk_{\text{B}}T\, \partial_\omega I|_{\omega=0} \tag{3.58}$$

where we substituted $\beta^{-1} = k_{\mathrm{B}}T$ to highlight the dependence on the temperature. Indeed, this relation enables to infer the temperature of a sample by measuring the current noise S^I, and the conductance $q\,\partial_\omega I|_{\omega=0}$. Instead, for large driving frequencies, i.e. $\beta\hbar\omega \gg 1$, Eq. (3.57) reduces to

$$S^I \approx |qI|, \tag{3.59}$$

making the noise proportional to the current. This is referred to as Schottky regime [114], and is used to determine the amount q of the observable transferred by taking the ratio of the measured noise and current. For instance, this technique has been used to detect Cooper pair transfers [30, 31], or even the exchange of fractional charges in the fractional quantum Hall effect [28, 29]. Naturally, the current and the noise of Eqs. (3.54, 3.56) can be and have been derived without the use of the two-point measurement scheme by studying the current operator

$$\hat{I}(t) = -\frac{i}{\hbar}\left[\hat{O}, \hat{H}(t)\right]. \tag{3.60}$$

The average current is obtained by taking the expectation value of $\hat{I}$, and the noise through the current-current correlations as

$$I = \langle \hat{I}(t) \rangle, \tag{3.61a}$$

$$S^I = \int_{-\infty}^{\infty} dt \langle \delta\hat{I}(t)\delta\hat{I}(0)\rangle, \tag{3.61b}$$

with $\delta\hat{I}(t) \equiv \hat{I}(t) - I$. Under the same assumptions of weak-coupling and absence of a temperature bias, Eq. (3.57) is derived. Beyond these assumptions, the relation between the noise and the current is not straigthforward, and the noise can have more intricate features. However, these features cannot be arbitrary. Indeed, in Chapter 4, we show that there are constraints on the noise that depend on the thermodynamic condition of the system. Specifically, in Paper IV and in Sec. 4.2 we study the noise within the weak-coupling approximation presented in this section, but we allow for a temperature bias. This makes the simple detailed balance relation of Eq. (3.52) break down, and, consequently, the noise does not satisfy Eq. (3.57) any more. Still, the transition rates (and therefore also the noise) are constrained by the heat dissipation required to establish the temperature bias.

4 Constraints on out-of-equilibrium noise

This chapter puts in relation the main results of the appended papers. All of them put forward inequalities involving the noise in out-of-equilibrium systems. Specifically, Sec. 4.1 summarizes the main results of Papers I-III, Sec. 4.2 addresses Paper IV, and Sec. 4.3 focuses on Papers V,VI. In the former two sections we establish constraints on the out-of-equilibrium noise generated by a temperature bias, which is of interest for heat engines. These results therefore go beyond the fluctuation-dissipation theorem decribed in Sec. 2.3, where the response coefficients are calculated at equilibrium, as in Eq. (2.36b). Additionally, the presence of a temperature bias complements previous relations between current and noise that require a uniform temperature in the system, as in Eq. (3.57). Crucially, the constraints of Papers I-IV can be saturated in the presence of a *large* temperature bias. Thus, they provide additional insigths into the noise in far-from-equilibrium setups. In Sec. 4.3 the constraints on the noise take the form of an upper-bound on the precision of an arbitrary current, namely on the ratio betwen the squared average current and its noise. We identify such a constraint with the kinetic uncertainty relations discussed in Sec. 2.4.2. Indeed, in the classical limit, the upper-bound reduces to the dynamical activity, see Eq. (2.54). However, when quantum effects are included, the precision can exceed the limit set by the (classical) dynamical activity. In Markovian open quantum systems the dynamical activity was modified to take into account the (coherent) quantum dynamics [22, 24, 25, 27]. In a similar fashion, in Paper VI we show how the limits on the precision are modified in coherent scatterers. Furthermore, we express these limits in terms of experimentally accessible quantities, like the particle current and its noise. Interestingly, the limits on the precision depend strongly on whether the system is bosonic or fermionic. This difference is, at its core, due to the bunching or anti-bunching of bosons or fermions, respectively, which diminish or enhance the maximum attainable precision.

4.1 Out-of-equilibrium fluctuation-dissipation bound

Papers I-III deal with the noise in fermionic systems described by scattering theory, see Sec. 3.1, subject to external temperature, chemical potential, or spin biases. Papers I, II focus on a two-terminal setup under a combination of biases

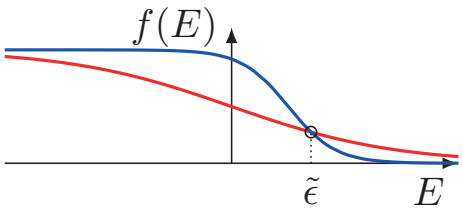

Figure 4.1: *A hot (red) and a cold (blue) Fermi distribution as functions of energy. They cross only at the energy $\tilde{\epsilon}$. For energies larger than $\tilde{\epsilon}$ the hotter distribution is larger than the cold one, and vice-versa.*

for which the average current vanishes. This condition is particularly relevant when studying devices operating close to their thermovoltage, where the average charge current vanishes, or in the stalling condition for other kinds of currents. Furthermore, having out-of-equilibrium noise at zero average current has recently attracted interest in the context of the so-called delta-T noise [34–36]. This noise is an instance of out-of-equilibrium noise generated by a temperature bias, hence the name. Indeed, in the presence of a temperature bias, the noise is not simply the sum of thermal noises at different temperatures, but some additional noise is also present. This additional out-of-equilibrium noise was measured recently for the first time, paving the way for both experimental and theoretical studies on the opportunities for spectroscopy offered by the delta-T noise [92, 127–138]. Papers I, II were written within this context, and extend the analysis of delta-T noise to other kinds of currents and to more general bias combinations.

Paper III generalizes the results of Papers I, II to arbitrary many terminals and arbitrary biases, thereby allowing for nonvanishing average charge current. This allowed us to extend the reach of Paper III beyond the delta-T noise and to compare its results with the fluctuation-dissipation theorem and the thermodynamic uncertainty relation, which we discussed in Chapter 2. Indeed, the results of Paper III not only hold when the system is *producing* power, but they also establish constraints between this average power produced and its noise. For this reason we now focus on the inequalities published in Paper III, which relate the average charge current (or power) to their noise at a given out-of-equilibrium condition.

The main idea that allowed to prove such inequalities is the observation that, given two Fermi distributions at *different temperatures* and possibly different chemical potentials, say $f_{\text{hot}}(E)$ and $f_{\text{cold}}(E)$, there is exactly one energy $\tilde{\epsilon}$ for which $f_{\text{hot}}(\tilde{\epsilon}) = f_{\text{cold}}(\tilde{\epsilon})$. Calling $T_{\text{hot/cold}}, \mu_{\text{hot/cold}}$ the temperatures and chemical potentials of the hot/cold Fermi distribution such that $T_{\text{hot}} > T_{\text{cold}}$, this crossing energy reads

$$\tilde{\epsilon} = \frac{\mu_{\text{cold}} T_{\text{hot}} - \mu_{\text{hot}} T_{\text{cold}}}{T_{\text{hot}} - T_{\text{cold}}}. \tag{4.1}$$

The crossing energy is not only unique, but also determines which Fermi distribution is larger. Indeed, for $E \gtrless \tilde{\epsilon}$, we always have that $f_{\text{hot}}(E) \gtrless f_{\text{cold}}(E)$,

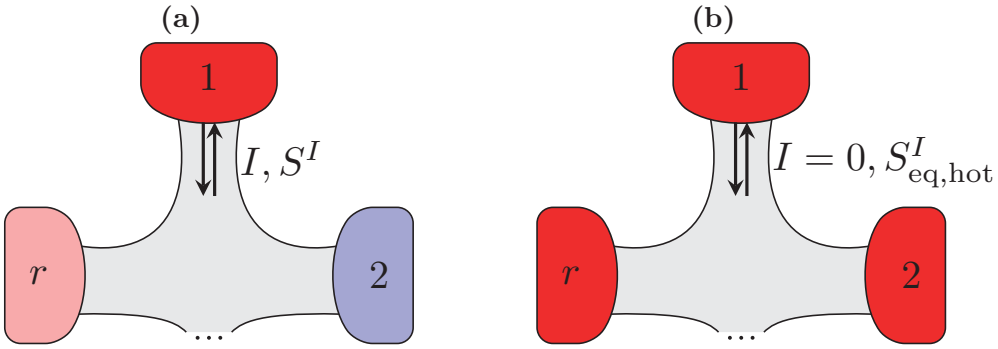

Figure 4.2: **(a)**: *Out-of-equilibrium setup in which reservoir 1 is the hottest. The other reservoirs* $2, \cdots, r$ *have different temperatures and chemical potentials. An average current* I *flows into reservoir 1 with noise* S^I. **(b)**: *Hot equilibrium setup in which all reservoirs have the same (hot) temperature and chemical potential as reservoir 1. On average, no current flows into reservoir 1, but there is still the equilibrium noise* $S^I_{eq,hot}$.

as shown in Fig. 4.1. If transport were to happen only at energies close to $\tilde{\epsilon}$, it would be hard to distinguish between the out-of-equilibrium setup, where the temperature and potential bias are present, and the equilibrium setup. This property of the Fermi distributions suggests to compare the out-of-equilibrium setup in which the terminals have different temperatures and chemical potentials with the equilibrium setup in which there is no bias. Such a comparison is not only appealing from a technical point of view, but also from a practical one: Before operating the device out of equilibrium, it is often useful to "benchmark" its noise at equilibrium. Indeed, this equilibrium noise acts a natural reference for the out-of-equilibrium noise, especially since, at equilibrium, the fluctuation-dissipation theorem discussed in Sec. 2.3 applies, and the equilibrium noise takes a much simpler form.

First, we compare the out-of-equilibrium setup, see Fig. 4.2a, to the *hot* equilibrium setup, see Fig. 4.2b. In the latter, all temperatures and chemical potentials are the same as the hottest terminal in the out-of-equilibrium setup. We focus on the difference between the charge-current noise measured in the hottest contact in these two setups, i.e. $S^I - S^I_{\text{eq,hot}}$. Here, we use the crossing property of the Fermi distributions discussed previously combined with the fact that $f_{\text{hot}}(E)$ is a monotonically decreasing function of energy to establish an inequality between this excess charge-current noise and the average current I in the out-of-equilibrium setup. Note that the crossing property and the monotonicity of the occupations $f_{\text{hot/cold}}(E)$ are the necessary conditions to establish the inequality. This means that, while having *thermal* Fermi distributions as occupations is sufficient, the result also holds for more general *nonthermal* occupations, i.e. occupations that do not have a well-defined temperature and chemical potential, as long as they satisfy the crossing and monotonicity conditions. In the two-terminal case the

inequality reads

$$S^I - S^I_{\text{eq,hot}} \leq -qI_{\text{hot}} \tanh\left(\frac{\Delta\mu}{2k_B\Delta T}\right), \tag{4.2}$$

where q is the particle charge and the biases are defined as $\Delta T \equiv T_{\text{hot}} - T_{\text{cold}} > 0$, $\Delta\mu \equiv \mu_{\text{hot}} - \mu_{\text{cold}}$. The average current I_{hot} in the out-of-equilibrium setup is positive when flowing into the hot contact, and S^I is its noise, whereas $S^I_{\text{eq,hot}}$ is the current noise in the hot equilibrium setup. Notably, Eq. (4.2) holds for any temperatures $T_{\text{hot}} > T_{\text{cold}}$, any chemical potentials, and any scattering matrix. The same insight can also be used to compare the noise in the out-of-equilibrium setup with the noise in the *cold* equilibrium setup. In this equilibrium setup all temperatures and chemical potentials are the same as the coldest terminal in the out-of-equilibrium setup. In constrast with Eq. (4.2), the inequality generated by this comparison has the opposite direction, and applies only to the classical component of the out-of-equilibrium noise $S^{I,\text{cl}}$, namely

$$S^{I,\text{cl}} - S^I_{\text{eq,cold}} \geq -qI_{\text{cold}} \tanh\left(\frac{\Delta\mu}{2k_B\Delta T}\right), \tag{4.3}$$

where the average current I_{cold} is positive when flowing into the cold contact, and $S^I_{\text{eq, cold}}$ is the current noise in the cold equilibrium setup. Indeed, one would expect the (large) hot thermal noise $S^I_{\text{eq,hot}}$ to be an upper-bound for the out-of-equilibrium noise, and the (small) cold thermal noise $S^I_{\text{eq,cold}}$ to be a lower-bound. This intuition is confirmed and honed by Eqs. (4.2, 4.3), where the average current and the biases affect the upper and lower bounds. However, the change in the direction of the inequality in Eq. (4.3) is the reason why it is limited to the classical noise contribution [Eq. (3.27a)] only. Indeed, unlike Eq. (4.2), here we cannot use the negativity of the quantum contribution to the noise [Eq. (3.27b)] of fermionic particles to extend the inequality to the full current noise. Still, in the weak-coupling regime, the quantum noise contributions are negligible, and Eq. (4.3) provides a lower bound on the out-of-equilbrium noise.

Both Eqs. (4.2, 4.3) can be generalized to the multi-terminal case, see Paper III, and, for $I_{\text{hot}} = 0$, Eq. (4.2) reproduces the results of Papers I, II. In these latter papers, instead of splitting the noise into a "classical" and a "quantum" contribution, we decompose it in the sum of thermal noise contributions $\Theta^I_{\text{hot/cold}}$ and a shot noise contribution S^I_{shot}, i.e. $S^I = \Theta^I_{\text{hot}} + \Theta^I_{\text{cold}} + S^I_{\text{shot}}$. The thermal and shot contributions are given by

$$\Theta^I_{\text{hot/cold}} \equiv \frac{q^2}{h}\int dE D(E) f_{\text{hot/cold}}(E)[1 - f_{\text{hot/cold}}(E)], \tag{4.4a}$$

$$S^I_{\text{shot}} \equiv \frac{q^2}{h}\int dE D(E)[1 - D(E)][f_{\text{hot}}(E) - f_{\text{cold}}(E)]^2, \tag{4.4b}$$

where $D(E)$ is the transmission probability at energy E. This decomposition is common in the context of delta-T noise, where one is particularly interested in

the deviations of the total noise from the thermal noise alone. Indeed, when no bias is present, the noise is given only by the thermal noise. In particular, in hot equilibrium setup the noise reads $S^I_{\mathrm{eq,hot}} = 2\Theta^I_{\mathrm{hot}}$. Instead, when a temperature bias is present, the additional noise S^I_{shot} is present on top of the thermal noises at the different temperatures $\Theta^I_{\mathrm{hot}} + \Theta^I_{\mathrm{cold}}$. For this reason, we identify the shot noise contribution with the delta-T noise. Then, substituting this noise decomposition into Eq. (4.2) we find

$$S^I_{\mathrm{shot}} \leq \Theta^I_{\mathrm{hot}} - \Theta^I_{\mathrm{cold}} - qI_{\mathrm{hot}} \tanh\left(\frac{\Delta\mu}{2k_{\mathrm{B}}\Delta T}\right) \overset{I_{\mathrm{hot}}=0}{=} \Theta^I_{\mathrm{hot}} - \Theta^I_{\mathrm{cold}}. \tag{4.5}$$

In the zero-current condition $I_{\mathrm{hot}} = 0$, Eq. (4.5) reduces to the constraint of Papers I, II, which states that the shot noise contribution that arises out-of-equilibrium is limited by the difference in the thermal noises. However, as shown in Papers I, II, Eq. (4.5) does not hold for any kind of current. Indeed, energy and heat currents do not fulfil such an inequality because the quantity transferred is energy-dependent. Then, with an appropriate choice of the scattering matrix, it is possible to violate the inequality even in the absence of an average current. This is not the case for the particle and the charge current, where the quantity transferred is energy-independent.

This requirement of constant amount of quantity transferred is not peculiar of the results presented here, but is also necessary to derive the relation between current and noise of Eq. (3.57). However, unlike the extension of the fluctuation-dissipation theorem of Eq. (3.57), the fluctuation-dissipation bound of Eq. (4.2) also holds in the presence of a temperature bias and is not limited to the weak-coupling regime. A crucial difference is furthermore that Eq. (3.57) is an equality, whereas Eq. (4.2) is an inequality. Thus, if the temperature bias is much smaller than the chemical potential bias $|\Delta\mu|$, Eq. (4.2) is less informative than Eq. (3.57). However, the fluctuation-dissipation bound shines when the temperature bias is sizable, i.e. when Eq. (3.57) does not hold. Indeed, inequality Eq. (4.2) can be saturated when one takes the weak-coupling limit [which is also required for Eq. (3.57)], and when the temperature bias ΔT is the *largest* energy scale, such that $k_{\mathrm{B}}T_{\mathrm{hot}} \gg \gamma \gg k_{\mathrm{B}}T_{\mathrm{cold}}$, where γ is the energy-width of the transmission window generated by the scattering matrix. The latter requirement is in stark contrast with Eq. (3.57), where instead the temperature bias needs to be the *smallest* energy scale. Thus, the fluctuation-dissipation bound of Eq. (4.2) complements the previously known results on noise by including the effect of a temperature bias, and, by becoming an equality in the far-from-equilibrium case where the temperature bias is large.

Having a temperature bias is not only interesting in the context of out-of-equilibrium noise, but is also instrumental for thermoelectric devices. There, the temperature bias is used to drive a current against a chemical potential bias $\Delta\mu$, thereby generating the average (electro-chemical) power $P = I_{\mathrm{hot}}\frac{\Delta\mu}{q}$. This

connection between the power and the current allows us to study how the noise is related to the power using Eq. (4.2). A first connection between them is seen in the large temperature bias limit, where Eq. (4.2) becomes

$$S^I - S^I_{\text{eq,hot}} \leq -\frac{q^2}{2k_\text{B}}\frac{P}{\Delta T}, \quad \text{for} \quad k_\text{B}\Delta T \gg |\Delta\mu|, \tag{4.6}$$

which tells us that, if the device is *generating* power, i.e. $P > 0$, then the noise in the out-of-equilibrium setup is *necessarily smaller* than the noise in the hot equilibrium setup. Conversely, if the device is *dissipating* power, i.e. $P < 0$, then the out-of-equilibrium noise *can be larger* than the hot equilibrium noise, but by at most a factor proportional to the power.

Furthermore, since the power P is proportional to the current, one can write Eq. (4.2) for the noise of the power S^P rather than current noise S^I. Then, using the decomposition in thermal noise and shot noise of Eq. (4.4), we find

$$S^P \geq \Theta^P_\text{hot} - \Theta^P_\text{cold} - S^P_\text{shot} \geq P\Delta\mu \tanh\left(\frac{\Delta\mu}{2k_\text{B}\Delta T}\right), \tag{4.7}$$

where S^P is the noise in the power, while $\Theta^P_\text{hot/cold}$ and S^P_shot are its hot/cold thermal and shot noise contributions. Equation 4.7 tells us that, to have large average power P, it is necessary to have large hot thermal noise Θ^P_hot, and small cold thermal noise Θ^P_cold and shot noise S^P_shot. This is understood in terms of having a large hot temperature, a small cold temperature, and a scattering matrix that is either fully transmitting or fully reflecting, which does not produce any "friction" in the particle flow. Furthermore, the inequalities of Eq. (4.7) tells us that that a minimum amout of noise in the power output is required to produce the average power P.

The necessity of having noise to produce a finite average power reminds us of the thermodynamic uncertainty relation of Sec. 2.4.1. However, unlike Eq. (4.7), the TUR can be violated in systems described by scattering theory [88, 89, 91–96]. Such violations of the TUR are also possible when the device is producing power [90]. Furthermore, in contrast with the TUR, Eq. (4.7) does not expliticitely contain the entropy production. We address this latter issue by using the first and second law of thermodynamics to make Eq. (4.7) resemble the thermodynamic uncertainty relation, as detailed in App. E. We obtain the following constraint on the precision of the power output

$$\frac{P^2}{S^P} \leq \frac{\dot\sigma_\text{cold}}{k_\text{B} g\left(\frac{\Delta\mu}{k_\text{B}\Delta T}\right)} \geq \frac{\dot\sigma}{k_\text{B} g\left(\frac{\Delta\mu}{k_\text{B}\Delta T}\right)}, \tag{4.8}$$

where $g(x) \equiv x\tanh(x/2)$, while $\dot\sigma$ and $\dot\sigma_\text{cold}$ are, respectively, the global entropy production rate and the entropy current in the cold contact. The second inequality of Eq. (4.8) stems from requiring positive power production $P > 0$.

Crucially, this second inequality shows that it is not the global entropy production $\dot{\sigma}$ that sets a limit on the power precision, but only the entropy production in the cold contact $\dot{\sigma}_{\text{cold}}$. Furthermore, the biases determining the out-of-equilibrium condition, $\Delta\mu$ and ΔT also affect the maximum precision by entering in the function $g(\Delta\mu/k_{\text{B}}\Delta T)$. Moreover, one can write the limit on the power precision of Eq. (4.8) in terms of the efficiency $\eta \equiv P/(-J_{\text{hot}})$ as

$$\frac{P}{S^P}\frac{\eta}{1-\eta}k_{\text{B}}T_{\text{cold}}g\left(\frac{\Delta\mu}{k_{\text{B}}\Delta T}\right) \leq 1, \tag{4.9}$$

which now gives a trade-off relation between the average power P, its noise S^P, and the efficiency η at which the power is produced. The crucial difference of having the local entropy production $\dot{\sigma}_{\text{cold}}$ instead of the global one $\dot{\sigma}$ in Eq. (4.8) is now reflected in the $1-\eta$ term at the denominator. Indeed, in the TUR, the efficiency shows up as $\eta/(\eta_{\text{C}}-\eta)$, with η_{C} being the Carnot efficiency [12]. Interestingly, when $T_{\text{hot}} \gg T_{\text{cold}}$, this difference becomes negligible as $\eta_{\text{C}} \approx 1$. In this case, Eq. (4.9) tells us that, as long as the noise S^P does not diverge, when the efficiency η approaches the Carnot efficiency $\eta_{\text{C}} \approx 1$, the average power P necessarily approaches 0. However, at finite temperature T_{hot}, Eq. (4.9) does not forbid finite power production at Carnot efficiency. Still, this was shown to be impossible by finding the maximum efficiency at any given power output [139, 140]. However, when maximizing the efficiency, one does not take into account the noise S^P of the power output. Therefore, if one is interested not only in the average power P and the efficiency η at which this power is produced, but also in the noise S^P of the output power, Eq. (4.9) provides a trade-off relation between them.

4.2 Thermodynamic and energetic costs of transition rates

While the results presented in Sec. 4.1 hold in the presence of arbitrary biases, they were derived within the scattering theory formalism, in which particle-particle interactions are neglected. Therefore, the extent to which those results hold in the presence of possibly strong interactions is an open question. Still, the idea presented in Sec. 4.1 of comparing the out-of-equilibrium setup with the equilibrium one does not depend on the formalism used to describe transport. Indeed, in Paper IV we use this idea, albeit in a slightly different fashion, on the formalism described in Sec. 3.2. Here, two subsystems, L and R, have possibly strong (local) interactions, thereby going beyond the scattering theory formalism used in Sec. 4.1, but they are coupled weakly. Specifically, the subsystems are described by their own arbitrary Hamiltonians $\hat{H}_{\text{L,R}}$, while the coupling takes the form of Eq. (3.41), and is treated perturbatively. This coupling induces transitions between the subsystems at the rates $\Gamma_{\rightleftarrows}$, see Eq. (3.53), which fully determine the

average current and its noise. For this reason, we compare the out-of-equilibrium setup with the equilibrium one already at the level of the transition rates to find how they are constrained out of equilibrium.

Already at this point we can understand why the comparison between the out-of-equilibrium setup and the equilibrium one differs from the one in Sec. 4.1: Since we are considering arbitrary Hamiltonians $\hat{H}_{\mathrm{L,R}}$, the state occupation in each subsystem is generally not described by the Fermi function. Indeed, each local Hamiltonian can also describe bosons, or even a combination of bosons and fermions. Furthermore, even if the subsystems were comprised solely by fermions, the presence of interactions disrupts the single-particle average occupation described by the Fermi function. Therefore, to compare the out-of-equilibrium setup in which a temperature bias is present with the one in which it is absent, we consider states that are tensor products of Gibbs states $\tau_\alpha(\beta)$, namely

$$\rho(\beta_{\mathrm{L}},\beta_{\mathrm{R}}) = \tau_{\mathrm{L}}(\beta_{\mathrm{L}}) \otimes \tau_{\mathrm{R}}(\beta_{\mathrm{R}}) = \frac{e^{-\beta_{\mathrm{L}}\hat{H}_{\mathrm{L}}}}{Z_{\mathrm{L}}(\beta_{\mathrm{L}})} \otimes \frac{e^{-\beta_{\mathrm{R}}\hat{H}_{\mathrm{R}}}}{Z_{\mathrm{R}}(\beta_{\mathrm{R}})}, \tag{4.10}$$

where β_α is the inverse temperature of the $\alpha \in \{\mathrm{L}, \mathrm{R}\}$ subsystems, and $Z_\alpha(\beta) = \mathrm{Tr}_\alpha\left\{e^{-\beta\hat{H}_\alpha}\right\}$ is the corresponding partition function. Note that this choice of states is well justified within the weak-coupling approach. The occupation probability $p_n^{(\mathrm{L})}(\beta)$ of the eigenstate $|n\rangle$ of $\hat{H}_{\mathrm{L}}$ with energy $\epsilon_n^{(\mathrm{L})}$, follows a Boltzmann distribution,

$$p_n^{(\mathrm{L})}(\beta) = \frac{e^{-\beta\epsilon_n^{(\mathrm{L})}}}{Z_{\mathrm{L}}(\beta)}, \tag{4.11}$$

satisfying the same properties that were highlighted for the Fermi functions in Sec. 4.1. Namely, two such occupations at different temperatures, $p_n^{(\mathrm{L})}(\beta_{\mathrm{L}})$ and $p_n^{(\mathrm{L})}(\beta_{\mathrm{R}})$, with $\beta_{\mathrm{R}} > \beta_{\mathrm{L}}$, cross exactly once at the energy $\tilde{\epsilon}^{(\mathrm{L})}$, given by

$$\tilde{\epsilon}^{(\mathrm{L})} = \frac{1}{\beta_{\mathrm{R}} - \beta_{\mathrm{L}}} \log \frac{Z_{\mathrm{L}}(\beta_{\mathrm{L}})}{Z_{\mathrm{L}}(\beta_{\mathrm{R}})}. \tag{4.12}$$

Furthermore, as in Sec. 4.1, for $\epsilon_n^{(\mathrm{L})} \gtrless \tilde{\epsilon}^{(\mathrm{L})}$ we always have $p_n^{(\mathrm{L})}(\beta_{\mathrm{L}}) \gtrless p_n^{(\mathrm{L})}(\beta_{\mathrm{R}})$, as shown in Fig. 4.3. This means that the following inequality holds for any $\beta_{\mathrm{R}} > \beta_{\mathrm{L}}$

$$[p_n^{(\mathrm{L})}(\beta_{\mathrm{L}}) - p_n^{(\mathrm{L})}(\beta_{\mathrm{R}})][\epsilon_n^{(\mathrm{L})} - \tilde{\epsilon}^{(\mathrm{L})}] \geq 0. \tag{4.13}$$

This property only depends on the properties of the Gibbs state, and can therefore be used to constraint the two-point probability distributions discussed in Sec. 2.1. Indeed, multiplying Eq. (4.13) by the conditioned probability Eq. (3.45) we find an inequality that relates the probabilities of observing the same transition under different (thermal) initial conditions. Since we are exploiting only the properties of the initial states, this inequality holds for *any* unitary transformation. However, we now focus on the case in which the unitary transformation is treated

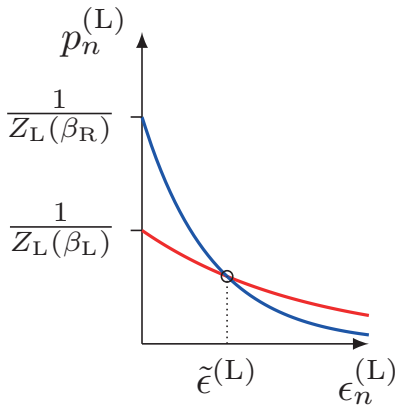

Figure 4.3: *A hot (red) and a cold (blue) Boltzmann distribution as functions of energy. They cross only at the energy $\tilde{\epsilon}^{(L)}$. For energies larger than $\tilde{\epsilon}^{(L)}$ the hotter distribution is larger, and vice-versa.*

perturbatively in the coupling, as discussed in Sec. 3.2, which allows for a simpler description of the current and its noise.

Like in Sec. 4.1, if all transitions happened close to energy $\tilde{\epsilon}^{(\mathrm{L})}$, the rates $\Gamma_{\rightleftarrows}(\beta_\mathrm{L}, \beta_\mathrm{R})$ in the setup with the temperature bias, in which the state is $\rho(\beta_\mathrm{L}, \beta_\mathrm{R})$, would coincide with the rates $\Gamma_{\rightleftarrows}(\beta_\mathrm{R}, \beta_\mathrm{R})$ in the setup without the temperature bias, in which the state is $\rho(\beta_\mathrm{R}, \beta_\mathrm{R})$. Furthermore, when the temperature bias is absent, the current and its noise obtained from the rates satisfy Eq. (3.57), which extends the fluctuation-dissipation theorem. For these reasons, we compare the out-of-equilibrium setup determined by a temperature bias with the equilibrium one in which the subsystems have the same temperature. In this comparison we only change the L subsystem's temperature, and keep the full Hamiltonian (including the coupling between the subsystems) unchanged. We study two different ways to implement such a comparison: The first one can be understood in terms of a fictitious thermodynamic cycle in which we heat up and cool down the L subsystem using a cold and a hot bath, while the second one consists of a heating stroke in which the temperature of the L subsystem slowly increases. These two fictitious protocol implementations are depicted in Fig. 4.4 and lead to two similar constraints on the out-of-equilibrium transition rates. The main difference between them is that, in the thermodynamic cycle, the heat dissipation plays a crucial role in the constraint, whereas in the heating stroke the energy needed to change the temperature of the L subsystem does.

Let's discuss the thermodynamic cycle first, see Fig. 4.4a. Other than the two subsystems L, R, we also include two macroscopic baths that we use to change the temperature of the L subsystem. Starting from the equilibrium condition in which both subsystem are at the cold temperature $k_\mathrm{B}T_\mathrm{R} = 1/\beta_\mathrm{R}$, the following protocol is carried out.

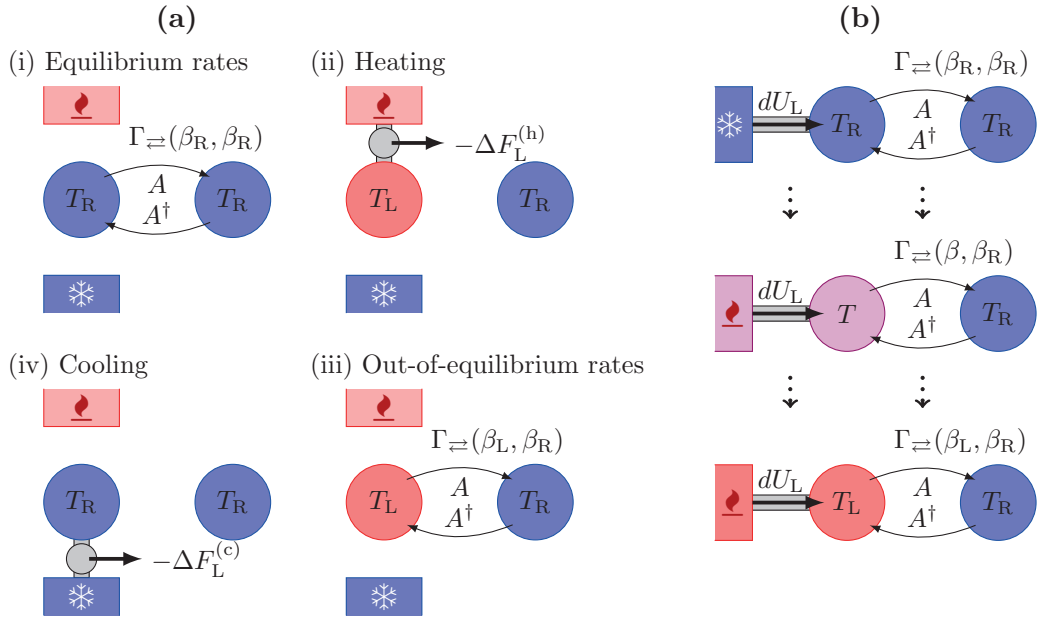

Figure 4.4: (a): *Thermodynamic cycle of a fictitious experiment. (i) The subsystem have the same (cold) temperature. (ii) The L subsystem is heated up by a bath, extracting work in the process. (iii) The subsystems have different temperatures. (iv) The L subsystems is cooled down to its initial temperature by a bath, extracting work in the process.* **(b)**: *Heating stroke of the L subsystem. As the temperature increases from T_R to T_L, the transition rates and the absorbed energy at each intermediate temperature are monitored.*

(i) *Equilibrium rates:* Transitions happen between the two subsystems at the rates $\Gamma_{\rightleftarrows}(\beta_R, \beta_R)$.

(ii) *Heating:* The hot bath at temperature $k_B T_L = 1/\beta_L$ is brought into contact with the L subsystem. Heat flows from the bath and is dissipated in the subsystem until the latter reaches the bath temperature T_L. While the heating takes place it is possible to extract at most the work $-\Delta F_L^{(h)}$, where

$$\Delta F_L^{(h)} \equiv \Delta U_L - T_L \Delta S_L \tag{4.14}$$

is the nonequilibrium free energy change. This depends on the internal energy variation ΔU_L and entropy variation ΔS_L, given by

$$\Delta U_L \equiv U_L(\beta_L) - U_L(\beta_R) = \mathrm{Tr}\left\{\hat{H}_L \left[\rho(\beta_L, \beta_R) - \rho(\beta_R, \beta_R)\right]\right\} \tag{4.15a}$$

$$\Delta S_L \equiv S_{vN}\left[\tau_L(\beta_L)\right] - S_{vN}\left[\tau_L(\beta_R)\right], \tag{4.15b}$$

where $S_{vN}[\rho] \equiv -k_B \mathrm{Tr}\{\rho \log \rho\}$ is the von Neumann entropy. Interestingly, when the work extraction is maximized, the energy change in the system is lower-bounded by

$$\Delta U_L \geq -\Delta F_L^{(h)} \frac{T_R}{T_L - T_R} \equiv -\Delta F_L^{(h)} \eta^{(c)}, \tag{4.16}$$

where $\eta^{(c)}$ is the Carnot efficiency of a refrigerator. Crucially, at the end of the heating process there is a temperature bias between the two subsystems.

(iii) *Out-of-equilibrium rates:* In the out-of-equilibrium setup transitions happen between the two subsystems at the rates $\Gamma_{\rightleftarrows}(\beta_{\rm L}, \beta_{\rm R})$.

(iv) *Cooling:* To get back to the initial condition, the cold bath at temperature $k_{\rm B}T_{\rm R} = 1/\beta_{\rm R}$ is brought into contact with the L subsystem. Heat flows from the subsystem and is dissipated into the bath until the former reaches the bath temperature $T_{\rm R}$. Similarly to the heating step, one can extract at most the work $-\Delta F_{\rm L}^{(c)}$, where

$$\Delta F_{\rm L}^{(c)} \equiv -\Delta U_{\rm L} + T_{\rm R}\Delta S_{\rm L} \tag{4.17}$$

is the nonequilibrium free energy change. Interestingly, when the work extraction is maximized, the heat dissipated in the cold bath is lower-bounded by

$$\Delta Q_{\rm cold} \geq -\Delta F_{\rm L}^{(c)} \frac{T_{\rm R}}{T_{\rm L} - T_{\rm R}} \equiv -\Delta F_{\rm L}^{(c)} \eta^{(h)}, \tag{4.18}$$

where $\eta^{(h)}$ is the Carnot efficiency of a heat pump.

We use the quantities encountered in this cycle to define a thermodynamic cost as

$$\mathcal{W}_{\rightleftarrows}^{(\rm Thermo)} \equiv -\Delta F_{\rm L}^{(c)} \eta^{(h)} \Gamma_{\rightleftarrows}(\beta_{\rm L}, \beta_{\rm R}) - \Delta F_{\rm L}^{(h)} \eta^{(c)} \Gamma_{\rightleftarrows}(\beta_{\rm R}, \beta_{\rm R}), \tag{4.19}$$

in which the equilibrium and out-of-equilibrium rates are weighted by a lower-bound of the heat dissipated to establish and deplete, respectively, the temperature bias. By definition, this cost is positive $\mathcal{W}_{\rightleftarrows}^{(\rm Thermo)} \geq 0$. However, using the crossing property of the occupation probabilities, we prove that this thermodynamic cost is limited by

$$\mathcal{W}_{\rightleftarrows}^{(\rm Thermo)} \geq \mathcal{W}_{\rightleftarrows}^{(\rm Resp)} \tag{4.20}$$

where the rate response $\mathcal{W}_{\rightleftarrows}^{(\rm Resp)}$ is defined as

$$\mathcal{W}_{\rightleftarrows}^{(\rm Resp)} \equiv \partial_{\rm L}\Gamma_{\rightleftarrows}(\beta_{\rm L}, \beta_{\rm R}) - \partial_{\rm L}\Gamma_{\rightleftarrows}(\beta_{\rm R}, \beta_{\rm R}). \tag{4.21}$$

Here, $\partial_{\rm L} f(x,y) \equiv \frac{\partial f}{\partial x}(x,y)$ is the derivative with respect to the left argument. Thus, $\mathcal{W}_{\rightleftarrows}^{(\rm Resp)}$ corresponds to the difference between the out-of-equilibrium response and the equilibrium response of the rates.

Notably, the rate response $\mathcal{W}_{\rightleftarrows}^{(\rm Resp)}$ acts as lower bound also for the constraint obtained in the heating stroke, see Fig. 4.4b. However, unlike Eq. (4.19), the cost associated to this process involves only the internal energy $U_{\rm L}(\beta)$. In the heating stroke, we continuously increase the temperature of the L subsystem from the colder $T_{\rm R}$ to the hotter $T_{\rm L}$. At each intermediate temperature $k_{\rm B}T = 1/\beta$

transition events between the two subsystems happen at the rates $\Gamma_{\rightleftarrows}(\beta, \beta_{\mathrm{R}})$, and to reach the next (infinitesimally larger) temperature, the energy $dU_{\mathrm{L}}(\beta)$ needs to be provided to the L subsystem. Then, similarly to the thermodynamic cost of Eq. (4.19), we define the *energetic cost* by weighting the transition rates by the energy required to change the temperature of the L subsystem

$$\mathcal{W}_{\rightleftarrows}^{(\mathrm{Energy})} \equiv \int_{U_{\mathrm{L}}(\beta_{\mathrm{R}})}^{U_{\mathrm{L}}(\beta_{\mathrm{L}})} \Gamma_{\rightleftarrows}(\beta, \beta_{\mathrm{R}}) d[U_{\mathrm{L}}(\beta)]. \tag{4.22}$$

Like the thermodynamic cost, the energetic cost is also positive $\mathcal{W}_{\rightleftarrows}^{(\mathrm{Energy})} \geq 0$ by definition, and lower-bounded by the rate response

$$\mathcal{W}_{\rightleftarrows}^{(\mathrm{Energy})} \geq \mathcal{W}_{\rightleftarrows}^{(\mathrm{Resp})}. \tag{4.23}$$

Note that both thermodynamic and energetic costs take the form of a transport quantity, namely the transition rates $\Gamma_{\rightleftarrows}$ multiplied by an *extensive* quantity of subsystem L, whereas the rate response contains the temperature-derivative of the transport quantity only. Therefore, taking the thermodynamic limit on the L subsystem, we expect different scalings between the left- and right-hand sides of both thermodynamic and energetic constraints. Indeed, in such a limit, the thermodynamic and energetic costs dominate over the rate response, making both constraints Eqs. (4.20, 4.23) trivial. Therefore, in small-scale systems, in which the thermodynamic limit is *not* fulfilled, the out-of-equilibrium rates are nontrivially constrained. Then, it is interesting to know not only when such constraints are possible, but also when they are tight. This happens trivially at equilibrium, i.e. when $\beta_{\mathrm{L}} = \beta_{\mathrm{R}}$, for both thermodynamic and energetic constraints since all the involved quantities vanish, $\mathcal{W}_{\rightleftarrows}^{(\mathrm{Thermo})} = \mathcal{W}_{\rightleftarrows}^{(\mathrm{Energy})} = \mathcal{W}_{\rightleftarrows}^{(\mathrm{Resp})} = 0$. However, it is also possible to approach the equality *far from equilibrium*, as shown in Paper IV, where neither the thermodynamic/energetic cost nor the rate response vanish. Specifically, the thermodynamic constraint Eq. (4.20) is saturated when the transitions happen close to the crossing energy $\tilde{\epsilon}^{(\mathrm{L})}$, whereas the energetic constraint Eq. (4.23) is saturated when the transitions happen close to the internal energy U_{L}.

The thermodynamic and energetic constraints of Eqs. (4.20, 4.23) go beyond the results of Sec. 4.1 by allowing for particle-particle interactions, albeit in the weak-coupling regime, and by focusing on the transition rates. Indeed, one can connect the statements on the rates to the current and its noise as long as all transitions transfer the same amount q of the considered observable. This is the case, for example, when one considers the particle (or charge) current and the coupling takes the tunneling form $\hat{V} \propto (\hat{c}_{\mathrm{L}}^{\dagger}\hat{c}_{\mathrm{R}} + \hat{c}_{\mathrm{R}}^{\dagger}\hat{c}_{\mathrm{L}})$. Then, the current and its noise fulfil Eq. (3.56), the transition rates $\Gamma_{\rightleftarrows}$ can be written in terms of the average current I and its noise S^I as

$$2q^2\Gamma_{\rightarrow} = S^I + qI, \tag{4.24a}$$

$$2q^2\Gamma_{\leftarrow} = S^I - qI. \tag{4.24b}$$

Therefore, the constraints Eqs. (4.20, 4.23) on the transition rates tell us *how much* the noise deviates from the Poissonian regime. Still, the results of Paper IV are not limited to this case in which all transitions transfer the same amount q of the observable considered. Indeed, independently on what this observable is, both constraints (4.20, 4.23) are also valid at the level of the individual transition rates $\Gamma_{a\rightleftarrows b}$ between the states $|a\rangle$ and $|b\rangle$, see Eqs. (3.48, 3.49). For a general observable that takes value $q_{a/b}$ on the state $|a/b\rangle$, the transition $\Gamma_{a\to b}$ transfers the amount $q_b - q_a$, producing a current. The noise of such a current is given by a linear combination of the rates, see Eq. (3.54). Therefore, this noise is also subject to the thermodynamic and energetic constraints of Eqs. (4.20, 4.23). This is in constrast with the results of Sec. 4.1, which do not apply when the transferred quantity depends on the energy at which the transition happens.

Even though the results of this Section and of Sec. 4.1 both stem from the idea of comparing the out-of-equiliubrium setup generated by a temperature bias with the corresponding equilibrium setup, their results are different. This is because the formalisms in which the comparison is made are different. However, the perturbative approach reproduces the scattering theory results in the weak-coupling regime under the necessary conditions, e.g. coupling of the tunneling form, negligible particle-particle interactions. Therefore, one may wonder what are the necessary conditions on the local Hamiltonians $\hat{H}_{\mathrm{L,R}}$ and the coupling $\hat{V}$ between the subsystems to recover the fluctuation-dissipation bound of Eq. (4.2) starting from the perturbative approach of Sec. 3.2.

4.3 Kinetic uncertainty relation in quantum transport

The results in Sections 4.1 and 4.2 focus on comparing out-of-equilibrium and equilibrium setups because, in the latter, the fluctuation-dissipation theorem (and its generalizations) hold. This comparison allowed us to find constraints on the out-of-equilibrium transport properties, most significantly between the charge current and its noise. Another way to compare an average current and its noise is through the precision, namely the ratio between the average current squared and its noise. As discussed in Sec. 2.4, trade-off relations limiting the maximum attainable precision were proven in classical Markovian systems. These are the thermodynamic and the kinetic uncertainty relations (TUR and KUR), see Eq. (2.48) and Eq. (2.53) respectively. In the former, the limit on the precision is given by the entropy production, a measure of dissipation, whereas in the latter, it is given by the activity, a measure of how many transitions happen in the system. However, the presence of coherent or non-Markovian dynamics was shown to disrupt such relations [89, 105]. For instance, systems in which transport is described by scattering theory, see Sec. 3.1, have been pointed out as examples of systems

where the classical formations of both TUR and KUR are violated. For this reason, how such relations need to be modified for quantum or non-Markovian systems is currently being investigated [24, 27, 93]. Paper VI contributes to this field of research by studying the kinetic uncertainty relation in quantum transport setups described by scattering theory. Specifically, we show how to recover the classical formulation of the KUR, and how to include the quantum effects into the constraint.

The first step in the proof of the kinetic uncertainty relations for quantum transport was actually published in Paper V in a very different context. There, we studied the role of noise in nonequilibrium demons [141, 142], i.e. systems in which a nonthermal contact is used as a resource to decrease the entropy production in the rest of the system, even in the absence of average energy or particle flow from the nonthermal contact. In particular, we showed that the average entropy production in such a nonthermal contact is limited by a combination of its noise and the particle current noise. This constraint was later extended in Paper VI to arbitrary currents, and refined in the form of the KUR. For this reason, we here focus on the results of Paper VI. These follow from applying the simple inequalities

$$x^2 - |x| + \frac{1}{4} \geq 0 \qquad \text{for} \quad x \in \mathbb{R} \tag{4.25a}$$

$$x_1 + x_2 \geq |x_1 - x_2| \qquad \text{for} \quad x_1, x_2 \geq 0 \tag{4.25b}$$

to the noise $S^{(X)}_{\alpha\alpha}$ of the current $I^{(X)}_\alpha$, see Eqs. (3.27) and (3.24), respectively. Then, as one may expect, the classical component of the noise $S^{(X)\mathrm{cl}}_{\alpha\alpha}$ leads to a kinetic uncertainty relation analogue to the one in Eq. (2.53), namely

$$\frac{\left(I^{(X)}_\alpha\right)^2}{S^{(X)\mathrm{cl}}_{\alpha\alpha}} \leq S^{(N)\mathrm{cl}}_{\alpha\alpha} = \Gamma^{\rightarrow}_\alpha + \Gamma^{\leftarrow}_\alpha \equiv \mathcal{K}_\alpha \tag{4.26}$$

where the rates of adding ($\Gamma^{\leftarrow}_\alpha$) or removing a particle ($\Gamma^{\rightarrow}_\alpha$) from reservoir α read

$$\Gamma^{\leftarrow}_\alpha = \frac{1}{h}\int dE \sum_{\beta\neq\alpha} D_{\alpha\beta}(E) f_\beta (1 \pm f_\alpha) \tag{4.27a}$$

$$\Gamma^{\rightarrow}_\alpha = \frac{1}{h}\int dE \sum_{\beta\neq\alpha} D_{\alpha\beta}(E) f_\alpha (1 \pm f_\beta) \tag{4.27b}$$

where the upper sign refers to bosons and the lower to fermions. Here, the activity $\mathcal{K}_\alpha$ only counts the transitions involving reservoir α. Indeed, the transitions that do not involve reservoir α do not contribute to either the current $I^{(X)}_\alpha$ or its noise $S^{(X)}_{\alpha\alpha}$. Thus, we refer to it as a *local* activity, which sets a tighter constraint on the precision compared to the global activity, namely $\mathcal{K}_\alpha \leq \mathcal{K} \equiv \sum_\alpha \mathcal{K}_\alpha$.

Of course, the noise can be well approximated by its classical component only in some specific regimes, for instance in the tunneling regime, where $D_{\alpha\beta} \ll 1$ for $\alpha \neq \beta$, or close to equilibrium, where $f_\beta \approx f_\alpha$. Here, we want to go beyond such approximations and consider the general case, in which the quantum contributions are sizable. Then, to extend the KUR of Eq. (4.26) to the full noise, we need to treat the quantum noise contribution in more detail. Here, the bosonic or fermionic nature of the particles play a crucial role because, for the former, the quantum noise contribution is positive, whereas for the latter it is negative. This difference in sign is a consequence of the bunching or anti-bunching of particles in a multi-particle scattering process.

Let's first focus on the bosonic case. There, we use Cauchy-Schwarz inequality on the space of square-integrable functions to obtain the following lower bound on the quantum noise contribution

$$S^{(X)\mathrm{qu}}_{\alpha\alpha,\mathrm{bos}} = \frac{1}{h}\int dE \left[x_\alpha \sum_\beta D_{\alpha\beta}(f_\beta - f_\alpha)\right]^2 \geq \frac{h}{B^{(X)}_\alpha}\left(I^{(X)}_\alpha\right)^2 \tag{4.28}$$

where we introduced the bandwidth $B^{(X)}_\alpha$ in terms of the characteristic function $\mathbf{1}_A(E)$ of the set $A \equiv \mathrm{supp}\left\{x_\alpha \sum_\beta D_{\alpha\beta}(f_\beta - f_\alpha)\right\}$, namely

$$B^{(X)}_\alpha \equiv \int dE \mathbf{1}_A(E), \qquad \mathbf{1}_A(E) = \begin{cases} 1 & \text{for} \quad E \in A \\ 0 & \text{otherwise} \end{cases}. \tag{4.29}$$

Essentially, the bandwidth is the energy range in which there is, on average, a finite flow (either positive or negative) of the quantity x_α. The bound of Eq. (4.28) then provides a lower limit on the quantum noise contribution for bosonic transport in terms of the average current and the bandwidth. Intuitively, this inequality is saturated when the flows of x_α are equally distributed over the bandwith, such that bunching effects are minimized. However, if the bandwidth becomes infinitely large, $B^{(X)}_\alpha \to \infty$, Eq. (4.28) becomes uninformative since it reduces to the positivity of the quantum noise contribution. Still, even though the bandwidth $B^{(X)}_\alpha$ may be infinite in a mathematical sense, in a realistic setup we expect it to be finite because the contributions at large E are typically exponentially suppressed. For instance, when f_α are Bose-Einstein distributions, their temperature $k_\mathrm{B}T$ sets a natural energy scale cut-off (which depends on the desired accuracy) on the bandwidth because the contributions of energy larger than a multiple of $k_\mathrm{B}T$ can be neglected.

As a next step, we combine the constraint on the quantum noise contribution of Eq. (4.28) with the constraint on the precision of Eq. (4.26) to extend the latter to the full noise. To this end, we use Eq. (4.28) to estimate from above the classical contribution to the noise by means of the "bunching-modified" noise

$$\tilde{S}^{(X)}_{\alpha\alpha,\mathrm{bos}} \equiv S^{(X)}_{\alpha\alpha,\mathrm{bos}} - \frac{h}{B^{(X)}_\alpha}\left(I^{(X)}_\alpha\right)^2 \geq S^{(X)\mathrm{cl}}_{\alpha\alpha,\mathrm{bos}}, \tag{4.30}$$

which is defined in terms of experimentally accessible quantities, namely the full noise, the current, and the bandwidth. With this notion, the classical KUR of Eq. (4.26) is extended to the full noise as

$$\frac{\left(I_\alpha^{(X)}\right)^2}{S_{\alpha\alpha,\mathrm{bos}}^{(X)}} \leq \frac{\tilde{S}_{\alpha\alpha,\mathrm{bos}}^{(N)}}{1+\frac{h}{B_\alpha^{(X)}}\tilde{S}_{\alpha\alpha,\mathrm{bos}}^{(N)}} \leq S_{\alpha\alpha,\mathrm{bos}}^{(N)}. \tag{4.31}$$

Here, the bosonic bunching allows not only to set the full particle noise $S_{\alpha\alpha,\mathrm{bos}}^{(N)}$ as an upper limit on the precision, but also to establish a tighter constraint in terms of the bunching-modified noise.

For fermions, we follow a different approach compared to the one in Eq. (4.28), which is required because the fermionic quantum noise contribution is negative. Using that the fermionic occupation numbers take values between 0 and 1, $f_\alpha \in [0,1]$, we find the following lower bound on the quantum noise contribution

$$S_{\alpha\alpha,\mathrm{fer}}^{(X)\mathrm{qu}} \geq -\frac{1}{h}\int dE\,[x_\alpha]^2\,[1-D_{\alpha\alpha}]\sum_\beta D_{\alpha\beta}|f_\beta - f_\alpha|. \tag{4.32}$$

We first use this inequality on the quantum noise contribution, and only then use the inequalities of Eq. (4.25) to produce a quadratic form. In particular, calling $R_\alpha \equiv \inf_{E\in A} D_{\alpha\alpha}$ the infimum of the reflection probability in the transmission window, we find the following limit on the precision in fermionic systems

$$\frac{\left(I_\alpha^{(X)}\right)^2}{S_{\alpha\alpha,\mathrm{fer}}^{(X)}} \leq \frac{1}{R_\alpha^2} S_{\alpha\alpha,\mathrm{fer}}^{(N)} \geq S_{\alpha\alpha,\mathrm{fer}}^{(N)}. \tag{4.33}$$

Here, the limit on the precision is *not* given by the full particle noise $S_{\alpha\alpha,\mathrm{fer}}^{(N)}$, but it is larger. Indeed, the full particle noise divided by the infimum of the reflection probability squared R_α^2 is the maximum attainable precision. Equations (4.31) and (4.33) showcase the effect that bunching and anti-bunching have on the limits on the precision for bosonic and fermionic transport, respectively. In the bosonic case, bunching effects provide a more restrictive constraint on the precision, whereas the anti-bunching effects provide less restrictive contraints in the fermionic case. This means that fermionic systems can achieve higher precision compared to their bosonic counterparts. In particular, when the reflection probability vanishes, i.e. $R_\alpha = 0$, Eq. (4.33) does not set any limit whatsoever on the precision. In this case, it is possible to drive large average currents in far-from-equilibrium setups while the noise remains small due to Pauli exclusion principle. For example, consider a fully transparent scatterer where a large chemical potential bias $\Delta\mu$ and uniform temperature T is imposed on the contact. Then, the average particle current is proportional to chemical potential bias, $I^{(\mathrm{N})} \propto \Delta\mu$. Instead, in the fully transparent case the noise is simply given by the thermal noise, namely

$S^I \propto T$. Therefore, by increasing the ratio $\Delta\mu/k_\mathrm{B}T$, one can have arbitrarily large precision.

Furthermore, using the same inequalities Eq. (4.25), we also find a different limit on the precision of fermionic currents

$$\frac{\left(I_\alpha^{(X)}\right)^2}{S^{(X)}_{\alpha\alpha,\mathrm{fer}}} \leq \frac{1}{hR_\alpha}\int dE \sum_\beta D_{\alpha\beta}|f_\beta - f_\alpha| \leq \frac{1}{R_\alpha} S^{(N)\mathrm{cl}}_{\alpha\alpha,\mathrm{fer}}. \tag{4.34}$$

Here, unlike Eq. (4.33), the upper limit on the precision scales with R_α^{-1}, but is not expressed with the more accessible full particle noise $S^{(N)}_{\alpha\alpha,\mathrm{fer}}$. Still, Eq. (4.34) is particularly interesting when compared to the precision constraint of Eq. (2.61). There, the precision is limited by $\mathcal{K}/(1-\mathcal{K})$, with $\mathcal{K}$ being the probability of a transition happening. Intuitively, we expect the reflection probability R_α to be connected to $1-\mathcal{K}$, representing the probability of returning into the same state. Similary, the numerator of the precision constraint in Eq. (4.34) is linear in the transmission probabilities $D_{\alpha\beta}$ with $\alpha \neq \beta$ and is expected to be connected to $\mathcal{K}$. However, to confirm this intuition, and establish more concrete connections between the precision limit of Eq. (2.61) and not only the results of this section, but also other formulations of the KUR in, for instance, open quantum systems [22, 27], more work is required.

5 Conclusion

5.1 Summary

In this thesis we first discussed out-of-equilibrium fluctuations in the context of two-point measurement scheme, to then describe transport statistics from the same perspective. This approach provides a broader context for the constraints on the out-of-equilibrium noise derived in the appended papers and discussed in chapter 4, and allows us to compare both results and techniques with the ones previously known, and discussed in chapter 2.

In particular, by comparing the out-of-equilibrium setup with the same setup under (hot) equilibrium conditions, we find constraints on the noise as discussed in Sec. 4.1 and Sec. 4.2. Unlike the fluctuation-dissipation theorem presented in Sec. 2.3, which links fluctuations and response at equilibrium, these constraints offer additional insights into the out-of-equilibrium fluctuations generated by a temperature bias.

Additionally, we established limits on the precision of currents in a quantum transport setup which recall the kinetic uncertainty relation. Specifically, we find that the upper limit on the precision is given by the particle current noise, and is enhanced for fermions and diminished for bosons.

Crucially, all the results discussed in this thesis apply to the out-of-equilibrium noise, which plays an important role in characterizing the performance of small-scale engines.

5.2 Open questions

Throughout the thesis, some of the questions opened (or left open) in this thesis have beed identified. For instance, in Sec. 4.2 we pointed out how Paper III and Paper IV are based on comparing a system under a temperature bias with the same system without the bias. However, the resulting constraints differ, see Eq. (4.2) and Eq. (4.20). Intuitively, we expect that adding assumptions on the Hamiltonians considered in Paper IV allows to recover the results of Paper III. However, what are the (strictly) necessary condition is not known.

Furthermore, we mentioned how systems described by steady-state scattering theory can exhibit violations of the thermodynamic uncertainty relation. It is important to stress that such violations have been seen when using the thermo-

dynamic entropy production rate, see Sec. 3.1.2. Therefore, we expect the TUR to be preserved when the stochastic entropy change discussed in Sec. 2.4.1 is used. Then, clarifying the connection of this entropy change to the thermodynamic entropy production rate, as well as to non-Markovian dynamics would be interesting.

In the case of the kinetic uncertainty relation (KUR), several points need clarification. Even for Markovian open system dynamics, multiple non-equivalent extensions of the classical KUR have been developed [22, 27]. Giving an intuitive definition to the activity in the quantum case, where both jumps and coherent dynamics take place, remains challenging. This challenge persists in the quantum transport setup studied in Paper VI. There, we instead formulated the precision bounds in terms of the particle current noise, which corresponds to the activity only in the classical limit. However, a concrete connection between the particle current noise and the probability of a transition happening, which we discussed in Sec. 2.4.2, is still missing.

Finally, a natural question emerging from the results of Paper III is whether a generalization to periodically driven systems is possible. Although this is an ongoing project and not included in the thesis, preliminary findings suggest that it is indeed possible to extend the results to the driven case. The generalization leads to results similar to the multi-terminal case, with contributions from all Floquet quanta of the driving.

Appendices

Appendix A

Thermodynamic uncertainty relation in a multi-measurement process

The thermodynamic uncertainty relation also holds for processes in which many consecutive measurements take place. This generalizes the two-point measurement scheme by repeating the application of a (possibly different) unitary transformation followed by a measurement, as sketched in Fig. A.1(a). Calling $\rho(0)$ the initial state, $\hat{\mathcal{U}}_i$ the applied unitary transformation between times t_{i-1} and t_i, and $\{\hat{\Pi}_a^{(i)}\}_a$ the complete set of projectors describing the measurement at time t_i, we sequentially combine the unitary evolution Eq. (2.2) with a transformation induced by the measurements, Eq. (2.5), to calculate the probability of a single realization of the process. Calling a_i the outcome of the i-th measurement, the stochastic trajectory $\gamma = (a_n, t_n; \dots; a_1, t_1; a_0, t_0)$ happens with probability

$$\begin{aligned} p[\gamma] &= p(a_n, t_n; \dots; a_1, t_1; a_0, t_0) \\ &= \mathrm{Tr}\left\{\hat{\Pi}_{a_n}^{(n)}\hat{\mathcal{U}}_n \cdots \hat{\Pi}_{a_1}^{(1)}\hat{\mathcal{U}}_1\hat{\Pi}_{a_0}^{(0)}\rho(0)\hat{\Pi}_{a_0}^{(0)}\hat{\mathcal{U}}_1^\dagger\hat{\Pi}_{a_1}^{(1)}\cdots\hat{\mathcal{U}}_n^\dagger\hat{\Pi}_{a_n}^{(n)}\right\}. \end{aligned} \tag{A.1}$$

Then, in the same fashion as in the two-point measurement case, we consider "current-like" observables Q, which are anti-symmetric under the inversion of the outcome order, namely

$$Q[\gamma] = -Q[\gamma^*] \tag{A.2}$$

where $\gamma^* = (a_0, t_n; \dots; a_{n-1}, t_1; a_n, t_0)$. Similarly to Eq. (2.43), we define the entropy change at the trajectory level by comparing the probability of the forward protocol $p[\gamma]$, with the probability $p[\gamma^*]$ of observing the outcomes in the opposite order,

$$\tilde{\sigma}[\gamma] \equiv \log\left(\frac{p[\gamma]}{p[\gamma^*]}\right). \tag{A.3}$$

Again, we stress here that this entropy change is generally different from the one obtained by comparing the forward and the time-reversed processes. Indeed, as sketched in Fig. A.1(b), the "opposite" process differs from the forward one only in the order of the outcomes, not on the order at which measurements and unitary transformations are applied.

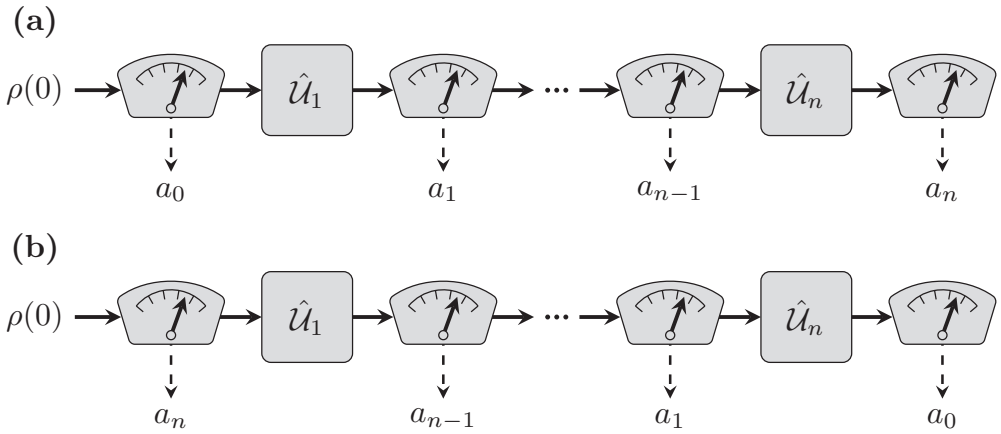

Figure A.1: (a) *Forward multi-measurement process. The initial state* $\rho(0)$ *undergoes a series of measurements and unitary transformations. In a single realization, the measurements have oucomes* $a_0, \ldots, a_n$.**(b)** *"Opposite" multi-measurement process. The initial state* $\rho(0)$ *undergoes the same series of measurements and unitary transformations as in the forward process, but the order of the measurement outcomes* $a_n, \ldots, a_0$ *is inverted.*

Then, applying the same techniques as discussed in the two-point measurement case, the thermodynamic uncertainty relation takes on the same forms, i.e. Eq. (2.50).

Appendix B

Scattering theory revisited

In this Appendix detailed derivations that complement Sec. 3.1 are provided.

B.1 Reduced conditional state and probability

B.1.1 Fermionic scattering

For fermionic particles we use the anticommutation relation of the creation operators to write the scattering evolution of Eq. (3.5) as

$$|\overrightarrow{\alpha i}\rangle \to \sum_{\beta_1 j_1 < \cdots < \beta_k j_k} \det\left[S^{\overrightarrow{\beta j}}_{\overrightarrow{\alpha i}}\right] |\overrightarrow{\beta j}\rangle \tag{B.1}$$

where $|\overrightarrow{\alpha i}\rangle \equiv \hat{c}^\dagger_{\alpha_1 i_1} \cdots \hat{c}^\dagger_{\alpha_k i_k} |\varnothing\rangle$, and $\det\left[S^{\overrightarrow{\beta j}}_{\overrightarrow{\alpha i}}\right]$ is the determinant of the matrix

$$S^{\overrightarrow{\beta j}}_{\overrightarrow{\alpha i}} \equiv \begin{pmatrix} s_{\beta_1 j_1, \alpha_1 i_1} & \cdots & s_{\beta_1 j_1, \alpha_k i_k} \\ \vdots & \ddots & \vdots \\ s_{\beta_k j_k, \alpha_1 i_1} & \cdots & s_{\beta_k j_k, \alpha_k i_k} \end{pmatrix}. \tag{B.2}$$

In Eq. (B.1) the summation over the lead-channel indices $\beta_1 j_1, \cdots, \beta_k j_k$ is restricted to the k-tuples ordered lexicographically. This ordering is defined through

$$\beta j < \gamma l \quad \Leftrightarrow \quad \begin{cases} \beta < \gamma, \\ \beta = \gamma, \quad j < l, \end{cases} \tag{B.3}$$

where we recall that the lead indices take values in $\{1, \cdots, r\}$, and the channel indices of lead β take values in $\{1, \cdots, M_\beta\}$. Without loss of generality, we calculate the marginal state on lead 1 given the initial state $\overrightarrow{\alpha i}$. To do so, we need to evaluate the partial trace on all other leads

$$\rho_{1|\overrightarrow{\alpha i}} = \mathrm{Tr}_{\overline{1}} \left\{ \sum_{\beta_1 j_1 < \cdots < \beta_k j_k} \sum_{\gamma_1 l_1 < \cdots < \gamma_k l_k} \det[S^{\overrightarrow{\beta j}}_{\overrightarrow{\alpha i}}] \det[S^{\overrightarrow{\gamma l}}_{\overrightarrow{\alpha i}}]^* \, |\overrightarrow{\beta j}\rangle\langle\overrightarrow{\gamma l}| \right\}. \tag{B.4}$$

Crucially, the trace only acts on the ketbra $|\overrightarrow{\beta j}\rangle\langle\overrightarrow{\gamma l}|$. In particular, if the states $|\overrightarrow{\beta j}\rangle$ and $|\overrightarrow{\gamma l}\rangle$ have different numbers of particles in lead 1, the trace vanishes because the remaining leads also have different numbers of particles. This is the reason behind the block structure of Eq. (3.10). If instead both states have n particles in lead 1, the trace yields

$$\mathrm{Tr}_{\overline{1}}\left\{|\overrightarrow{\beta j}\rangle\langle\overrightarrow{\gamma l}|\right\} = |\overrightarrow{1x}\rangle\langle\overrightarrow{1y}|\left(\prod_{\xi=1}^{n}\delta_{\beta_\xi,1}\delta_{\gamma_\xi,1}\right)\left(\prod_{\xi=n+1}^{k}\delta_{\beta_\xi j_\xi,\gamma_\xi l_\xi}[1-\delta_{\beta_\xi,1}]\right), \tag{B.5}$$

where the first n lead indices are equal to 1, i.e. $\beta_1 = \gamma_1 = \cdots = \beta_n = \gamma_n = 1$, and we renamed the lead indices $j_1 = x_1, \cdots, j_n = x_n$ and $l_1 = y_1, \cdots, l_n = y_n$, such that $\overrightarrow{1x} = (1x_1, \cdots, 1x_n)$ describes an arrangement of n particles in lead 1. The ordering introduced in Eq. (B.1) guarantees that the only the first n lead indices refer to lead 1. Furthermore, the ordering also generates the Kronecker deltas $\delta_{\beta_\xi j_\xi,\gamma_\xi l_\xi}$ for $\xi = n+1, \cdots, k$ since the remaining particles must be in the same state for the trace to be non-vanishing. Then, the diagonal block in the Fock subspace of n particles reads

$$\rho_{1,n|\overrightarrow{\alpha i}} = \sum_{x_1<\cdots<x_n}\sum_{y_1<\cdots<y_n}\sum_{1M_1<\beta_{n+1}j_{n+1}<\cdots<\beta_k j_k}\det\left[S^{\overrightarrow{1x}\overrightarrow{\beta j}}_{\overrightarrow{\alpha i}}\right]\det\left[S^{\overrightarrow{1y}\overrightarrow{\beta j}}_{\overrightarrow{\alpha i}}\right]^*|\overrightarrow{1x}\rangle\langle\overrightarrow{1y}|\,. \tag{B.6}$$

where $\overrightarrow{1x}\overrightarrow{\beta j} = (1x_1, \cdots, 1x_n, \beta_{n+1}j_{n+1}, \cdots, \beta_k j_k)$ incorporates the constraints emerging from the Kronecker deltas stemming from the partial trace. The last summation in Eq. (B.6) is performed on the remaining $k-n$ lead-channel indices $\beta_{n+1}j_{n+1}, \cdots, \beta_k j_k$ and does not allow them to describe a particle in lead 1 through the constraint $1M_1 < \beta_{n+1}j_{n+1} \cdots < \beta_k j_k$. The matrix in Eq. (B.6) is still cumbersome to work with, and contains too much information if one is interested only in the number of particles after the scattering process. From now on we focus instead on the probability $p_{n|\overrightarrow{\alpha i}}$ of finding n particles after the scattering of the initial state $\overrightarrow{\alpha i}$. As stated in Eq. (3.11), this probability is given by the trace of the corresponding block matrix, namely

$$p_{n|\overrightarrow{\alpha i}} = \mathrm{Tr}\left\{\rho_{1,n|\overrightarrow{\alpha i}}\right\} = \sum_{x_1<\cdots<x_n}\sum_{1M_1<\beta_{n+1}j_{n+1}<\cdots<\beta_k j_k}\left|\det\left[S^{\overrightarrow{1x}\overrightarrow{\beta j}}_{\overrightarrow{\alpha i}}\right]\right|^2. \tag{B.7}$$

Here, we use the properties of the determinant to write this probability in a more convenient form. In particular, the deteminant vanishes when two rows or columns are equal, and its absolute value does not change under the exchange of two rows or columns. This allows us to change the summations from ordered to unrestrained by taking into account the double-counting emerging from the permutation of $x_1, \cdots, x_n$ and $\beta_{n+1}j_{n+1}, \cdots, \beta_k j_k$. This leads to

$$p_{n|\overrightarrow{\alpha i}} = \frac{1}{n!(k-n)!}\sum_{x_1,\cdots,x_n}\sum_{1M_1<\beta_{n+1}j_{n+1},\cdots,\beta_k j_k}\left|\det\left[S^{\vec{1x}\overrightarrow{\beta j}}_{\overrightarrow{\alpha i}}\right]\right|^2. \tag{B.8}$$

Now, we explicitely write the determinants in terms of summations over the permutations of the matrix columns and use the unitarity of the scattering matrix, namely

$$\sum_{\gamma l} s_{\alpha i,\gamma l} s^*_{\beta j,\gamma l} = \sum_{\gamma l} s^*_{\gamma l,\beta j} s_{\gamma l,\alpha i} = \delta_{\alpha i,\beta j}, \tag{B.9}$$

to find

$$\begin{aligned} p_{n|\overrightarrow{\alpha i}} = \frac{1}{n!(k-n)!} \sum_{\sigma,\sigma' \in \mathcal{S}_k} \Bigg\{ (-1)^{\sigma+\sigma'} \left[\prod_{\xi=1}^{n} \left(\sum_x s_{1x,\sigma(\alpha_\xi i_\xi)} s^*_{1x,\sigma'(\alpha_\xi i_\xi)} \right) \right] \times \\ \times \left[\prod_{\xi=n+1}^{k} \left(\delta_{\sigma(\alpha_\xi i_\xi)\sigma'(\alpha_\xi i_\xi)} - \sum_x s_{1x,\sigma(\alpha_\xi i_\xi)} s^*_{1x,\sigma'(\alpha_\xi i_\xi)} \right) \right] \Bigg\}. \end{aligned} \tag{B.10}$$

Note that this form of the conditional probability corresponds to Eq. (3.12) since, for fermions, $\langle \overrightarrow{\alpha i} | \overrightarrow{\alpha i} \rangle = 1$ for all admissible initial states.

The product structure of Eq. (3.12), or equivalently Eq. (B.10), is the key element behind the recursive relation of Eq. (3.13), which we now show. Indeed, for $n < k$, we split off the last term of the second product and expand it, obtaining

$$\begin{aligned} p_{n|\overrightarrow{\alpha i}} = \frac{1}{n!(k-n)!} \sum_{\sigma,\sigma' \in \mathcal{S}_k} \Bigg\{ (-1)^{\sigma+\sigma'} \left[\prod_{\xi=1}^{n} \left(\sum_x s_{1x,\sigma(\alpha_\xi i_\xi)} s^*_{1x,\sigma'(\alpha_\xi i_\xi)} \right) \right] \times \\ \times \left[\prod_{\xi=n+1}^{k-1} \left(\delta_{\sigma(\alpha_\xi i_\xi)\sigma'(\alpha_\xi i_\xi)} - \sum_x s_{1x,\sigma(\alpha_\xi i_\xi)} s^*_{1x,\sigma'(\alpha_\xi i_\xi)} \right) \right] \delta_{\sigma(\alpha_k i_k)\sigma'(\alpha_k i_k)} + \\ - (-1)^{\sigma+\sigma'} \left[\prod_{\xi=1}^{n} \left(\sum_x s_{1x,\sigma(\alpha_\xi i_\xi)} s^*_{1x,\sigma'(\alpha_\xi i_\xi)} \right) \right] \left(\sum_x s_{1x,\sigma(\alpha_k i_k)} s^*_{1x,\sigma'(\alpha_k i_k)} \right) \times \\ \times \left[\prod_{\xi=n+1}^{k-1} \left(\delta_{\sigma(\alpha_\xi i_\xi)\sigma'(\alpha_\xi i_\xi)} - \sum_x s_{1x,\sigma(\alpha_\xi i_\xi)} s^*_{1x,\sigma'(\alpha_\xi i_\xi)} \right) \right] \Bigg\}. \end{aligned} \tag{B.11}$$

Here, we notice that the first contribution resembles the probability of having n particles in lead 1 after the scattering process of an initial state that has $k-1$ of the k particles of $\overrightarrow{\alpha i}$. In particular, the Kronecker delta $\delta_{\sigma(\alpha_k i_k)\sigma'(\alpha_k i_k)}$ selecs only the permutations that can be decomposed as

$$\sigma = \tilde{\sigma} \circ \pi_x, \qquad \sigma' = \tilde{\sigma}' \circ \pi_x$$

with π_x exchanging x and k, and $\tilde{\sigma}, \tilde{\sigma}'$ being permutations of the $k-1$ elements that do not include x. Then, the sign associated to the permutations fulfils $(-1)^{\sigma+\sigma'} = (-1)^{\tilde{\sigma}+\tilde{\sigma}'}$, and we can reduce the summation from the permutations of k elements to the permutations of $k-1$ elements. The second contribution of Eq. (B.11) is instead proportional to the probability of having $n+1$ particles in lead 1 after

the scattering process of the initial state $\overrightarrow{\alpha i}$. Combining everything together we get the recursive relation of Eq. (3.13), namely

$$p_{n|\overrightarrow{\alpha i}} = \frac{1}{k-n}\sum_{x=1}^{k} p_{n|\overrightarrow{\alpha i}\setminus\{\alpha_x,i_x\}} - \frac{n+1}{k-n}p_{n+1|\overrightarrow{\alpha i}}, \qquad \text{for} \quad n<k, \tag{B.12}$$

where $\overrightarrow{\alpha i}\setminus\{\alpha_x,i_x\}$ denotes the state $\overrightarrow{\alpha i}$ *without* the x-th particle.

To solve this recursive relation a boundary condition is required. This is given by the probability of having all the particles in the initial state in the desired lead after the scattering process. For fermions, this is given by setting $n=k$ in Eq. (B.10) and reads

$$p_{k|\overrightarrow{\alpha i}} = \frac{1}{k!}\sum_{x_1,\cdots,x_k}\left|\det\left[S^{\overrightarrow{1x}}_{\overrightarrow{\alpha i}}\right]\right|^2. \tag{B.13}$$

Note that, if there are more fermions than the number of channels in the lead, i.e. $k>M_1$, then the probability $p_{k|\overrightarrow{\alpha i}}$ must vanish because of Pauli exclusion principle. This is confirmed in the presence of the determinants in Eq. (B.13), which, for $k>M_1$, vanish because (by pidgeonhole principle) at least two rows of the matrices considered are equal.

B.1.2 Bosonic scattering

For bosonic particles we use the commutation of the creation operators to write the scattering evolution of Eq. (3.5) as

$$|\overrightarrow{\alpha i}\rangle \to \sum_{\beta_1 j_1\le\cdots\le\beta_k j_k}\frac{\operatorname{perm}\left[S^{\overrightarrow{\beta j}}_{\overrightarrow{\alpha i}}\right]}{\langle\overrightarrow{\beta j}|\overrightarrow{\beta j}\rangle}|\overrightarrow{\beta j}\rangle \tag{B.14}$$

where instead of the determinant we now have the permanent of the matrix given in Eq. (B.2). Furthermore, since the indices $\beta_x j_x$ can now take on the same value, to avoid double-counting, we divide the permanent by

$$\langle\overrightarrow{\beta j}|\overrightarrow{\beta j}\rangle = n_{11}^{\overrightarrow{\beta j}}!\cdots n_{rM_r}^{\overrightarrow{\beta j}}! \tag{B.15}$$

where $n_{\gamma l}^{\overrightarrow{\beta j}}$ is the number of particles in lead γ, channel l in the state $|\overrightarrow{\beta j}\rangle$. As for the fermionic case, we calculate without loss of generality the marginal state on lead 1, namely

$$\rho_{1|\overrightarrow{\alpha i}} = \frac{1}{\langle\overrightarrow{\alpha i}|\overrightarrow{\alpha i}\rangle}\operatorname{Tr}_{\bar{1}}\left\{\sum_{\beta_1 j_1\le\cdots\le\beta_k j_k}\sum_{\gamma_1 l_1\le\cdots\le\gamma_k l_k}\frac{\operatorname{perm}\left[S^{\overrightarrow{\beta j}}_{\overrightarrow{\alpha i}}\right]}{\langle\overrightarrow{\beta j}|\overrightarrow{\beta j}\rangle}\frac{\operatorname{perm}\left[S^{\overrightarrow{\gamma l}}_{\overrightarrow{\alpha i}}\right]^*}{\langle\overrightarrow{\gamma l}|\overrightarrow{\gamma l}\rangle}|\overrightarrow{\beta j}\rangle\langle\overrightarrow{\gamma l}|\right\}, \tag{B.16}$$

where the prefactor $\langle\overrightarrow{\alpha i}|\overrightarrow{\alpha i}\rangle^{-1}$ guarantees the normalization of the density matrix. Again, we first evaluate the partial trace since it only acts on the ketbra $|\overrightarrow{\beta j}\rangle\langle\overrightarrow{\gamma l}|$. As in the fermionic case, the bra and the ket may have different numbers of particles in each channel, but the *total* number of particles in lead 1 must be equal for the trace not to vanish. As for the fermionic case, this is what leads to the block structure in the Fock basis of the reduced density matrix, see Eq. (3.10). Thus, calling n the number of particles in lead 1 for both $\overrightarrow{\beta j}$ and $\overrightarrow{\gamma l}$, the partial trace reads

$$\begin{aligned}\mathrm{Tr}_{\overline{1}}\left\{|\overrightarrow{\beta j}\rangle\langle\overrightarrow{\gamma l}|\right\} = |\overrightarrow{1x}\rangle\langle\overrightarrow{1y}|\left(\prod_{\xi=1}^{n}\delta_{\beta_\xi,1}\delta_{\gamma_\xi,1}\right)\times \\ \times\left(\prod_{\xi=n+1}^{k}\delta_{\beta_\xi j_\xi,\gamma_\xi l_\xi}[1-\delta_{\beta_\xi,1}]\right) n_{21}^{\overrightarrow{\beta j}}!\cdots n_{rM_r}^{\overrightarrow{\beta j}}!,\end{aligned} \tag{B.17}$$

where the ordering introduced in Eq. (B.14) guarantees the first n lead indices β_ξ, γ_ξ for $\xi = 1, \cdots, n$ to be equal to 1. The remaining $k-n$ particles in both ket and bra must be described by the same collection of indices. Here, the factor $n_{21}^{\overrightarrow{\beta j}}!\cdots n_{rM_r}^{\overrightarrow{\beta j}}!$ appears because the states $|\overrightarrow{\beta j}\rangle$ are not normalized in the bosonic case. Then, the diagonal block in the Fock subspace of n particles reads

$$\rho_{1,n|\overrightarrow{\alpha i}} = \frac{1}{\langle\overrightarrow{\alpha i}|\overrightarrow{\alpha i}\rangle}\sum_{\substack{x_1\leq\cdots\leq x_n\\ y_1\leq\cdots\leq y_n\\ 1M_1<\beta_{n+1}j_{n+1}\leq\cdots\leq\beta_k j_k}}\frac{\mathrm{perm}\left[S_{\overrightarrow{\alpha i}}^{\overrightarrow{1x}\overrightarrow{\beta j}}\right]\mathrm{perm}\left[S_{\overrightarrow{\alpha i}}^{\overrightarrow{1y}\overrightarrow{\beta j}}\right]^*}{\langle\overrightarrow{1x}\overrightarrow{\beta j}|\overrightarrow{1x}\overrightarrow{\beta j}\rangle\,\langle\overrightarrow{1y}|\overrightarrow{1y}\rangle}|1\vec{x}\rangle\langle 1\vec{y}|\,, \tag{B.18}$$

where $\overrightarrow{1x}\overrightarrow{\beta j} = (1x_1, \cdots, 1x_n, \beta_{n+1}j_{n+1}, \cdots, \beta_k j_k)$ incorporates the constraints emerging from the Kronecker deltas stemming from the partial trace. Again, the block matrix of Eq. (B.18) is cumbersome to work with, especially if one is interested in the number of particles transferred during the scattering process. In that case, the probability $p_{n|\overrightarrow{\alpha i}}$ of having n particles in the lead after the scattering of the initial state $\overrightarrow{\alpha i}$ is sufficient. This probability is given by the trace of the block matrix $\rho_{1,n|\overrightarrow{\alpha i}}$ and reads

$$p_{n|\overrightarrow{\alpha i}} = \mathrm{Tr}\left\{\rho_{1,n|\overrightarrow{\alpha i}}\right\} = \frac{1}{\langle\overrightarrow{\alpha i}|\overrightarrow{\alpha i}\rangle}\sum_{\substack{x_1\leq\cdots\leq x_n\\ 1M_1<\beta_{n+1}j_{n+1}\leq\cdots\leq\beta_k j_k}}\frac{\left|\mathrm{perm}\left[S_{\overrightarrow{\alpha i}}^{\overrightarrow{1x}\overrightarrow{\beta j}}\right]\right|^2}{\langle\overrightarrow{1x}\overrightarrow{\beta j}|\overrightarrow{1x}\overrightarrow{\beta j}\rangle}. \tag{B.19}$$

Here, we use the properties of the permanent to write this probability in a more convenient form. In particular, the permanent does not change when two rows or columns are exchanged. This allows us to change the summations from ordered

to unrestrained by taking into account the double-counting emerging from the permutations of $x_1, \cdots, x_n$ and $\beta_{n+1} j_{n+1}, \cdots, \beta_k j_k$. This leads to

$$\begin{aligned} p_{n|\overrightarrow{\alpha i}} &= \frac{1}{\langle \overrightarrow{\alpha i} | \overrightarrow{\alpha i} \rangle} \sum_{\substack{x_1, \cdots, x_n \\ 1 M_1 < \beta_{n+1} j_{n+1}, \cdots, \beta_k j_k}} \frac{\langle \overrightarrow{1 x \beta j} | \overrightarrow{1 x \beta j} \rangle}{n!(k-n)!} \frac{\left| \mathrm{perm} \left[S^{\overrightarrow{1 x \beta j}}_{\overrightarrow{\alpha i}} \right] \right|^2}{\langle \overrightarrow{1 x \beta j} | \overrightarrow{1 x \beta j} \rangle} \\ &= \binom{k}{n} \frac{1}{k! \, \langle \overrightarrow{\alpha i} | \overrightarrow{\alpha i} \rangle} \sum_{\substack{x_1, \cdots, x_n \\ 1 M_1 < \beta_{n+1} j_{n+1}, \cdots, \beta_k j_k}} \left| \mathrm{perm} \left[S^{1 \overrightarrow{x \beta j}}_{\overrightarrow{\alpha i}} \right] \right|^2 , \end{aligned} \tag{B.20}$$

where the factor $\langle \overrightarrow{1 x \beta j} | \overrightarrow{1 x \beta j} \rangle$ at the numerator stems from counting the permutations with repeated indices. Now, we explicitely write the permanents in terms of summations over the permutations of the matrix columns and use the unitarity of the scattering matrix [Eq. (B.9)] to find

$$\begin{aligned} p_{n|\overrightarrow{\alpha i}} = \binom{k}{n} \frac{1}{k! \, \langle \overrightarrow{\alpha i} | \overrightarrow{\alpha i} \rangle} \sum_{\sigma, \sigma' \in \mathcal{S}_k} \Bigg\{ \Bigg(\prod_{\xi=1}^{n} \sum_x s_{1x, \sigma(\alpha_\xi i_\xi)} s^*_{1x, \sigma'(\alpha_\xi i_\xi)} \Bigg) \times \\ \times \Bigg(\prod_{\xi=n+1}^{k} \Big[\delta_{\sigma(\alpha_\xi i_\xi), \sigma'(\alpha_\xi i_\xi)} - \sum_x s_{1x, \sigma(\alpha_\xi i_\xi)} s^*_{1x, \sigma'(\alpha_\xi i_\xi)} \Big] \Bigg) \Bigg\} , \end{aligned} \tag{B.21}$$

which corresponds to Eq. (3.12).

In the same fashion as the fermionic case, we use the product structure of Eq. (B.21) to show that the recursive relation Eq. (3.13) holds. For $n < k$, we split off the last term of the product and expand it as

$$\begin{aligned} p_{n|\overrightarrow{\alpha i}} = \binom{k}{n} \frac{1}{k! \, \langle \overrightarrow{\alpha i} | \overrightarrow{\alpha i} \rangle} \sum_{\sigma, \sigma' \in \mathcal{S}_k} \Bigg\{ \delta_{\sigma(\alpha_k i_k), \sigma'(\alpha_k i_k)} \Bigg(\prod_{\xi=1}^{n} \sum_x s_{1x, \sigma(\alpha_\xi i_\xi)} s^*_{1x, \sigma'(\alpha_\xi i_\xi)} \Bigg) \times \\ \times \Bigg(\prod_{\xi=n+1}^{k-1} \Big[\delta_{\sigma(\alpha_\xi i_\xi), \sigma'(\alpha_\xi i_\xi)} - \sum_x s_{1x, \sigma(\alpha_\xi i_\xi)} s^*_{1x, \sigma'(\alpha_\xi i_\xi)} \Big] \Bigg) + \\ - \Bigg(\prod_{\xi=1}^{n} \sum_x s_{1x, \sigma(\alpha_\xi i_\xi)} s^*_{1x, \sigma'(\alpha_\xi i_\xi)} \Bigg) \Bigg[\sum_x s_{1x, \sigma(\alpha_k i_k)} s^*_{1x, \sigma'(\alpha_k i_k)} \Bigg] \times \\ \times \Bigg(\prod_{\xi=n+1}^{k-1} \Big[\delta_{\sigma(\alpha_\xi i_\xi), \sigma'(\alpha_\xi i_\xi)} - \sum_x s_{1x, \sigma(\alpha_\xi i_\xi)} s^*_{1x, \sigma'(\alpha_\xi i_\xi)} \Big] \Bigg) \Bigg\} . \end{aligned} \tag{B.22}$$

Here, we notice that the first contribution resembles the probability of having n particles in lead 1 after the scattering process of an initial state that has $k-1$ of the k particles of $\overrightarrow{\alpha i}$. In particular, the Kronecker delta $\delta_{\sigma(\alpha_k i_k) \sigma'(\alpha_k i_k)}$ tells us which particle has been removed from the state $\overrightarrow{\alpha i}$. Let the permutation σ map the k-th label into the x-th label, i.e. $\sigma(\alpha_k i_k) = \alpha_x i_x$. Since we are dealing with

bosons, the final label is repeated $n^{\overrightarrow{\alpha i}}_{\alpha_x i_x} \geq 1$ times, meaning that there can be multiple particles in the same state. Then, the second permutation σ' can map the k-th label into $n^{\overrightarrow{\alpha i}}_{\alpha_x i_x}$ different labels while fulfilling the condition imposed by the Kronecker delta. Luckily, this additional multiplicity combines with the norm of $|\overrightarrow{\alpha i}\rangle$ as

$$\frac{n^{\overrightarrow{\alpha i}}_{\alpha_x i_x}}{\langle \overrightarrow{\alpha i}|\overrightarrow{\alpha i}\rangle} = \frac{1}{\langle \overrightarrow{\alpha i} \setminus \{\alpha_x i_x\}|\overrightarrow{\alpha i} \setminus \{\alpha_x i_x\}\rangle},$$

leading to the norm of the initial state with $k-1$ particles. The second contribution of Eq. (B.22) is directly proportional to the probability of having $n+1$ particles in lead 1 after the scattering of the initial state $\overrightarrow{\alpha i}$. Combining everything together we get the recursive relation of Eq. (3.13), namely

$$p_{n|\overrightarrow{\alpha i}} = \frac{1}{k-n}\sum_{x=1}^{k} p_{n|\overrightarrow{\alpha i}\setminus\{\alpha_x,i_x\}} - \frac{n+1}{k-n} p_{n+1|\overrightarrow{\alpha i}}, \qquad \text{for } n < k, \tag{B.23}$$

which is exactly the same as the fermionic one. The difference between the fermionic and bosonic case stems from the boundary condition necessary to solve for the probabilities. In the bosonic case, the boundary condition for $n = k$ reads

$$p_{k|\overrightarrow{\alpha i}} = \frac{1}{k!\,\langle \overrightarrow{\alpha i}|\overrightarrow{\alpha i}\rangle} \sum_{\sigma,\sigma'\in\mathcal{S}_k} \left(\prod_{\xi=1}^{k} \sum_{x} s_{1x,\sigma(\alpha_\xi i_\xi)} s^{*}_{1x,\sigma'(\alpha_\xi i_\xi)} \right). \tag{B.24}$$

B.1.3 Useful properties of the conditional probability

Since both fermionic and bosonic scattering processes exhibit the same recursive relation on the conditional probabilities, it is useful to look into what properties of expectation values emerge from such a recursive relation. In particular, we consider here expectation values of a variable $f_0(n, \overrightarrow{\alpha i})$, i.e.

$$\sum_{\overrightarrow{\alpha i}} \sum_{n} f_0(n, \overrightarrow{\alpha i}) p_{n|\overrightarrow{\alpha i}} p_{\overrightarrow{\alpha i}} = \sum_{k=0}^{\infty} \sum_{\overrightarrow{\alpha i}, |\overrightarrow{\alpha i}|=k} \left(\sum_{n=0}^{k} f_0(n, \overrightarrow{\alpha i}) p_{n|\alpha i} \right) p_{\overrightarrow{\alpha i}}, \tag{B.25}$$

where we ordered the sum according to the number of particles $|\overrightarrow{\alpha i}|$ in the initial state. Here, we focus on the summation over the final number of particles n because it contains the conditional probability. Furthermore, to ease the notation, we drop the $\overrightarrow{\alpha i}$ dependence of the function f_0 that we are calculating the expectation value of.

The goal is to write the conditioned expectation value as a sum over the boundary conditions of the conditional probabilities. To this end, we start by "unravel-

ing" the conditional probabilities with the recursive relation,

$$\begin{aligned}
\sum_{n=0}^{k} f_0(n) p_{n|\overrightarrow{\alpha i}} &= f_0(k) p_{k|\overrightarrow{\alpha i}} + \sum_{n=0}^{k-1} f_0(n) p_{n|\overrightarrow{\alpha i}} \\
&= f_0(k) p_{k|\overrightarrow{\alpha i}} + \sum_{n=0}^{k-1} \frac{f_0(n)}{k-n} \left(\sum_{x=1}^{k} p_{n|\overrightarrow{\alpha i}\setminus\{\alpha_x i_x\}} - (n+1) p_{n+1|\overrightarrow{\alpha i}} \right) \\
&= f_0(k) p_{k|\overrightarrow{\alpha i}} + \left[\sum_{n=0}^{k-1} \frac{f_0(n)}{k-n} \sum_{x=1}^{k} p_{n|\overrightarrow{\alpha i}\setminus\{\alpha_x i_x\}} \right] - \sum_{n=0}^{k} \frac{n f_0(n-1)}{k-n+1} p_{n|\overrightarrow{\alpha i}} \\
&= \left[f_0(k) - k f_0(k-1) \right] p_{k|\overrightarrow{\alpha i}} + \left[\sum_{n=0}^{k-1} \frac{f_0(n)}{k-n} \sum_{x=1}^{k} p_{n|\overrightarrow{\alpha i}\setminus\{\alpha_x i_x\}} \right] + \\
&\quad - \sum_{n=0}^{k-1} \frac{n f_0(n-1)}{k-n+1} p_{n|\overrightarrow{\alpha i}}
\end{aligned} \tag{B.26}$$

and so on. The end result reads

$$\sum_{n=0}^{k} f_0(n) p_{n|\overrightarrow{\alpha i}} = \left[\sum_{i=0}^{k} (-1)^i f_0(k-i) \binom{k}{i} \right] p_{k|\overrightarrow{\alpha i}} + \sum_{n=0}^{k-1} f_1(n) \sum_{x=1}^{k} p_{n|\overrightarrow{\alpha i}\setminus\{\alpha_x i_x\}}, \tag{B.27}$$

where

$$f_1(n) \equiv \sum_{i=0}^{n} \frac{(-1)^i f_0(n-i)}{k\binom{k-1}{n}} \binom{k}{n-i}. \tag{B.28}$$

For completeness, we now prove Eq. (B.27) by manipulating the right-hand side. First, we use the recursive relation Eq. (3.13) on the conditional probabilities to write the right-hand side of Eq. (B.27) as

$$\begin{aligned}
\text{RHS} &= \left[\sum_{i=0}^{k} (-1)^i f_0(k-i) \binom{k}{i} \right] p_{k|\overrightarrow{\alpha i}} + \sum_{n=0}^{k-1} f_1(n) \left[(k-n) p_{n|\overrightarrow{\alpha i}} + (n+1) p_{n+1|\overrightarrow{\alpha i}} \right] \\
&= \left[\sum_{i=0}^{k} (-1)^i f_0(k-i) \binom{k}{i} \right] p_{k|\overrightarrow{\alpha i}} + \\
&\quad + \sum_{n=0}^{k-1} \left[f_1(n)(k-n) + f_1(n-1) n \right] p_{n|\overrightarrow{\alpha i}} + f_1(k-1) k p_{k|\overrightarrow{\alpha i}}.
\end{aligned} \tag{B.29}$$

Here, we have two contributions: one proportional to $p_{k|\overrightarrow{\alpha i}}$ and one to $p_{n\neq k|\overrightarrow{\alpha i}}$.

Let's treat them separately. The first contribution has the proportionality factor

$$\begin{aligned}
&\left[\sum_{i=0}^{k}(-1)^i f_0(k-i)\binom{k}{i}\right] + f_1(k-1)k = \\
&\quad= \left[\sum_{i=0}^{k}(-1)^i f_0(k-i)\binom{k}{i}\right]\sum_{i=0}^{k-1}(-1)^i f_0(k-1-i)\binom{k}{k-1-i} \\
&\quad= f_0(k) - \sum_{i=0}^{k-1}(-1)^i f_0(k-1-i)\left[\binom{k}{1+i} - \binom{k}{k-1-i}\right] \\
&\quad= f_0(k),
\end{aligned} \tag{B.30}$$

where we used the definition of $f_1(n)$ and the symmetry property of the binomial coefficient $\binom{k}{n} = \binom{k}{k-n}$. The second contribution has the proportionality factor

$$\begin{aligned}
&f_1(n)(k-n) + f_1(n-1)n = \\
&= \sum_{i=0}^{n}\frac{(-1)^i f_0(n-i)(k-n)}{k\binom{k-1}{n}}\binom{k}{n-i} + \sum_{i=0}^{n-1}\frac{(-1)^i f_0(n-1-i)n}{k\binom{k-1}{n-1}}\binom{k}{n-1-i} \\
&= \frac{f_0(n)(k-n)}{k\binom{k-1}{n}}\binom{k}{n} - \sum_{i=0}^{n-1}(-1)^i f_0(n-1-i)\binom{k}{n-1-i}\left[\frac{k-n}{k\binom{k-1}{n}} - \frac{n}{k\binom{k-1}{n-1}}\right] \\
&= f_0(n),
\end{aligned} \tag{B.31}$$

where the square-bracket contribution vanishes. Putting everything together we have indeed proven Eq. (B.27) using the recursive relation Eq. (3.13).

Note that Eq. (B.27) is still a recursive relation: The expectation value given an initial state $\overrightarrow{\alpha i}$ of k particles is given in terms of the boundary condition, i.e. having all k particles in the final state, *and* in terms of the expectation values of a possibly different function given the initial states with $k-1$ particles obtained from $\overrightarrow{\alpha i}$ by removing one of its particles. For some relevant choices of f_0, additional calculations are carried out below.

Normalization of probabilities

An instructive example is given by considering $f_0(n) = 1$. In this case, the expectation value

$$\sum_{n=0}^{k} p_{n|\overrightarrow{\alpha i}} = 1$$

because the probabilities are normalized. Here, we verify that this is the case given the recursive relation of Eq. (B.27). The first step is finding $f_1(n)$, namely

$$f_1(n) = \sum_{i=0}^{n}\frac{(-1)^i}{k\binom{k-1}{n}}\binom{k}{n-i} = \frac{1}{k\binom{k-1}{n}}\binom{k-1}{n} = \frac{1}{k} \tag{B.32}$$

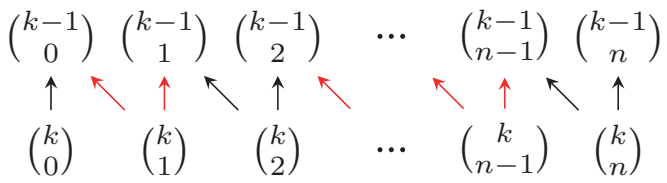

Figure B.1: *Two consecutive rows of Pascal triangle. The sum in Eq. (B.32) runs over the lower row with alternate signs. Each entry in the lower row is given by the sum of two entries in the upper row depicted with the arrows. Black and red arrows indicate opposite signs in the sum. The only contribution that does not cancel out is therefore* $\binom{k-1}{n}$.

where we used the property

$$\binom{k}{n} + \binom{k}{n+1} = \binom{k+1}{n+1}$$

to identify a telescopic sum on the Pascal triangle, as shown in Fig. B.1. Furthermore, the $p_{k|\overrightarrow{\alpha i}}$ contribution vanishes whenever $k > 0$ since

$$\sum_{i=0}^{k} (-1)^k \binom{k}{i} = (1-1)^k = 0.$$

With these considerations, we find

$$\begin{aligned}
\sum_{n=0}^{k} p_{n|\overrightarrow{\alpha i}} &= \frac{1}{k} \sum_{n=0}^{k-1} \sum_{x_1=1}^{k} p_{n|\overrightarrow{\alpha i}\setminus\{\alpha_{x_1} i_{x_1}\}} \\
&= \frac{1}{k(k-1)} \sum_{n=0}^{k-2} \sum_{x_1=1}^{k} \sum_{x_2=1, x_2\neq x_1}^{k} p_{n|\overrightarrow{\alpha i}\setminus\{\alpha_{x_1} i_{x_1}\}\setminus\{\alpha_{x_2} i_{x_2}\}} \\
&= \frac{1}{k!} \sum_{x_1} \sum_{x_2\neq x_1} \cdots \sum_{x_k\neq x_1,\cdots,x_{k-1}} p_{0|\varnothing} = 1,
\end{aligned} \tag{B.33}$$

where we are removing, one by one, each particle in the initial state $\overrightarrow{\alpha i}$. In the last step we used that the probability $p_{0|\varnothing}$ of having 0 particles in the lead after the scattering process of 0 initial particle is unity, i.e. $p_{0|\varnothing} = 1$. Then, the summations reduce to counting in how many ways we can remove the particles from the initial state, leading to $k!$.

Average of n

To calculate the average number of transferred particles in the scattering process we need to know the expectation value of the final number of particles n. Therefore, let's study the case $f_0(n) = n$. Using the following property of the binomial

coefficients

$$n\binom{k}{n} = k\binom{k-1}{n-1},$$

we see that $f_1(n)$ reads

$$f_1(n) = \sum_{i=0}^{n} \frac{(-1)^i(n-i)}{k\binom{k-1}{n}} \binom{k}{n-i} = \sum_{i=0}^{n} \frac{(-1)^i}{\binom{k-1}{n}} \binom{k-1}{n-1-i} = \frac{\binom{k-2}{k-1}}{\binom{k-1}{n}} = \frac{n}{k-1}, \tag{B.34}$$

where once again we identified the telescopic sum on the Pascal triangle, see Fig. B.1. Crucially, $f_1(n) \propto f_0(n)$, as was also the case for $f_0(n) = 1$. Furthermore, the $p_{k|\overrightarrow{\alpha i}}$ contribution in Eq. (B.27) vanishes for $k \neq 1$ since

$$\sum_{i=0}^{k}(-1)^i(k-i)\binom{k}{i} = \sum_{i=0}^{k}(-1)^i(k-i)\binom{k}{k-i} = \sum_{i=0}^{k}(-1)^i k\binom{k-1}{k-1-i} = 0.$$

Therefore, when we unravel the expectation value with the recursive relation Eq. (B.27), the only nonvanishing term is given by the initial states with only 1 particle,

$$\begin{aligned}
\sum_{n=0}^{k} n p_{n|\overrightarrow{\alpha i}} &= \frac{1}{k-1} \sum_{n=0}^{k-1} n \sum_{x_1=1}^{k} p_{n|\overrightarrow{\alpha i}\setminus\{\alpha_{x_1} i_{x_1}\}} \\
&= \frac{1}{(k-1)(k-2)} \sum_{n=0}^{k-2} n \sum_{x_1=1}^{k} \sum_{x_2=1, x_2\neq x_1}^{k} p_{n|\overrightarrow{\alpha i}\setminus\{\alpha_{x_1} i_{x_1}\}\setminus\{\alpha_{x_2} i_{x_2}\}} \\
&= \frac{1}{(k-1)!} \sum_{x_1} \sum_{x_2\neq x_1} \cdots \sum_{x_{k-1}\neq x_1,\cdots,x_{k-2}} p_{1|\overrightarrow{\alpha i}\setminus\{\alpha_{x_1} i_{x_1}\}\cdots\setminus\{\alpha_{x_{k-1}} i_{x_{k-1}}\}} \\
&= \sum_{x} p_{1|\{\alpha_x i_x\}}.
\end{aligned} \tag{B.35}$$

Here, the $(k-1)!$ in the denominator cancels out with the double-counting of the summations. Indeed, given the particle indexed with $\alpha_x i_x$ of the initial state $\overrightarrow{\alpha i}$, we are simply counting the number of ways to remove the other $k-1$ particles, which is $(k-1)!$.

Average of $n(n-1)$

To calculate the variance of number of transferred particles we need to know the expectation value of n^2. In this case, it is convenient to look at $f_0(n) = n(n-1)$

due to the binomial nature of the process. Indeed, $f_1(n)$ then reads

$$\begin{aligned} f_1(n) &= \sum_{i=0}^{n} \frac{(-1)^i (n-i)(n-i-1)}{k\binom{k-1}{n}} \binom{k}{n-i} \\ &= \sum_{i=0}^{n} \frac{(-1)^i (k-1)}{\binom{k-1}{n}} \binom{k-2}{n-2-i} \\ &= \frac{(k-1)\binom{k-3}{k-2}}{\binom{k-1}{n}} = \frac{n(n-1)}{k-2}. \end{aligned} \tag{B.36}$$

Again, $f_1(n) \propto f_0(n)$, making the recursive relation much more useful. Furthermore, the $p_{k|\overrightarrow{\alpha i}}$ contribution vanishes for $k \neq 2$ since

$$\begin{aligned} \sum_{i=0}^{k} (-1)^i (k-i)(k-i-1) \binom{k}{k-i} &= \sum_{i=0}^{k} (-1)^i k(k-i-1) \binom{k-1}{k-1-i} \\ &= \sum_{i=0}^{k} (-1)^i k(k-1) \binom{k-2}{k-2-i} = 0. \end{aligned}$$

Therefore, when we unravel the expectation value with the recursive relation Eq. (B.27), the only nonvanishing term is given by the initial states with only 2 particles,

$$\begin{aligned} \sum_{n=0}^{k} n(n-1) p_{n|\overrightarrow{\alpha i}} &= \frac{1}{k-2} \sum_{n=0}^{k-1} n(n-1) \sum_{x_1=1}^{k} p_{n|\overrightarrow{\alpha i}\setminus\{\alpha_{x_1} i_{x_1}\}} \\ &= \frac{1}{(k-2)(k-3)} \sum_{n=0}^{k-2} n(n-1) \sum_{x_1=1}^{k} \sum_{x_2=1, x_2\neq x_1}^{k} p_{n|\overrightarrow{\alpha i}\setminus\{\alpha_{x_1} i_{x_1}\}\setminus\{\alpha_{x_2} i_{x_2}\}} \\ &= \frac{2}{(k-2)!} \sum_{x_1} \sum_{x_2\neq x_1} \cdots \sum_{x_{k-2}\neq x_1,\cdots,x_{k-3}} p_{2|\overrightarrow{\alpha i}\setminus\{\alpha_{x_1} i_{x_1}\}\cdots\setminus\{\alpha_{x_{k-2}} i_{x_{k-2}}\}} \\ &= 2 \sum_{x_1} \sum_{x_2\neq x_1} p_{2|(\alpha_{x_1} i_{x_1}, \alpha_{x_2} i_{x_2})}. \end{aligned} \tag{B.37}$$

Here the factor 2 comes from evaluating $n(n-1)$ for the number of particles $n = 2$ ending up in lead 1, and the factor $(k-2)!$ at the denominator cancels out with the number of ways to remove $k-2$ particles from the initial state $\overrightarrow{\alpha i}$ leaving $(\alpha_{x_1} i_{x_1}, \alpha_{x_2} i_{x_2})$ as the remaining particles.

B.2 Relevant transport quantities

In this section we use the insights of the previous section combined with the choice of initial thermal states to calculate the average and the variance of the number of particles transferred in the scattering process.

B.2.1 Average transferred particle number

To calculate the average number of transferred particles we need to know how many particles accumulate in a given lead, say lead 1, during a scattering process. This means that, calling $n_1(\overrightarrow{\alpha i})$ the number of particles in lead 1 given the state $\overrightarrow{\alpha i}$, we need to calculate the expectation value of $n - n_1(\overrightarrow{\alpha i})$, namely

$$\langle n - n_1(\overrightarrow{\alpha i})\rangle = \sum_k \sum_{\overrightarrow{\alpha i},|\alpha i|=k} \sum_{n=0}^{k} [n - n_1(\overrightarrow{\alpha i})] p_{n|\overrightarrow{\alpha i}} p_{\overrightarrow{\alpha i}} \tag{B.38}$$

From now on we assume that the initial state is a tensor product over the leads and the channels, and that on each lead the density matrix is diagonal with respect to the number of particles in each channel. This allows us to write the probability of finding the initial state $\overrightarrow{\alpha i}$ in terms of the number of particles that the state has in each channel $n_{\beta j}$, namely

$$p_{\overrightarrow{\alpha i}} = \prod_{\beta j} p_{n_{\beta j}}. \tag{B.39}$$

Then, the expectation value of $n_1(\overrightarrow{\alpha i}) = n_{11} + \cdots + n_{1N_1}$ is simply given by

$$\langle n_1(\overrightarrow{\alpha i})\rangle = \sum_x \langle n_{1x}\rangle \tag{B.40}$$

because the conditional probabilities trivially sum up to 1. Instead, using Eq. (B.35), the expectation value of n is given by the probabilities of transfering one particle given the initial states with exactly one particle through

$$\langle n\rangle = \sum_{n_{11}} \cdots \sum_{n_{rM_r}} \left[n_{11} p_{1|11} + \cdots + n_{rM_r} p_{1|rM_r} \right] \left(\prod_{\beta j} p_{n_{\beta j}} \right). \tag{B.41}$$

For both bosons and fermions, we use Eq. (3.12) to write the single-particle conditional probability as

$$p_{1|\alpha i} = \sum_x |s_{1x,\alpha i}|^2, \tag{B.42}$$

which we then plug into $\langle n\rangle$ to find

$$\langle n\rangle = \sum_{x,\beta j} |s_{1x,\beta j}|^2 \langle n_{\beta j}\rangle. \tag{B.43}$$

Combining Eqs. (B.40, B.43), and assuming that the channels in a given lead have the same average number of particles, i.e. $\langle n_{\alpha i}\rangle = \langle n_{\alpha j}\rangle = \langle n_\alpha\rangle$, we find the

average number of transferred particles

$$\begin{aligned}\langle n - n_1(\overrightarrow{\alpha i})\rangle &= \left(\sum_{x,y}|s_{1x,1y}|^2 - M_1\right)\langle n_1\rangle + \sum_{\alpha\neq 1}\sum_{x,y}|s_{1x,\alpha y}|^2\langle n_\alpha\rangle \\ &= \left[\sum_{x=1}^{M_1}\left(1 - \sum_{\alpha\neq 1}\sum_{y}|s_{1x,\alpha y}|^2\right) - M_1\right]\langle n_1\rangle + \sum_{\alpha\neq 1}\sum_{x,y}|s_{1x,\alpha y}|^2\langle n_\alpha\rangle \\ &= \sum_{\alpha\neq 1}\sum_{xy}|s_{1x,\alpha y}|^2(\langle n_\alpha\rangle - \langle n_1\rangle) \\ &= \sum_{\alpha\neq 1}\mathrm{Tr}\left\{t_{1\alpha}t_{1\alpha}^\dagger\right\}(\langle n_\alpha\rangle - \langle n_1\rangle),\end{aligned} \tag{B.44}$$

where we used the unitarity of the scattering matrix to sum only over the transition probabilities from a different lead. In the last step we introduced the scattering sub-matrices $t_{\alpha\beta}$ defined through $[t_{\alpha\beta}]_{xy} \equiv s_{\alpha x,\beta y}$ which make the resemblance of Eq. (B.44) to the Landauer-Büttiker formula for the current more explicit. Note that Eq. (B.44) holds for both fermions and bosons: the difference between them is encoded in the average occupation of the initial state $\langle n_{\beta j}\rangle$.

B.2.2 Variance of transferred particle number

To calculate the variance of the transferred particle number we need to study the expectation value of $[n - n_1(\overrightarrow{\alpha i})]^2$, which is the second moment of the transferred particle number. We decompose this square in the following way

$$[n - n_1(\overrightarrow{\alpha i})]^2 = n^2 - 2nn_1(\overrightarrow{\alpha i}) + n_1^2(\overrightarrow{\alpha i}) = n(n-1) + n - 2nn_1(\overrightarrow{\alpha i}) + n_1^2(\overrightarrow{\alpha i})$$

so we can calculate the second moment by studying it piece by piece.

- $\langle n(n-1)\rangle$:

  First, let's look at the $n(n-1)$ contribution. As seen in Eq. (B.37), the sum over n reduces to the sum over the initial states with only two particles. Then, given any initial state, we need to count in how many ways we can get the same two-particles state $(\alpha_1 i_1, \alpha_2 i_2)$. Here, an important difference arises if the two particles are in the same state or not. If they are not, the number of ways to obtain the same state is simply given by the product $n_{\alpha_1 i_1} n_{\alpha_2 i_2}$. Instead, if they are in the same state $\alpha_1 i_1 = \alpha_2 i_2 = \alpha i$ it is given by the binomial coefficient $\binom{n_{\alpha i}}{2}$. The average of $n(n-1)$ then reads

$$\langle n(n-1)\rangle = \sum_{\alpha_1 i_1 < \alpha_2 i_2} 2p_{2|(\alpha_1 i_1,\alpha_2 i_2)}\langle n_{\alpha_1 i_1}\rangle\langle n_{\alpha_2 i_2}\rangle + \sum_{\alpha i} 2p_{2|(\alpha i,\alpha i)}\langle\frac{n_{\alpha i}(n_{\alpha i}-1)}{2}\rangle, \tag{B.45}$$

where we used $\langle n_{\alpha_1 i_1} n_{\alpha_2 i_2}\rangle = \langle n_{\alpha_1 i_1}\rangle\langle n_{\alpha_2 i_2}\rangle$ because the probability distribution of the initial state is taken to be uncorrelated. Notably, for fermions the second term of Eq. (B.45) vanishes because two fermions cannot occupy the same state.

- $\langle n\rangle$:

  We have previously discussed in Sec. B.2.1 how to deal with the average of n, and we have seen that it reduces to

$$\langle n\rangle = \sum_{\alpha i} p_{1|\alpha i}\langle n_{\alpha i}\rangle. \tag{B.46}$$

- $\langle -2nn_1(\overrightarrow{\alpha i})\rangle$:

  We first sum over n conditioned on a given state, reducing the problem to the conditional probabilities on single-particle states. Then, recalling that $n_1(\overrightarrow{\alpha i})$ is the number of particles in lead $\alpha = 1$ in the initial state, the average reads

$$\begin{aligned}\langle -2nn_1(\overrightarrow{\alpha i})\rangle &= -2\sum_{n_{11},\cdots,n_{rM_r}} \left[p_{1|11}n_{11} + \cdots + p_{1|rM_r}n_{rM_r}\right]\times \\ &\qquad \times \left[n_{11} + \cdots + n_{1M_1}\right]\left(\prod_{\beta j} p_{n_{\beta j}}\right) \\ &= -2\sum_{\alpha i,x} p_{1|\alpha i}\langle n_{\alpha i} n_{1x}\rangle \\ &= -2\left[\sum_{\alpha i,x} p_{1|\alpha i}\langle n_{\alpha i}\rangle\langle n_{1x}\rangle + \sum_x p_{1|1x}\mathrm{Var}[n_{1x}]\right]\end{aligned} \tag{B.47}$$

  where we once again used that the initial probability distribution is not correlated. Here, Var[•] denotes the variance.

- $\langle [n_1(\overrightarrow{\alpha i})]^2\rangle$:

  For this last term the scattering process is irrelevant because we are only looking at the initial particle number. Consequently, we sum up to 1 the conditional probabilities $p_{n|\overrightarrow{\alpha i}}$. We are left with

$$\langle [n_1(\overrightarrow{\alpha i})]^2\rangle = \sum_{xy}\langle n_{1x} n_{1y}\rangle = \sum_{x,y}\langle n_{1x}\rangle\langle n_{1y}\rangle + \sum_x \mathrm{Var}[n_{1x}]. \tag{B.48}$$

At this point we have all the tools to calculate the variance of the transferred particle number. In the following, we explicitely carry out the calculation for both fermions and bosons.

Variance of transferred fermions

Let's tackle first the contribution stemming from $n(n-1)$. For fermions, we cannot have particles in the same state, so the second contribution in Eq. (B.45) vanishes. The probability conditioned on the two-particle state reads

$$\begin{aligned} p_{2|(\alpha_1 i_1,\alpha_2 i_2)} &= \frac{1}{2}\sum_{xy} \left| s_{1x,\alpha_1 i_1} s_{1y,\alpha_2 i_2} - s_{1x,\alpha_2 i_2} s_{1y,\alpha_1 i_1} \right|^2 \\ &= \sum_{xy} \left[|s_{1x,\alpha_1 i_1}|^2 |s_{1y,\alpha_2 i_2}|^2 - s_{1x,\alpha_1 i_1} s^*_{1y,\alpha_1 i_1} s_{1y,\alpha_2 i_2} s^*_{1x,\alpha_2 i_2} \right]. \end{aligned} \tag{B.49}$$

Here it is convenient to write the averages in terms of the scattering submatrices $t_{\alpha\beta}$, and to assume that the average $\langle n_{\alpha i}\rangle = f_\alpha$ and the variance $\mathrm{Var}[n_{\alpha i}] = f_\alpha(1-f_\alpha)$ of the initial particle numbers do not depend on the channel. Then, the average of $n(n-1)$ reads

$$\begin{aligned} \langle n(n-1)\rangle &= \frac{1}{2}\sum_{\alpha_1 i_1,\alpha_2 i_2} 2 p_{2|(\alpha_1 i_1,\alpha_2 i_2)} \langle n_{\alpha_1 i_1}\rangle \langle n_{\alpha_2 i_2}\rangle \\ &= \sum_{\alpha_1\alpha_2} \left[\mathrm{Tr}\left\{ t_{1\alpha_1} t^\dagger_{1\alpha_1} \right\} \mathrm{Tr}\left\{ t_{1\alpha_2} t^\dagger_{1\alpha_2} \right\} - \mathrm{Tr}\left\{ t_{1\alpha_1} t^\dagger_{1\alpha_1} t_{1\alpha_2} t^\dagger_{1\alpha_2} \right\} \right] f_{\alpha_1} f_{\alpha_2} \end{aligned} \tag{B.50}$$

where we first symmetrized the summation over $\alpha_1 i_1, \alpha_2 i_2$ by noticing that, on the diagonal, the conditional probability vanishes. Using that

$$f_{\alpha_1} f_{\alpha_2} = (f_{\alpha_1} - f_1)(f_{\alpha_2} - f_1) + f_1 f_{\alpha_1} + f_1 f_{\alpha_2} - f_1^2 \tag{B.51}$$

and calling

$$X \equiv \sum_\alpha t_{1\alpha} t^\dagger_{1\alpha} (f_\alpha - f_1), \tag{B.52}$$

such that the average of the transferred particle number reads $\langle n - n_1(\overrightarrow{\alpha i})\rangle = \mathrm{Tr}\{X\}$, the average of $n(n-1)$ becomes

$$\begin{aligned} \langle n(n-1)\rangle &= \mathrm{Tr}\{X\}^2 - \mathrm{Tr}\left\{X^2\right\} + \\ &\quad + f_1 \left[2(M_1 - 1) \sum_\alpha \mathrm{Tr}\left\{ t_{1\alpha} t^\dagger_{1\alpha} \right\} f_\alpha \right] - f_1^2 \left[M_1^2 - M_1 \right] \\ &= \mathrm{Tr}\{X\}^2 - \mathrm{Tr}\left\{X^2\right\} + \\ &\quad + f_1 \left[2(M_1 - 1) \left(\mathrm{Tr}\{X\} + M_1 f_1 \right) \right] - f_1^2 \left[M_1^2 - M_1 \right] \\ &= \mathrm{Tr}\{X\}^2 - \mathrm{Tr}\left\{X^2\right\} + f_1 \left[2(M_1 - 1)\mathrm{Tr}\{X\} \right] + f_1^2 \left[M_1^2 - M_1 \right]. \end{aligned} \tag{B.53}$$

Here, we used the unitarity of the scattering matrix, which, for the sub-matrix formulation reads

$$\sum_\gamma t_{\alpha\gamma} t^\dagger_{\beta\gamma} = \mathbb{1}_\alpha \delta_{\alpha\beta}.$$

Note that the first term of $\langle n(n-1)\rangle$ in Eq. (B.53), i.e. $\mathrm{Tr}\left\{X\right\}^2$, would cancel out with $\langle n - n_1(\overrightarrow{\alpha i})\rangle^2$ when we calculate the variance. Additionally, the second term in Eq. (B.53), i.e. $-\mathrm{Tr}\left\{X^2\right\}$, represents the "anti-bunching" contribution to the variance. We will later see that the remaining terms combine neatly with the remaining contributions of $\langle[n - n_1(\overrightarrow{\alpha i})]^2\rangle$.

Now, let's look at the remaining contributions to the variance. Here, for the sake of conciseness, the argument of $n_1(\overrightarrow{\alpha i})$ is dropped, and we write

$$\begin{aligned}
\langle n - 2nn_1 + n_1^2\rangle &= \sum_\alpha \mathrm{Tr}\left\{t_{1\alpha}t_{1\alpha}^\dagger\right\} f_\alpha - 2\Bigg[f_1 M_1 \sum_\alpha \mathrm{Tr}\left\{t_{1\alpha}t_{1\alpha}^\dagger\right\} f_\alpha + \\
&\quad + \mathrm{Tr}\left\{t_{11}t_{11}^\dagger\right\} f_1(1-f_1)\Big] + M_1^2 f_1^2 + M_1 f_1(1-f_1) \\
&= \mathrm{Tr}\left\{X\right\} + M_1 f_1 - 2\Big[M_1 f_1 \mathrm{Tr}\left\{X\right\} + M_1^2 f_1^2 + M_1 f_1(1-f_1) + \\
&\quad - \sum_{\alpha\neq 1} \mathrm{Tr}\left\{t_{1\alpha}t_{1\alpha}^\dagger\right\} f_1(1-f_1)\Bigg] + M_1 f_1 + f_1^2[M_1^2 - M_1] \\
&= \mathrm{Tr}\left\{X\right\} + f_1\left[2\sum_{\alpha\neq 1} \mathrm{Tr}\left\{t_{1\alpha}t_{1\alpha}^\dagger\right\} - 2M_1 \mathrm{Tr}\left\{X\right\}\right] + \\
&\quad + f_1^2\left[M_1 - M_1^2 - 2\sum_{\alpha\neq 1} \mathrm{Tr}\left\{t_{1\alpha}t_{1\alpha}^\dagger\right\}\right],
\end{aligned} \tag{B.54}$$

where once again we used the unitarity of the scattering matrix. We now take the sum of Eq. (B.53) and (B.54) to find the second moment of $n - n_1$

$$\langle (n-n_1)^2\rangle = \mathrm{Tr}\left\{X\right\}^2 - \mathrm{Tr}\left\{X^2\right\} + \sum_{\alpha\neq 1} \mathrm{Tr}\left\{t_{1\alpha}t_{1\alpha}^\dagger\right\}\left[f_\alpha + f_1 - 2f_1 f_\alpha\right]. \tag{B.55}$$

When taking the variance of the transferred particle number, the $\mathrm{Tr}\left\{X\right\}^2$ term cancels out and we are left with

$$\mathrm{Var}[n-n_1] = \sum_{\alpha\neq 1} \mathrm{Tr}\left\{t_{1\alpha}t_{1\alpha}^\dagger\right\}\left[f_\alpha(1-f_1) + f_1(1-f_\alpha)\right] - \mathrm{Tr}\left\{X^2\right\}, \tag{B.56}$$

which is exactly the integrand in the zero-frequency current noise for fermionic scattering.

Variance of transferred bosons

As for the fermionic case, let's start from the average of $n(n-1)$. If the initial particles are in different channels, i.e. $\alpha_1 i_1 \neq \alpha_2 i_2$, the conditional probability reads

$$p_{2|(\alpha_1 i_1, \alpha_2 i_2)} = \frac{1}{2}\sum_{xy}\left[2|s_{1x,\alpha_1 i_1}|^2 |s_{1y,\alpha_2 i_2}|^2 + 2 s_{1x,\alpha_1 i_1} s^*_{1y,\alpha_1 i_1} s_{1y,\alpha_2 i_2} s^*_{1x,\alpha_2 i_2}\right]. \tag{B.57}$$

Instead, when the initial particles are in the same channel, we have

$$\begin{aligned} p_{2|(\alpha_1 i_1,\alpha_1 i_1)} &= \frac{1}{4}\sum_{xy}\left[2|s_{1x,\alpha_1 i_1}|^2|s_{1y,\alpha_1 i_1}|^2 + 2s_{1x,\alpha_1 i_1}s^*_{1y,\alpha_1 i_1}s_{1y,\alpha_1 i_1}s^*_{1x,\alpha_1 i_1}\right], \\ &= \sum_{xy}|s_{1x,\alpha_1 i_1}|^2|s_{1y,\alpha_1 i_1}|^2. \end{aligned} \tag{B.58}$$

Assuming that the initial distribution does not depend on the specific channel, and taking a thermal distributions of bosons, such that $\langle n_{\alpha i}\rangle = f_\alpha$ and $\mathrm{Var}[n_{\alpha i}] = f_\alpha(1+f_\alpha)$, we calculate the average of $n(n-1)$ as

$$\begin{aligned} \langle n(n-1)\rangle &= \frac{1}{2}\sum_{\alpha_1 i_1\neq\alpha_2 i_2} 2p_{2|(\alpha_1 i_1,\alpha_2 i_2)}\langle n_{\alpha_1 i_1}\rangle\langle n_{\alpha_2 i_2}\rangle + \sum_{\alpha i} 2p_{2|(\alpha i,\alpha i)}\langle\frac{n_{\alpha i}(n_{\alpha i}-1)}{2}\rangle \\ &= \sum_{\alpha_1 i_1\neq\alpha_2 i_2} p_{2|(\alpha_1 i_1,\alpha_2 i_2)}f_{\alpha_1}f_{\alpha_2} + \sum_{\alpha i} p_{2|(\alpha i,\alpha i)}[f_\alpha(1+f_\alpha)+f_\alpha^2-f_\alpha] \\ &= \sum_{\alpha_1 i_1\neq\alpha_2 i_2,xy}\left[|s_{1x,\alpha_1 i_1}|^2|s_{1y,\alpha_2 i_2}|^2 + s_{1x,\alpha_1 i_1}s^*_{1y,\alpha_1 i_1}s_{1y,\alpha_2 i_2}s^*_{1x,\alpha_2 i_2}\right]f_{\alpha_1}f_{\alpha_2} + \\ &\qquad + \sum_{\alpha i,xy}|s_{1x,\alpha i}|^2|s_{1y,\alpha i}|^2 2f_\alpha^2 \\ &= \sum_{\alpha_1 i_1,\alpha_2 i_2,xy}\left[|s_{1x,\alpha_1 i_1}|^2|s_{1y,\alpha_2 i_2}|^2 + s_{1x,\alpha_1 i_1}s^*_{1y,\alpha_1 i_1}s_{1y,\alpha_2 i_2}s^*_{1x,\alpha_2 i_2}\right]f_{\alpha_1}f_{\alpha_2} \\ &= \sum_{\alpha_1,\alpha_2}\left[\mathrm{Tr}\left\{t_{1\alpha_1}t^\dagger_{1\alpha_1}\right\}\mathrm{Tr}\left\{t_{1\alpha_2}t^\dagger_{1\alpha_2}\right\} + \mathrm{Tr}\left\{t_{1\alpha_1}t^\dagger_{1\alpha_1}t_{1\alpha_2}t^\dagger_{1\alpha_2}\right\}\right]f_{\alpha_1}f_{\alpha_2}. \end{aligned} \tag{B.59}$$

In the same fashion as before, we decompose the product of the average occupation numbers as done in Eq. (B.51) and use the matrix X defined in Eq. (B.52) to write the average of $n(n-1)$ as

$$\begin{aligned} \langle n(n-1)\rangle &= \mathrm{Tr}\{X\}^2 + \mathrm{Tr}\left\{X^2\right\} + f_1\left[2(M_1+1)\sum_\alpha \mathrm{Tr}\left\{t_{1\alpha}t^\dagger_{1\alpha}\right\}f_\alpha\right] + \\ &\qquad - f_1^2\left[M_1^2+M_1\right] \\ &= \mathrm{Tr}\{X\}^2 + \mathrm{Tr}\left\{X^2\right\} + f_1\left[2(M_1+1)(\mathrm{Tr}\{X\}+M_1f_1)\right] + \\ &\qquad - f_1^2\left[M_1^2+M_1\right] \\ &= \mathrm{Tr}\{X\}^2 + \mathrm{Tr}\left\{X^2\right\} + f_1\left[2(M_1+1)\mathrm{Tr}\{X\}\right] + f_1^2\left[M_1^2+M_1\right]. \end{aligned} \tag{B.60}$$

Here, we see that the first term will cancel out when taking the variance, while the second term represents the "bunching" contribution to the variance. The other two terms combine with the remaining contributions of $\langle[n-n_1(\overrightarrow{\alpha i})]^2\rangle$.

Now, let's look at the remaining contributions. Again, for the sake of concise-

ness, the argument of $n_1(\overrightarrow{\alpha i})$ is dropped.

$$\begin{aligned}\langle n - 2nn_1 + n_1^2\rangle &= \sum_\alpha \mathrm{Tr}\left\{t_{1\alpha}t_{1\alpha}^\dagger\right\} f_\alpha - 2\Big[f_1 M_1 \sum_\alpha \mathrm{Tr}\left\{t_{1\alpha}t_{1\alpha}^\dagger\right\} f_\alpha + \\ &\quad + \mathrm{Tr}\left\{t_{11}t_{11}^\dagger\right\} f_1(1+f_1)\Big] + M_1^2 f_1^2 + M_1 f_1(1+f_1) \\ &= \mathrm{Tr}\left\{X\right\} + M_1 f_1 - 2M_1 f_1\left[\mathrm{Tr}\left\{X\right\} + M_1 f_1\right] - 2M_1 f_1 - 2M_1 f_1^2 + \\ &\quad + 2\sum_{\alpha\neq 1} \mathrm{Tr}\left\{t_{1\alpha}t_{1\alpha}^\dagger\right\} f_1(1+f_1) + M_1 f_1 + M_1 f_1^2 + M_1^2 f_1^2 \\ &= \mathrm{Tr}\left\{X\right\} + f_1\left[-2M_1\mathrm{Tr}\left\{X\right\} + 2\sum_{\alpha\neq 1}\mathrm{Tr}\left\{t_{1\alpha}t_{1\alpha}^\dagger\right\}\right] + \\ &\quad + f_1^2\left[-M_1 - M_1^2 + 2\sum_{\alpha\neq 1}\mathrm{Tr}\left\{t_{1\alpha}t_{1\alpha}^\dagger\right\}\right].\end{aligned} \tag{B.61}$$

Taking the sum of Eqs. (B.59) and (B.61), we find the second moment of the transferred particle number

$$\langle (n-n_1)^2\rangle = \mathrm{Tr}\left\{X\right\}^2 + \mathrm{Tr}\left\{X^2\right\} + \sum_{\alpha\neq 1}\mathrm{Tr}\left\{t_{1\alpha}t_{1\alpha}^\dagger\right\}\left[f_\alpha + f_1 + 2f_1 f_\alpha\right]. \tag{B.62}$$

When taking the variance of the transferred particle number, the $\mathrm{Tr}\left\{X\right\}^2$ term cancels out and we are left with

$$\mathrm{Var}[n-n_1] = \mathrm{Tr}\left\{X^2\right\} + \sum_{\alpha\neq 1}\mathrm{Tr}\left\{t_{1\alpha}t_{1\alpha}^\dagger\right\}\left[f_\alpha(1+f_1) + f_1(1+f_\alpha)\right], \tag{B.63}$$

which is exactly the integrand in the zero-frequency noise for bosonic scattering.

Appendix C

From variance of transferred particles to current noise

Consider an observable $O(t)$ and its associated stochastic current $I^{(O)}(t)$. For simplicity we consider here the case $O(0) = 0$. The observable and its current are related by the differential equation

$$dO(t) = I^{(O)}(t)dt \quad \Rightarrow \quad O(t) = \int_0^t I^{(O)}(s)ds. \tag{C.1}$$

The average value of the observable is then given by

$$\langle O(t)\rangle = \int_0^t \langle I^{(O)}(s)\rangle ds, \tag{C.2}$$

while the variance reads

$$\mathrm{Var}[O(t)] = \int_0^t \int_0^t \langle \delta I^{(O)}(s_1)\delta I^{(O)}(s_2)\rangle ds_1 ds_2, \tag{C.3}$$

where $\delta I^{(O)}(s) \equiv I^{(O)}(s) - \langle I^{(O)}(s)\rangle$ denotes the deviation from the average. Taking the derivative with respect to time and assuming time-translation invariance we find

$$\begin{aligned} \partial_t \mathrm{Var}[O(t)] &= 2\int_0^t ds \langle \delta I^{(O)}(t)\delta I^{(O)}(s)\rangle = 2\int_{-t}^0 ds \langle \delta I^{(O)}(t)\delta I^{(O)}(t+s)\rangle \\ &= \int_{-t}^t ds \langle \delta I^{(O)}(t)\delta I^{(O)}(t+s)\rangle \\ &= \int_{-t}^t ds \langle \delta I^{(O)}(0)\delta I^{(O)}(s)\rangle \overset{t\to\infty}{\to} S^{(O)}. \end{aligned} \tag{C.4}$$

Therefore, in the long-time limit, the zero-frequency noise of the current $I^{(O)}$ corresponds to the time-derivative of the variance of the associated observable $O(t)$.

In the scattering process described in Sec. 3.1 the observable $O(t)$ considered is the number of particles $N_\gamma(t)$ accumulated in reservoir γ through the scattering events. Let δt be the time interval between two consecutive scattering events and

$dN_\gamma(s)$ be the number of particles transferred in the scattering event taking place at time s. Then, the number of particles accumulated in lead γ is given by

$$N_\gamma(t) = \sum_{n=0}^{t/\delta t} dN_\gamma\left(\frac{n\delta t}{t}\right). \tag{C.5}$$

Crucially, the scattering events are statistically independent and do not depend on time, such that the average and variance of $N_\gamma(t)$ read

$$\langle N_\gamma(t)\rangle = \frac{t}{\delta t}\langle dN_\gamma\rangle, \tag{C.6a}$$

$$\mathrm{Var}[N_\gamma(t)] = \frac{t}{\delta t}\mathrm{Var}[dN_\gamma]. \tag{C.6b}$$

This means that all we need is the statistics of a single scattering event. In particular, we need the statistics of the transferred number of particles Q_γ defined in Sec. 3.1.1. Again, since the scattering events at different energies are independent, the average and variance of the accumulated particle number dN_γ in reservoir γ at all energies are given by

$$\langle dN_\gamma(t)\rangle = \frac{\delta t}{h}\int dE\langle Q_\gamma\rangle, \tag{C.7a}$$

$$\mathrm{Var}[dN_\gamma(t)] = \frac{\delta t}{h}\int dE\mathrm{Var}[Q_\gamma], \tag{C.7b}$$

respectively. Combining Eqs. (C.6, C.7) with the Eqs. (C.2, C.4) for the average current and its noise we find

$$I_\gamma^{(N)} = \langle \dot{N}_\gamma(t)\rangle = \partial_t\langle N_\gamma(t)\rangle = \frac{1}{h}\int\langle Q_\gamma\rangle dE, \tag{C.8a}$$

$$S_{\gamma\gamma}^{(N)} = \partial_t\mathrm{Var}[N_\gamma(t)] = \frac{1}{h}\int\mathrm{Var}[Q_\gamma]dE, \tag{C.8b}$$

which are proportional to the charge currents of Eqs. (3.24, 3.25). Indeed, since each particle carries the same amount of charge q, the charge current and its noise fulfil $I_\gamma = qI_\gamma^{(N)}$, $S_{\gamma\gamma}^I = q^2S_{\gamma\gamma}^{(N)}$.

Note that, the current $I_\gamma^{(X)}$ and its noise $S^{(X)}$ of an energy-dependent quantity $x(E)$ carried by the particles at energy E, like energy or heat current, is generally not proportional to the particle current and noise. Still, the procedure described here is still valid up to Eq. (C.7), where now the energy-dependent quantity enters in the integrals as

$$\langle dX_\gamma(t)\rangle = \frac{\delta t}{h}\int dEx(E)\langle Q_\gamma\rangle, \tag{C.9a}$$

$$\mathrm{Var}[dX_\gamma(t)] = \frac{\delta t}{h}\int dE[x(E)]^2\mathrm{Var}[Q_\gamma]. \tag{C.9b}$$

Then, the average current and its noise take the intuitive form

$$I_\gamma^{(X)} = \frac{1}{h}\int x(E)\langle Q_\gamma\rangle dE, \tag{C.10a}$$

$$S_{\gamma\gamma}^{(X)} = \frac{1}{h}\int [x(E)]^2 \mathrm{Var}[Q_\gamma] dE. \tag{C.10b}$$

Appendix D

Clausius' relation

In this appendix we explicitely show that in a thermal and large bath the entropy production obeys Clausius' relation

$$\Delta S_{\mathrm{B}} = \frac{\Delta \mathcal{Q}_{\mathrm{B}}}{T_{\mathrm{B}}} \tag{D.1}$$

where T_{B} is the temperature of the bath, while ΔS_{B} is the variation of the entropy and $\Delta \mathcal{Q}_{\mathrm{B}}$ is the heat absorbed by the bath.

We start by decomposing the entropy production as

$$\begin{aligned} \frac{1}{k_{\mathrm{B}}} \Delta S_{\mathrm{B}} &= S_{\mathrm{vN}}[\rho(\tau)] - S_{\mathrm{vN}}[\rho(0)] \\ &= \mathrm{Tr}\left\{\rho(0)\log\rho(0) - \rho(\tau)\log\rho(\tau)\right\} \\ &= \mathrm{Tr}\left\{[\rho(0)-\rho(\tau)]\log\rho(0)\right\} + \mathrm{Tr}\left\{\rho(\tau)[\log\rho(0) - \log\rho(\tau)]\right\}. \end{aligned} \tag{D.2}$$

where $\rho(0)$ and $\rho(\tau)$ are the density matrices of the bath at times $t = 0$ and $t = \tau$. Here, the assumption of a large bath comes into play. Writing the final state as $\rho(\tau) = \rho(0) + \delta\rho$, in a large bath $\delta\rho$ is a small correction. This means that the second term in Eq. (D.2) is $\mathcal{O}(\delta\rho^2)$ and can therefore be neglected because the first term is a first order correction in $\delta\rho$. This is seen by taking the definition of the logarithm of a matrix B in terms of a series, namely

$$\log(B) = \sum_{k=1}^{\infty} \frac{(-1)^{k+1}}{k} (B - \mathbb{1})^k, \tag{D.3}$$

and using it to expand the second term of Eq. (D.2) in $\delta\rho$. From now on, we drop

the time-argument of the density matrix, calling $\rho \equiv \rho(0)$. The logarithm reads

$$\begin{aligned}
\log(\rho+\delta\rho) &= \sum_{k=1}^{\infty} \frac{(-1)^{k+1}}{k}(\rho - \mathbb{1} + \delta\rho)^k \\
&= \sum_{k=1}^{\infty} \frac{(-1)^{k+1}}{k}\Big[(\rho-\mathbb{1})^k + \delta\rho(\rho-\mathbb{1})^{k-1} + \\
&\quad + (\rho-\mathbb{1})\delta\rho(\rho-\mathbb{1})^{k-2} + \cdots + (\rho-\mathbb{1})^{k-1}\delta\rho\Big] + \mathcal{O}(\delta\rho^2) \\
&= \log\rho + \sum_{k=1}^{\infty} \frac{(-1)^{k+1}}{k}\Big[\delta\rho(\rho-\mathbb{1})^{k-1} + \\
&\quad + (\rho-\mathbb{1})\delta\rho(\rho-\mathbb{1})^{k-2} + \cdots + (\rho-\mathbb{1})^{k-1}\delta\rho\Big] + \mathcal{O}(\delta\rho^2).
\end{aligned}$$

Then, the second term of Eq. (D.2) reads

$$\begin{aligned}
&\mathrm{Tr}\left\{(\rho+\delta\rho)[\log\rho - \log(\rho+\delta\rho)]\right\} = \\
&\quad = -\mathrm{Tr}\left\{\rho \sum_{k=1}^{\infty} \frac{(-1)^{k+1}}{k}\left[\delta\rho(\rho-\mathbb{1})^{k-1} + \cdots + (\rho-\mathbb{1})^{k-1}\delta\rho\right]\right\} + \mathcal{O}(\delta\rho^2) \\
&\quad = -\mathrm{Tr}\left\{\rho \sum_{k=1}^{\infty} \frac{(-1)^{k+1}}{k}\left[k\delta\rho(\rho-\mathbb{1})^{k-1}\right]\right\} + \mathcal{O}(\delta\rho^2) \\
&\quad = -\mathrm{Tr}\left\{\delta\rho \sum_{k=1}^{\infty}\left[(-1)^{k+1}(\rho-\mathbb{1})^{k-1}\right]\rho\right\} + \mathcal{O}(\delta\rho^2) \\
&\quad = -\mathrm{Tr}\left\{\delta\rho\right\} + \mathcal{O}(\delta\rho^2) = \mathcal{O}(\delta\rho^2),
\end{aligned} \tag{D.4}$$

where we used the cyclic property of the trace and recognized the series of

$$\frac{1}{\rho} = \frac{1}{\mathbb{1} + (\rho - \mathbb{1})} = \sum_{k=0}^{\infty}(-1)^k(\rho-\mathbb{1})^k. \tag{D.5}$$

In the last step of Eq. (D.4) we used that $\mathrm{Tr}\{\delta\rho\} = 0$.

Therefore, if the bath is large, the first term of Eq. (D.2) approximates the entropy production well. Additionally, if the initial state is thermal, namely $\rho(0) = e^{-\beta\hat{H}_\mathrm{B}}/Z$ we have

$$\frac{1}{k_\mathrm{B}}\Delta S_\mathrm{B} = \mathrm{Tr}\left\{[\rho(0) - \rho(\tau)][-\beta\hat{H}_\mathrm{B}]\right\} = \frac{\Delta\mathcal{Q}_\mathrm{B}}{k_\mathrm{B}T_\mathrm{B}}, \tag{D.6}$$

which corresponds to Eq. (3.33).

Appendix E

Fluctuation-dissipation bound and thermodynamic uncertainty relation

In this Appendix we show a connection between the out-of-equilibrium fluctuation-dissipation bound discussed in Sec. 4.1, and the thermodynamic uncertainty relation introduced in Sec. 2.4.1.

The starting point is the inequality between the average power output P and its noise S^P given in Eq. (4.7), which we write as

$$S^P \geq P k_{\mathrm{B}} \Delta T \, g\left(\frac{\Delta\mu}{k_{\mathrm{B}}\Delta T}\right) \tag{E.1}$$

where we defined

$$g\left(x\right) \equiv x \tanh\left(\frac{x}{2}\right). \tag{E.2}$$

Since we are focusing on the case in which power is produced, $P > 0$, we can multiply both sides of Eq. (E.1) by P without altering the direction of the inequality. Rearrenging the terms we find the constraint on the precision of the output power

$$\frac{P^2}{S^P} \leq \frac{P}{k_{\mathrm{B}}\Delta T \, g\left(\frac{\Delta\mu}{k_{\mathrm{B}}\Delta T}\right)}. \tag{E.3}$$

At this point, Eq. (E.3) starts resembling the thermodynamic uncertainty relation of Eq. (2.49). Indeed, in the steady-state regime, the TUR limits the precision of the steady-state power P as

$$\frac{P^2}{S^P} \leq \frac{\dot{\sigma}}{2}, \tag{E.4}$$

where $\dot{\sigma}$ is the *global* entropy production rate [12]. The main difference between Eq. (E.3) and Eq. (E.4) is that the upper limit on the precision is given by the average power P in place of the entropy current $\dot{\sigma}$. Then, we can use the first and the second law of thermodynamics to write the power P in terms of the entropy production. Specifically, the first and second law in this steady-state system read

$$P = -J_{\mathrm{hot}} - J_{\mathrm{cold}} \geq 0, \tag{E.5a}$$

$$\dot{\sigma} = \dot{\sigma}_{\mathrm{hot}} + \dot{\sigma}_{\mathrm{cold}} = \frac{J_{\mathrm{hot}}}{T_{\mathrm{hot}}} + \frac{J_{\mathrm{cold}}}{T_{\mathrm{cold}}} \geq 0, \tag{E.5b}$$

respectively. Here, $J_{\rm hot/cold}$ is the heat flow into the hot/cold contact, and $\dot\sigma_{\rm hot/cold}$ is the *local* entropy production in the hot/cold contact. Then, calling $\eta_{\rm C}\equiv 1-\frac{T_{\rm cold}}{T_{\rm hot}}$ the Carnot efficiency, we write Eq. (E.3) as

$$\begin{aligned}\frac{P^2}{S^P} &\leq -\frac{J_{\rm hot}+J_{\rm cold}}{k_{\rm B}\Delta T g\left(\frac{\Delta\mu}{k_{\rm B}\Delta T}\right)} = \frac{T_{\rm hot}}{k_{\rm B}\Delta T g\left(\frac{\Delta\mu}{k_{\rm B}\Delta T}\right)}\left[-\dot\sigma+\frac{J_{\rm cold}}{T_{\rm cold}}\eta_{\rm C}\right],\\ &\leq \frac{1}{k_{\rm B}\eta_{\rm C} g\left(\frac{\Delta\mu}{k_{\rm B}\Delta T}\right)}\left[\dot\sigma_{\rm cold}(\eta_{\rm C}-1)-\dot\sigma_{\rm hot}\right] \leq \frac{\dot\sigma_{\rm cold}}{k_{\rm B} g\left(\frac{\Delta\mu}{k_{\rm B}\Delta T}\right)},\end{aligned} \tag{E.6}$$

where in the last step we used the second law $-\dot\sigma_{\rm hot}\leq\dot\sigma_{\rm cold}$. Crucially, the limit on the power precision is not given by the *global dissipation* $\dot\sigma$ as in Eq. (E.4), but by the *local dissipation* in the cold contact. Furthermore, since we require the output power to be positive, this local dissipation is actually larger than the global one, namely

$$\frac{P^2}{S^P} \leq \frac{\dot\sigma_{\rm cold}}{k_{\rm B} g\left(\frac{\Delta\mu}{k_{\rm B}\Delta T}\right)} \geq \frac{\dot\sigma}{k_{\rm B} g\left(\frac{\Delta\mu}{k_{\rm B}\Delta T}\right)}. \tag{E.7}$$

Note that one can write the limit on the power precision of Eq. (E.7) in terms of the efficiency $\eta\equiv P/(-J_{\rm hot})$ by combining the first law Eq. (E.5a) with Clausius' relation $\dot\sigma_{\rm cold}=J_{\rm cold}/T_{\rm cold}$. The outcome reads

$$\frac{P}{S^P}\frac{\eta}{1-\eta}k_{\rm B}T_{\rm cold}g\left(\frac{\Delta\mu}{k_{\rm B}\Delta T}\right)\leq 1, \tag{E.8}$$

and sets a constraint on the combination of average power P, noise S^P and efficiency η. Note that, in contrast with the classical TUR, we have the factor $1-\eta$ instead of $\eta_{\rm C}-\eta$ at the denominator [12]. Even though this may suggest that it is possiblt to achieve finite power at Carnot efficiency, this is not the case. Indeed, Carnot efficiency is achieved when transport happens in a narrow energy window $\delta\epsilon$ close to the crossing energy $\tilde\epsilon$ of Eq. (4.1). However, the output power is then going to be propotional to $\delta\epsilon^2$, guaranteeing a vanishing power output at Carnot efficiency.

References

[1] E. Fermi, *Thermodynamics* (Dover Publications, Mineola, NY, USA, June 1956) (cit. on p. 1).

[2] M. A. Kastner, "The single-electron transistor", Rev. Mod. Phys. **64**, 849–858 (1992) (cit. on p. 1).

[3] F. Giazotto, T. T. Heikkilä, A. Luukanen, A. M. Savin, and J. P. Pekola, "Opportunities for mesoscopics in thermometry and refrigeration: Physics and applications", Rev. Mod. Phys. **78**, 217–274 (2006) (cit. on p. 1).

[4] C. Van den Broeck and M. Esposito, "Ensemble and trajectory thermodynamics: A brief introduction", Physica A **418**, 6–16 (2015) (cit. on p. 1).

[5] U. Seifert, "Stochastic thermodynamics: From principles to the cost of precision", Physica A **504**, 176–191 (2018) (cit. on p. 1).

[6] P. Strasberg and P. Strasberg, *Quantum Stochastic Thermodynamics* (Oxford University Press, Oxford, England, UK, Jan. 2022) (cit. on pp. 1, 9).

[7] Y. V. Nazarov and Y. M. Blanter, *Quantum Transport: Introduction to Nanoscience* (Cambridge University Press, Cambridge, England, UK, May 2009) (cit. on p. 1).

[8] M. V. Moskalets, *Scattering Matrix Approach to Non-Stationary Quantum Transport* (World Scientific Publishing Company, London, England, UK, Sept. 2011) (cit. on p. 1).

[9] G. Benenti, G. Casati, K. Saito, and R. S. Whitney, "Fundamental aspects of steady-state conversion of heat to work at the nanoscale", Phys. Rep. **694**, 1–124 (2017) (cit. on p. 2).

[10] R. S. Whitney, R. Sánchez, and J. Splettstoesser, "Quantum Thermodynamics of Nanoscale Thermoelectrics and Electronic Devices", in *Thermodynamics in the Quantum Regime* (Springer, Cham, Switzerland, Apr. 2019), pp. 175–206 (cit. on p. 2).

[11] A. C. Barato and U. Seifert, "Thermodynamic Uncertainty Relation for Biomolecular Processes", Phys. Rev. Lett. **114**, 158101 (2015) (cit. on pp. 3, 16, 19).

[12] P. Pietzonka and U. Seifert, "Universal Trade-Off between Power, Efficiency, and Constancy in Steady-State Heat Engines", Phys. Rev. Lett. **120**, 190602 (2018) (cit. on pp. 3, 16, 53, 97, 98).

[13] A. Dechant, "Multidimensional thermodynamic uncertainty relations", J. Phys. A: Math. Theor. **52**, 035001 (2018) (cit. on pp. 3, 16).

[14] A. M. Timpanaro, G. Guarnieri, J. Goold, and G. T. Landi, "Thermodynamic Uncertainty Relations from Exchange Fluctuation Theorems", Phys. Rev. Lett. **123**, 090604 (2019) (cit. on pp. 3, 16).

[15] Y. Hasegawa and T. Van Vu, "Fluctuation Theorem Uncertainty Relation", Phys. Rev. Lett. **123**, 110602 (2019) (cit. on pp. 3, 16).

[16] P. P. Potts and P. Samuelsson, "Thermodynamic uncertainty relations including measurement and feedback", Phys. Rev. E **100**, 052137 (2019) (cit. on pp. 3, 16, 20).

[17] J. M. Horowitz and T. R. Gingrich, "Thermodynamic uncertainty relations constrain non-equilibrium fluctuations", Nat. Phys. **16**, 15–20 (2020) (cit. on pp. 3, 16).

[18] S. K. Manikandan, D. Gupta, and S. Krishnamurthy, "Inferring Entropy Production from Short Experiments", Phys. Rev. Lett. **124**, 120603 (2020) (cit. on pp. 3, 16).

[19] Y. Hasegawa, "Thermodynamic Uncertainty Relation for General Open Quantum Systems", Phys. Rev. Lett. **126**, 010602 (2021) (cit. on pp. 3, 16).

[20] I. Di Terlizzi and M. Baiesi, "Kinetic uncertainty relation", J. Phys. A: Math. Theor. **52**, 02LT03 (2018) (cit. on pp. 3, 16, 20).

[21] J. Yan, A. Hilfinger, G. Vinnicombe, and J. Paulsson, "Kinetic Uncertainty Relations for the Control of Stochastic Reaction Networks", Phys. Rev. Lett. **123**, 108101 (2019) (cit. on pp. 3, 16).

[22] Y. Hasegawa, "Quantum Thermodynamic Uncertainty Relation for Continuous Measurement", Phys. Rev. Lett. **125**, 050601 (2020) (cit. on pp. 3, 16, 21, 47, 63, 66).

[23] K. Hiura and S.-i. Sasa, "Kinetic uncertainty relation on first-passage time for accumulated current", Phys. Rev. E **103**, L050103 (2021) (cit. on pp. 3, 16).

[24] Y. Hasegawa, "Thermodynamic uncertainty relation for quantum first-passage processes", Phys. Rev. E **105**, 044127 (2022) (cit. on pp. 3, 16, 47, 60).

[25] T. Nishiyama and Y. Hasegawa, "Exact solution to quantum dynamical activity", Phys. Rev. E **109**, 044114 (2024) (cit. on pp. 3, 16, 21, 47).

[26] J. Bourgeois, G. Blasi, S. Khandelwal, and G. Haack, "Finite-Time Dynamics of an Entanglement Engine: Current, Fluctuations and Kinetic Uncertainty Relations", Entropy **26**, 497 (2024) (cit. on pp. 3, 16).

[27] K. Prech, P. P. Potts, and G. T. Landi, "Role of Quantum Coherence in Kinetic Uncertainty Relations", arXiv (2024) 10.1103/PhysRevLett.134.020401, eprint: 2407.14147 (cit. on pp. 3, 16, 21, 47, 60, 63, 66).

[28] R. De-Picciotto, M. Reznikov, M. Heiblum, V. Umansky, G. Bunin, and D. Mahalu, "Direct observation of a fractional charge", Nature **389**, 162–164 (1997) (cit. on pp. 3, 45).

[29] L. Saminadayar, D. C. Glattli, Y. Jin, and B. Etienne, "Observation of the $e/3$ Fractionally Charged Laughlin Quasiparticle", Phys. Rev. Lett. **79**, 2526–2529 (1997) (cit. on pp. 3, 45).

[30] A. A. Kozhevnikov, R. J. Schoelkopf, and D. E. Prober, "Observation of Photon-Assisted Noise in a Diffusive Normal Metal–Superconductor Junction", Phys. Rev. Lett. **84**, 3398–3401 (2000) (cit. on pp. 3, 45).

[31] X. Jehl, M. Sanquer, R. Calemczuk, and D. Mailly, "Detection of doubled shot noise in short normal-metal/ superconductor junctions", Nature **405**, 50–53 (2000) (cit. on pp. 3, 45).

[32] D. R. White, R. Galleano, A. Actis, H. Brixy, M. De Groot, J. Dubbeldam, A. L. Reesink, F. Edler, H. Sakurai, R. L. Shepard, and J. C. Gallop, "The status of Johnson noise thermometry", Metrologia **33**, 325 (1996) (cit. on p. 3).

[33] L. Spietz, K. W. Lehnert, I. Siddiqi, and R. J. Schoelkopf, "Primary Electronic Thermometry Using the Shot Noise of a Tunnel Junction", Science **300**, 1929–1932 (2003) (cit. on p. 3).

[34] O. S. Lumbroso, L. Simine, A. Nitzan, D. Segal, and O. Tal, "Electronic noise due to temperature differences in atomic-scale junctions", Nature **562**, 240–244 (2018) (cit. on pp. 3, 48).

[35] E. Sivre, H. Duprez, A. Anthore, A. Aassime, F. D. Parmentier, A. Cavanna, A. Ouerghi, U. Gennser, and F. Pierre, "Electronic heat flow and thermal shot noise in quantum circuits", Nat. Commun. **10**, 1–8 (2019) (cit. on pp. 3, 48).

[36] S. Larocque, E. Pinsolle, C. Lupien, and B. Reulet, "Shot Noise of a Temperature-Biased Tunnel Junction", Phys. Rev. Lett. **125**, 106801 (2020) (cit. on pp. 3, 48).

[37] R. Bisognin, A. Marguerite, B. Roussel, M. Kumar, C. Cabart, C. Chapdelaine, A. Mohammad-Djafari, J.-M. Berroir, E. Bocquillon, B. Plaçais, A. Cavanna, U. Gennser, Y. Jin, P. Degiovanni, and G. Fève, "Quantum tomography of electrical currents", Nat. Commun. **10**, 1–12 (2019) (cit. on p. 3).

[38] E. S. Tikhonov, A. O. Denisov, S. U. Piatrusha, I. N. Khrapach, J. P. Pekola, B. Karimi, R. N. Jabdaraghi, and V. S. Khrapai, "Spatial and energy resolution of electronic states by shot noise", Phys. Rev. B **102**, 085417 (2020) (cit. on p. 3).

[39] U. Thupakula, V. Perrin, A. Palacio-Morales, L. Cario, M. Aprili, P. Simon, and F. Massee, "Coherent and Incoherent Tunneling into Yu-Shiba-Rusinov States Revealed by Atomic Scale Shot-Noise Spectroscopy", Phys. Rev. Lett. **128**, 247001 (2022) (cit. on p. 3).

[40] J. B. Johnson, "Thermal Agitation of Electricity in Conductors", Nature **119**, 50–51 (1927) (cit. on pp. 3, 15, 44).

[41] H. Nyquist, "Thermal Agitation of Electric Charge in Conductors", Phys. Rev. **32**, 110–113 (1928) (cit. on pp. 3, 15, 44).

[42] H. B. Callen and T. A. Welton, "Irreversibility and Generalized Noise", Phys. Rev. **83**, 34–40 (1951) (cit. on pp. 3, 15, 43).

[43] M. S. Green, "Markoff Random Processes and the Statistical Mechanics of Time-Dependent Phenomena. II. Irreversible Processes in Fluids", J. Chem. Phys. **22**, 398–413 (1954) (cit. on p. 3).

[44] R. Kubo, "Statistical-Mechanical Theory of Irreversible Processes. I. General Theory and Simple Applications to Magnetic and Conduction Problems", J. Phys. Soc. Jpn. **12**, 570–586 (1957) (cit. on pp. 3, 15).

[45] C. Jarzynski, "Nonequilibrium Equality for Free Energy Differences", Phys. Rev. Lett. **78**, 2690–2693 (1997) (cit. on p. 3).

[46] G. E. Crooks, "Entropy production fluctuation theorem and the nonequilibrium work relation for free energy differences", Phys. Rev. E **60**, 2721–2726 (1999) (cit. on p. 3).

[47] H. Tasaki, "Jarzynski Relations for Quantum Systems and Some Applications", arXiv (2000) 10.48550/arXiv.cond-mat/0009244, eprint: cond-mat/0009244 (cit. on p. 3).

[48] D. Andrieux and P. Gaspard, "A fluctuation theorem for currents and nonlinear response coefficients", J. Stat. Mech.: Theory Exp. **2007**, P02006 (2007) (cit. on pp. 3, 13, 15).

[49] C. Jarzynski, "Comparison of far-from-equilibrium work relations", C. R. Phys. **8**, 495–506 (2007) (cit. on p. 3).

[50] D. Andrieux, P. Gaspard, T. Monnai, and S. Tasaki, "The fluctuation theorem for currents in open quantum systems", New J. Phys. **11**, 043014 (2009) (cit. on pp. 3, 15).

[51] M. Esposito, U. Harbola, and S. Mukamel, "Nonequilibrium fluctuations, fluctuation theorems, and counting statistics in quantum systems", Rev. Mod. Phys. **81**, 1665–1702 (2009) (cit. on pp. 3, 9, 11, 13, 15).

[52] T. Sagawa and M. Ueda, "Nonequilibrium thermodynamics of feedback control", Phys. Rev. E **85**, 021104 (2012) (cit. on p. 3).

[53] O.-P. Saira, Y. Yoon, T. Tanttu, M. Möttönen, D. V. Averin, and J. P. Pekola, "Test of the Jarzynski and Crooks Fluctuation Relations in an Electronic System", Phys. Rev. Lett. **109**, 180601 (2012) (cit. on p. 3).

[54] G. N. Bochkov and Y. E. Kuzovlev, "Fluctuation–dissipation relations. Achievements and misunderstandings", Phys.-Usp. **56**, 590 (2013) (cit. on p. 3).

[55] P. P. Potts and P. Samuelsson, "Detailed Fluctuation Relation for Arbitrary Measurement and Feedback Schemes", Phys. Rev. Lett. **121**, 210603 (2018) (cit. on p. 3).

[56] G. Rubino, K. V. Hovhannisyan, and P. Skrzypczyk, "Revising the quantum work fluctuation framework to encompass energy conservation", (2024), arXiv:2406.18632 [quant-ph] (cit. on p. 3).

[57] K. Prech and P. P. Potts, "Quantum Fluctuation Theorem for Arbitrary Measurement and Feedback Schemes", Phys. Rev. Lett. **133**, 140401 (2024) (cit. on p. 3).

[58] D. Rogovin and D. J. Scalapino, "Fluctuation phenomena in tunnel junctions", Ann. Phys. **86**, 1–90 (1974) (cit. on pp. 3, 40, 44).

[59] L. S. Levitov and M. Reznikov, "Counting statistics of tunneling current", Phys. Rev. B **70**, 115305 (2004) (cit. on pp. 3, 44).

[60] B. Altaner, M. Polettini, and M. Esposito, "Fluctuation-Dissipation Relations Far from Equilibrium", Phys. Rev. Lett. **117**, 180601 (2016) (cit. on pp. 3, 16).

[61] N. Shiraishi, "Time-Symmetric Current and Its Fluctuation Response Relation around Nonequilibrium Stalling Stationary State", Phys. Rev. Lett. **129**, 020602 (2022) (cit. on pp. 3, 16).

[62] M. Josefsson, A. Svilans, A. M. Burke, E. A. Hoffmann, S. Fahlvik, C. Thelander, M. Leijnse, and H. Linke, "A quantum-dot heat engine operating close to the thermodynamic efficiency limits", Nat. Nanotechnol. **13**, 920–924 (2018) (cit. on p. 4).

[63] J. V. Koski, V. F. Maisi, J. P. Pekola, and D. V. Averin, "Experimental realization of a Szilard engine with a single electron", Proc. Natl. Acad. Sci. U.S.A. **111**, 13786–13789 (2014) (cit. on p. 4).

[64] H. van Houten, L. W. Molenkamp, C. W. J. Beenakker, and C. T. Foxon, "Thermo-electric properties of quantum point contacts", Semicond. Sci. Technol. **7**, B215–B221 (1992) (cit. on p. 4).

[65] S. Roddaro, D. Ercolani, M. A. Safeen, S. Suomalainen, F. Rossella, F. Giazotto, L. Sorba, and F. Beltram, "Giant Thermovoltage in Single InAs Nanowire Field-Effect Transistors", Nano Lett. **13**, 3638–3642 (2013) (cit. on p. 4).

[66] D. Prete, P. A. Erdman, V. Demontis, V. Zannier, D. Ercolani, L. Sorba, F. Beltram, F. Rossella, F. Taddei, and S. Roddaro, "Thermoelectric Conversion at 30 K in InAs/InP Nanowire Quantum Dots", Nano Lett. **19**, 3033–3039 (2019) (cit. on p. 4).

[67] L. D. Hicks and M. S. Dresselhaus, "Effect of quantum-well structures on the thermoelectric figure of merit", Phys. Rev. B **47**, 12727–12731 (1993) (cit. on p. 4).

[68] G. D. Mahan and J. O. Sofo, "The best thermoelectric.", Proc. Natl. Acad. Sci. U.S.A. **93**, 7436–7439 (1996) (cit. on p. 4).

[69] M. S. Dresselhaus, G. Chen, M. Y. Tang, R. G. Yang, H. Lee, D. Z. Wang, Z. F. Ren, J.-P. Fleurial, and P. Gogna, "New Directions for Low-Dimensional Thermoelectric Materials", Adv. Mater. **19**, 1043–1053 (2007) (cit. on p. 4).

[70] L. Szilard, "über die Entropieverminderung in einem thermodynamischen System bei Eingriffen intelligenter Wesen", Z. Phys. **53**, 840–856 (1929) (cit. on p. 4).

[71] J. M. R. Parrondo, J. M. Horowitz, and T. Sagawa, "Thermodynamics of information", Nature Physics **11**, 131–139 (2015) (cit. on p. 4).

[72] A. Alemany, A. Mossa, I. Junier, and F. Ritort, "Experimental free-energy measurements ofÂ kinetic molecular states using fluctuationÂ theorems", Nature Physics **8**, 688–694 (2012) (cit. on p. 4).

[73] S. Ciliberto, "Experiments in Stochastic Thermodynamics: Short History and Perspectives", Phys. Rev. X **7**, 021051 (2017) (cit. on p. 4).

[74] R. Kosloff, "A quantum mechanical open system as a model of a heat engine", J. Chem. Phys. **80**, 1625–1631 (1984) (cit. on p. 4).

[75] S. W. Kim, T. Sagawa, S. De Liberato, and M. Ueda, "Quantum Szilard Engine", Phys. Rev. Lett. **106**, 070401 (2011) (cit. on p. 4).

[76] R. Kosloff and A. Levy, "Quantum Heat Engines and Refrigerators: Continuous Devices", Annu. Rev. Phys. Chem., 365–393 (2014) (cit. on p. 4).

[77] J. P. Pekola, "Towards quantum thermodynamics in electronic circuits", Nat. Phys. **11**, 118–123 (2015) (cit. on p. 4).

[78] M. Campisi, J. Pekola, and R. Fazio, "Nonequilibrium fluctuations in quantum heat engines: theory, example, and possible solid state experiments", New J. Phys. **17**, 035012 (2015) (cit. on p. 4).

[79] G. Marchegiani, P. Virtanen, F. Giazotto, and M. Campisi, "Self-Oscillating Josephson Quantum Heat Engine", Phys. Rev. Appl. **6**, 054014 (2016) (cit. on p. 4).

[80] M. Łobejko, P. Mazurek, and M. Horodecki, "Thermodynamics of Minimal Coupling Quantum Heat Engines", Quantum **4**, 375 (2020), eprint: 2003.05788v4 (cit. on p. 4).

[81] R. Alicki, M. Horodecki, A. Jenkins, M. Łobejko, and G. Suárez, "The Josephson junction as a quantum engine", New J. Phys. **25**, 113013 (2023) (cit. on p. 4).

[82] S. Sundelin, M. A. Aamir, V. M. Kulkarni, C. Castillo-Moreno, and S. Gasparinetti, "Quantum refrigeration powered by noise in a superconducting circuit", arXiv (2024) 10.48550/arXiv.2403.03373, eprint: 2403.03373 (cit. on p. 4).

[83] L. M. Cangemi, C. Bhadra, and A. Levy, "Quantum engines and refrigerators", Phys. Rep. **1087**, 1–71 (2024) (cit. on p. 4).

[84] M. A. Aamir, P. Jamet Suria, J. A. Marín Guzmán, C. Castillo-Moreno, J. M. Epstein, N. Yunger Halpern, and S. Gasparinetti, "Thermally driven quantum refrigerator autonomously resets a superconducting qubit", Nat. Phys., 1–6 (2025) (cit. on p. 4).

[85] J. B. Brask, G. Haack, N. Brunner, and M. Huber, "Autonomous quantum thermal machine for generating steady-state entanglement", New J. Phys. **17**, 113029 (2015) (cit. on p. 4).

[86] A. Tavakoli, G. Haack, N. Brunner, and J. B. Brask, "Autonomous multipartite entanglement engines", Phys. Rev. A **101**, 012315 (2020) (cit. on p. 4).

[87] S. Khandelwal, B. Annby-Andersson, G. F. Diotallevi, A. Wacker, and A. Tavakoli, "Maximal steady-state entanglement in autonomous quantum thermal machines", arXiv (2024) 10.48550/arXiv.2401.01776, eprint: 2401.01776 (cit. on p. 4).

[88] K. Brandner, T. Hanazato, and K. Saito, "Thermodynamic Bounds on Precision in Ballistic Multiterminal Transport", Phys. Rev. Lett. **120**, 090601 (2018) (cit. on pp. 5, 52).

[89] B. K. Agarwalla and D. Segal, "Assessing the validity of the thermodynamic uncertainty relation in quantum systems", Phys. Rev. B **98**, 155438 (2018) (cit. on pp. 5, 52, 59).

[90] J. Liu and D. Segal, "Thermodynamic uncertainty relation in quantum thermoelectric junctions", Phys. Rev. E **99**, 062141 (2019) (cit. on pp. 5, 52).

[91] S. Saryal, H. M. Friedman, D. Segal, and B. K. Agarwalla, "Thermodynamic uncertainty relation in thermal transport", Phys. Rev. E **100**, 042101 (2019) (cit. on pp. 5, 52).

[92] H. M. Friedman, B. K. Agarwalla, O. Shein-Lumbroso, O. Tal, and D. Segal, "Thermodynamic uncertainty relation in atomic-scale quantum conductors", Phys. Rev. B **101**, 195423 (2020) (cit. on pp. 5, 48, 52).

[93] E. Potanina, C. Flindt, M. Moskalets, and K. Brandner, "Thermodynamic bounds on coherent transport in periodically driven conductors", Phys. Rev. X **11**, 021013 (2021) (cit. on pp. 5, 52, 60).

[94] T. Ehrlich and G. Schaller, "Broadband frequency filters with quantum dot chains", Phys. Rev. B **104**, 045424 (2021) (cit. on pp. 5, 52).

[95] M. Gerry and D. Segal, "Absence and recovery of cost-precision tradeoff relations in quantum transport", Phys. Rev. B **105**, 155401 (2022) (cit. on pp. 5, 52).

[96] A. M. Timpanaro, G. Guarnieri, and G. T. Landi, "Hyperaccurate thermoelectric currents", Phys. Rev. B **107**, 115432 (2023) (cit. on pp. 5, 52).

[97] H.-P. Breuer, F. Petruccione, H.-P. Breuer, and F. Petruccione, *The Theory of Open Quantum Systems* (Oxford University Press, Oxford, England, UK, June 2002) (cit. on p. 7).

[98] G. T. Landi and M. Paternostro, "Irreversible entropy production: From classical to quantum", Rev. Mod. Phys. **93**, 035008 (2021) (cit. on pp. 9, 11).

[99] G. Manzano, J. M. Horowitz, and J. M. R. Parrondo, "Quantum Fluctuation Theorems for Arbitrary Environments: Adiabatic and Nonadiabatic Entropy Production", Phys. Rev. X **8**, 031037 (2018) (cit. on p. 11).

[100] C. Jarzynski and D. K. Wójcik, "Classical and Quantum Fluctuation Theorems for Heat Exchange", Phys. Rev. Lett. **92**, 230602 (2004) (cit. on p. 11).

[101] F. C. Klebaner, *Introduction to stochastic calculus with applications* (World Scientific Publishing Company, 2012) (cit. on p. 12).

[102] S. K. Manikandan, L. Dabelow, R. Eichhorn, and S. Krishnamurthy, "Efficiency Fluctuations in Microscopic Machines", Phys. Rev. Lett. **122**, 140601 (2019) (cit. on p. 13).

[103] A. Dechant and S.-i. Sasa, "Fluctuation–response inequality out of equilibrium", Proc. Natl. Acad. Sci. U.S.A. **117**, 6430–6436 (2020) (cit. on p. 16).

[104] V. T. Vo, T. Van Vu, and Y. Hasegawa, "Unified thermodynamic–kinetic uncertainty relation", J. Phys. A: Math. Theor. **55**, 405004 (2022) (cit. on p. 16).

[105] K. Prech, P. Johansson, E. Nyholm, G. T. Landi, C. Verdozzi, P. Samuelsson, and P. P. Potts, "Entanglement and thermokinetic uncertainty relations in coherent mesoscopic transport", Phys. Rev. Res. **5**, 023155 (2023) (cit. on pp. 16, 59).

[106] J.-C. Delvenne and G. Falasco, "Thermokinetic relations", Phys. Rev. E **109**, 014109 (2024) (cit. on p. 16).

[107] Y. Zhang, "Comment on "Fluctuation Theorem Uncertainty Relation" and "Thermodynamic Uncertainty Relations from Exchange Fluctuation Theorems"", arXiv (2019) 10.48550/arXiv.1910.12862, eprint: 1910.12862 (cit. on p. 19).

[108] C. Maes, "Frenesy: Time-symmetric dynamical activity in nonequilibria", Phys. Rep. **850**, 1–33 (2020) (cit. on p. 20).

[109] Y. Hasegawa and T. Nishiyama, "Thermodynamic Concentration Inequalities and Trade-Off Relations", Phys. Rev. Lett. **133**, 247101 (2024) (cit. on p. 22).

[110] Y. Hasegawa, "Ultimate precision limit of quantum thermal machines", arXiv (2024) 10.48550/arXiv.2412.07271, eprint: 2412.07271 (cit. on p. 22).

[111] R. Landauer, "Electrical resistance of disordered one-dimensional lattices", Philosophical Magazine: A Journal of Theoretical Experimental and Applied Physics **21**, 863–867 (1970) (cit. on p. 25).

[112] M. Büttiker, Y. Imry, R. Landauer, and S. Pinhas, "Generalized many-channel conductance formula with application to small rings", Phys. Rev. B **31**, 6207–6215 (1985) (cit. on p. 25).

[113] M. Büttiker, "Four-Terminal Phase-Coherent Conductance", Phys. Rev. Lett. **57**, 1761–1764 (1986) (cit. on p. 25).

[114] Ya. M. Blanter and M. Büttiker, "Shot noise in mesoscopic conductors", Phys. Rep. **336**, 1–166 (2000) (cit. on pp. 34, 45).

[115] C. W. J. Beenakker, C. Emary, M. Kindermann, and J. L. van Velsen, "Proposal for Production and Detection of Entangled Electron-Hole Pairs in a Degenerate Electron Gas", Phys. Rev. Lett. **91**, 147901 (2003) (cit. on p. 37).

[116] A. Bruch, C. Lewenkopf, and F. von Oppen, "Landauer-B\"uttiker Approach to Strongly Coupled Quantum Thermodynamics: Inside-Outside Duality of Entropy Evolution", Phys. Rev. Lett. **120**, 107701 (2018) (cit. on p. 37).

[117] G. Zhang, C. Hong, T. Alkalay, V. Umansky, M. Heiblum, I. Gornyi, and Y. Gefen, "Measuring statistics-induced entanglement entropy with a Hong–Ou–Mandel interferometer", Nat. Commun. **15**, 1–8 (2024) (cit. on p. 37).

[118] M. Esposito, M. A. Ochoa, and M. Galperin, "Quantum Thermodynamics: A Nonequilibrium Green's Function Approach", Phys. Rev. Lett. **114**, 080602 (2015) (cit. on p. 37).

[119] N. Seshadri and M. Galperin, "Entropy and information flow in quantum systems strongly coupled to baths", Phys. Rev. B **103**, 085415 (2021) (cit. on p. 37).

[120] J. Zhou, A. Li, and M. Galperin, "Quantum thermodynamics: Inside-outside perspective", Phys. Rev. B **109**, 085408 (2024) (cit. on p. 37).

[121] P. Strasberg, G. Schaller, N. Lambert, and T. Brandes, "Nonequilibrium thermodynamics in the strong coupling and non-Markovian regime based on a reaction coordinate mapping", New J. Phys. **18**, 073007 (2016) (cit. on p. 37).

[122] L. P. Bettmann, M. J. Kewming, G. T. Landi, J. Goold, and M. T. Mitchison, "Quantum stochastic thermodynamics in the mesoscopic-leads formulation", arXiv (2024) 10.48550/arXiv.2404.06426, eprint: 2404.06426 (cit. on p. 37).

[123] M. Esposito, K. Lindenberg, and C. Van den Broeck, "Entropy production as correlation between system and reservoir", New J. Phys. **12**, 013013 (2010) (cit. on p. 38).

[124] M. Aspelmeyer, T. J. Kippenberg, and F. Marquardt, "Cavity optomechanics", Rev. Mod. Phys. **86**, 1391–1452 (2014) (cit. on p. 40).

[125] I. Safi, "Time-dependent Transport in arbitrary extended driven tunnel junctions", arXiv (2014) 10.48550/arXiv.1401.5950, eprint: 1401.5950 (cit. on p. 44).

[126] I. Safi, "Driven quantum circuits and conductors: A unifying perturbative approach", Phys. Rev. B **99**, 045101 (2019) (cit. on p. 44).

[127] J. Rech, T. Jonckheere, B. Grémaud, and T. Martin, "Negative Delta-T Noise in the Fractional Quantum Hall Effect", Phys. Rev. Lett. **125**, 086801 (2020) (cit. on p. 48).

[128] M. Hasegawa and K. Saito, "Delta-T noise in the Kondo regime", Phys. Rev. B **103**, 045409 (2021) (cit. on p. 48).

[129] R. A. Melcer, B. Dutta, C. Spånslätt, J. Park, A. D. Mirlin, and V. Umansky, "Absent thermal equilibration on fractional quantum Hall edges over macroscopic scale", Nat. Commun. **13**, 1–7 (2022) (cit. on p. 48).

[130] A. Popoff, J. Rech, T. Jonckheere, L. Raymond, B. Grémaud, S. Malherbe, and T. Martin, "Scattering theory of non-equilibrium noise and delta T current fluctuations through a quantum dot", J. Phys.: Condens. Matter **34**, 185301 (2022) (cit. on p. 48).

[131] G. Zhang, I. V. Gornyi, and C. Spånslätt, "Delta-T noise for weak tunneling in one-dimensional systems: Interactions versus quantum statistics", Phys. Rev. B **105**, 195423 (2022) (cit. on p. 48).

[132] M. Hübler and W. Belzig, "Light emission in delta-T-driven mesoscopic conductors", Phys. Rev. B **107**, 155405 (2023) (cit. on p. 48).

[133] A. Crépieux, T. Q. Duong, and M. Lavagna, "Fano factor, ΔT-noise and cross-correlations in double quantum dots", arXiv (2023) 10.48550/arXiv.2306.02146, eprint: 2306.02146 (cit. on p. 48).

[134] K. Iyer, J. Rech, T. Jonckheere, L. Raymond, B. Grémaud, and T. Martin, "Colored delta-T noise in fractional quantum Hall liquids", Phys. Rev. B **108**, 245427 (2023) (cit. on p. 48).

[135] M. Acciai, G. Zhang, and C. Spånslätt, "Role of scaling dimensions in generalized noises in fractional quantum Hall tunneling due to a temperature bias", arXiv (2024) 10.48550/arXiv.2408.04525, eprint: 2408.04525 (cit. on p. 48).

[136] O. Shein-Lumbroso, M. Gerry, A. Shastry, A. Vilan, D. Segal, and O. Tal, "Delta-T Flicker Noise Demonstrated with Molecular Junctions", Nano Lett. **24**, 1981–1987 (2024) (cit. on p. 48).

[137] L. Pierattelli, F. Taddei, and A. Braggio, "ΔT-noise in Multiterminal Hybrid Systems", arXiv (2024) 10.48550/arXiv.2411.12572, eprint: 2411.12572 (cit. on p. 48).

[138] M. Gerry, J. J. Wang, J. Li, O. Shein-Lumbroso, O. Tal, and D. Segal, "Machine learning delta-T noise for temperature bias estimation", arXiv (2024) 10.48550/arXiv.2412.00288, eprint: 2412.00288 (cit. on p. 48).

[139] R. S. Whitney, "Most Efficient Quantum Thermoelectric at Finite Power Output", Phys. Rev. Lett. **112**, 130601 (2014) (cit. on p. 53).

[140] R. S. Whitney, "Finding the quantum thermoelectric with maximal efficiency and minimal entropy production at given power output", Phys. Rev. B **91**, 115425 (2015) (cit. on p. 53).

[141] R. Sánchez, J. Splettstoesser, and R. S. Whitney, "Nonequilibrium System as a Demon", Phys. Rev. Lett. **123**, 216801 (2019) (cit. on p. 60).

[142] F. Hajiloo, R. Sánchez, R. S. Whitney, and J. Splettstoesser, "Quantifying nonequilibrium thermodynamic operations in a multiterminal mesoscopic system", Phys. Rev. B **102**, 155405 (2020) (cit. on p. 60).

Appended Papers